Visual dysfunction in macular telangiectasia type 2

Tjebo Frédéric Chomé Heeren

A dissertation submitted in partial fulfillment

of the requirements for the degree of

Doctor of Philosophy

of

University College London.

Institute of Ophthalmology

University College London

December 27, 2022

I, Tjebo Frédéric Chomé Heeren, confirm that the work presented in this thesis is my own. Where information has been derived from other sources, I confirm that this has been indicated in the work.

Abstract

Macular telangiectasia type 2 (macular telangiectasia type 2) is a bilateral neurodegenerative condition of the macula of the human eye which can lead to loss of central vision. There is evidence that metabolic dysfunction leads to slow degeneration of the retinal neuroglia, eventually leading to circumscribed loss of neuronal tissue (photoreceptor atrophy). A characteristic feature of macular telangiectasia type 2 is the temporal epicenter where the disease typically begins, and its limitation to a central oval shaped area of approximately five by ten degrees, called the *macular telangiectasia type 2 area*. Knowledge about visual function of people with macular telangiectasia type 2 was limited to visual acuity testing, investigations of reading performance, visual field testing with fundus-controlled perimetry (microperimetry), and scotopic perimetry (not fundus-controlled). This thesis summarises research aimed at exploring visual function in macular telangiectasia type 2 in more detail. In particular, visual acuity and reading performance are investigated in more detail, the (para)central scotomas are better characterised, and visual function in low light is elucidated by testing contrast sensitivity, low luminance visual acuity and dark-adapted microperimetry. Visual acuity data was collected as part of the international research collaboration *The macular telangiectasia type 2 study*, which started in 2005 and has since then accrued data of more than 3000 individuals with macular telangiectasia type 2. It was taken with Early Treatment of Diabetic Retinopathy Study (ETDRS) charts on a harmonised protocol. Distribution of visual acuity in the entire study cohort was investigated and eyes with low visual acuity were looked at in detail. It was found that only about half of eyes with very poor visual acuity showed evidence of neovascularisations, until recently still con-

sidered disease end stage, but nearly all eyes showed photoreceptor atrophy, which is therefore more likely to define the disease end stage. Scotomas were characterised further on retrospective analysis of microperimetry examinations from four large centers of the macular telangiectasia type 2 study. This analysis confirmed previous data which suggested mono-focality of the scotomas and the limitation to a specific size. Further microperimetry assessment was performed with a recently introduced new technology, allowing dark-adapted microperimetry with two wavelengths, aiding differentiation of cone and rod dysfunction. This test showed more general sensitivity reduction for blue light under low light conditions. This may be in keeping with the findings from contrast sensitivity testing in mesopic light conditions, showing strong impairment already in early disease stages, possibly indicating inner retinal dysfunction rather than photoreceptor dysfunction in those disease stages. Reading performance and the effect of binocularity was measured with Radner Reading charts. Reading was consistently slower when patients were using both eyes, strongly indicating binocular inhibition, in particular when arising from scotomas in left eyes. Based on the above, the findings resulted in new insights into visual function with implications on our understanding of the condition. Understanding visual impairment not only helps patient counselling, but also helps driving directions of future research.

Impact Statement

Being diagnosed with a potentially blinding disease of the eye can be a life-changing event. The typical age of onset of macular telangiectasia type 2 (MacTel) is between the fifth and sixth decade of life, in an age of productivity. Before this thesis was written, there was only limited knowledge about the impact of macular telangiectasia type 2 on visual function. For example, it was known that the simple test of reading letters on the chart only poorly reflects the very specific loss of vision which people with MacTel experience. It was known that there was an increasing blind spot in their central vision which could be measured with specific tools. The special location of the blind spot also accounted for particular problems with reading.

The herein presented studies further quantified and characterised details of functional loss in people with MacTel. Understanding how people are exactly affected will help direct future research in this condition, as it helps focussing research efforts and means on problems and questions that have more pertinence on affected people's lives. It is also essential to understand visual impairment better in order to help people retain their stable physical and mental health.

Especially the knowledge about early functional changes not only helps patient counselling, but also provides important clues to the disease mechanism. For example, the simple advice to improve lighting in the daily environment, in particular when performing common tasks such as reading, can be of life changing importance for the patient. Similarly,

encouraging people to try to read only with one eye open can help them reading more fluently and it is quite surprising how often patients have never tried to read in this way or have not dared to cover their eye because they might think it causes harm to do so. The studies presented in this thesis provide some more scientific ground to this commonplace advice, and it helps patients to understand why they might struggle with specific tasks so much. It also was shown that the likelihood of severe visual loss is very low - which most patients will find very reassuring.

New methods are being introduced to analyse results from still fairly new technologies such as fundus-controlled perimetry ("microperimetry"), which are lacking standardised analysis strategies. Microperimetry is a fascinating tool to quantify the visual field, and especially the size of blind spots in vision. The new analysis strategies used in this thesis will help provide ground for future groups working with similar methods.

The research presented in this thesis was published in six peer-reviewed articles [1–6] and has already influenced more than ten further studies. [7–17] It is expected that this study will continue to influence future research about visual disability in macular diseases in general, as methods and analytical approaches used in this study can be readily applied in other conditions such as age-related macular degeneration or diabetic maculopathy.

As a side project of this work, an open source R package was developed which will help future eye researchers to handle ophthalmic data in a more streamlined manner. In particular the often quite challenging inter-conversion of visual acuity notations, and other often astonishingly daunting tasks such as counting the number of patients and eyes has been made an easy task with this package. The software was published on the comprehensive R archive network (CRAN) under a Massachusetts Institute of Technology (MIT) licence, a permissive free

software license. People who are not proficient in R can use parts of the functionality of this software on www.va-converter.com, which is a website created for the purpose of converting visual acuity notations and is also free to use.

Acknowledgements

To begin with, I would like to thank my mentor and friend Peter Charbel Issa without whom I would not have started this venture. I also would like to thank my teacher and supervisor Catherine Egan and also my primary supervisor Prof. Marcus Fruttiger for being so relaxed but still firm about my progress. My friends who helped me find the strength to finish this thesis, foremost Marcela, Siggy, Abraham and Chris. Last, but not least, of course my parents who created me and shaped me in my early years - my memories of early childhood make me believe that I must have been a terribly annoying know-it-all, yet they tolerated me.

Contents

List of Figures

List of Tables

Chapter 1

Introduction

1.1 On a knife-edge

The human retina is a highly complex neuronal tissue organised in layers both of neuronal and non-neuronal cells. Neuronal cells are the photoreceptors (rods and cones), bipolar, amacrine, horizontal and ganglion cells, and non-neuronal cells are mostly neuroglial cells (microglia, astroglia, muller cells), and vascular cells (pericytes, endothelial cells). In a central area of approximately 6mm diameter there is an increased density of ganglion cells and cones [18], including the macula lutea. This area, so named after the macroscopically visible yellow colour of the central retina in dissected human eyes ("macula lutea" - latin for "yellow spot"), contains an even higher specialised area, the fovea centralis. The fovea, approximately of 1.5mm diameter, has the highest density of cones and ganglion cells with a cone to ganglion ratio of 1:1. This is the area of our sharpest vision (highest resolution). We focus on and explore things with our fovea. Due to the higher neuronal density it is presumed that the macula has higher metabolic demand than other retinal areas. [19] On the other hand there is reduced vascular supply to the fovea centralis. In fact, the very central fovea is devoid of blood vessels. [20, 21] It seems plausible that areas with increased metabolic demand but reduced oxygen supply may be more susceptible to even slight metabolic imbalances, making it more prone to macular disease. The image of neuronal tissue living "on a knife-edge" has been evoked. [22]

1.2 Macular telangiectasia type 2

Macular telangiectasia type 2 (MacTel) is such a disease which affects the macula. Being of neurodegenerative nature, it typically occurs bilaterally, i.e. in both eyes, and it leads to progressive loss of central vision. First symptoms usually occur in the fifth to sixth decade of life, an age in which most people are still working. Although considered a rare condition, its real prevalence is not yet known, but was estimated to be as high as one affected person of 1000 people. The earliest report of MacTel was likely in 1977, described as "bilateral parafoveal telangiectasis". [23] and the same author provided more detailed characterisation and classification over the next following decades. [24,25] In those early times, retinal diagnostics were largely limited to funduscopy, fundus photography and fluorescein angiography. Due to vascular changes seen in fluorescein angiography, MacTel was historically considered a disease of the retinal vasculature, hence its name. The term retinal telangiectasis (greek telos = end, angeion = vessel, ektasis = widening/ stretching out) was originally proposed by Reese in 1956. [26] The latest understanding of MacTel, however, suggests that MacTel might be associated with systemic metabolic dysregulation, those resulting in neurodegeneration and secondary vascular alterations. [7]

1.3 The MacTel study

In 2005, the MacTel study group was created by an international collaboration of retinal clinician specialists, geneticists, physiologists and histologists, with the aim to increase knowledge about MacTel, and eventually develop treatments. Patients were registered and followed in the MacTel Natural History Observation Study (NHOS), the register having two main aims - firstly the identification of potential participants in investigative studies, secondly it would allow for collection of data, most notably images and scans of the retina, clinical information about the patients as well as blood samples. The first approximately 550 patients were also followed up for at least 5 years. The registration study is still recruiting on the date of writing this thesis, however is limited to a one-time visit for each patient. The research presented in this thesis was part of this ongoing project.

At time of writing (January 2021), the MacTel study has enrolled 3943 participants. The diagnosis of MacTel was confirmed in 2749 (69.7%) participants by the Moorfields Eye Hospital Reading Centre (MEHRC), and in further 127 (27.1%) patients the diagnosis was uncertain (3.2%). The remaining 1067 participants were either unaffected family members or control participants without the condition who were also enrolled into the study. Participants underwent annual standardised examinations with slit lamp biomicroscopy, funduscopy after pupil dilation, colour fundus photography, fundus fluorescein angiography (FFA) and optical coherence tomography (OCT) imaging. Best-corrected visual acuity was tested following the Early Treatment for diabetic retinopathy study (ETDRS) protocol and charts [27]. Retinal images and scans were stored on servers of the MEHRC, whereas clinical information were stored in servers of the Emmes Corporation (Rockville, Massachusetts, US).

The following sections will provide further details about the methods used for imaging and functional testing and detail findings in MacTel for each modality.

1.4 Retinal imaging

1.4.1 Funduscopy and colour fundus photography

Slit lamp - based fundus examination constitutes a fundamental diagnostic tool in ophthalmology. Stereoscopic fundus examination is usually performed with pupils that are pharmacologically dilated (usually with tropicamide 1% and/or phenylephrine 2.5% eye drops). The image of the posterior section of the eye - vitreous, retina, retinal pigment epithelium, choroid, and sclera - is magnified to different degrees depending not only on the utilised lens, but also on the optical system of each individual eye (in particular, the cornea and the lens). In MacTel, pathologic changes are found exclusively in the macula, which can be found in the centre of the posterior pole, an ill-defined area between the large vessel arcades. The functional centre of the macula (and the retina) is the fovea, a small depression of neural tissue found primarily in humans and other primate species. [28–31]

Characteristic disease defining changes include the presence of retinal crys-

talline deposits, intraretinal pigment migration, so called "retinal greying", and the eponymous slightly blunted appearance of perifoveal vessels (telangiectasia). [32] All those are typical and recognised features of the disease but they are neither necessary criteria for the diagnosis, nor do they have an unambiguous relationship to visual function. Neovascularisations are found in approximately 10% of eyes [5] and it was unclear if they constitute the end stage of the condition before this thesis was conceived.

1.4.2 Fluorescein angiography (FFA)

By intravenously injecting the fluorescent agent fluorescein, fine retinal vasculature (including retinal capillaries) and retinal blood flow can be made visible in the living eye. This method was first described in 1961. [33] FFA is a dynamic examination, therefore time is an important variable for its evaluation. In pathologic vessels, where vessel walls show reduced tightness, fluorescein dye may extravasate and accumulate in perivascular tissue, resulting in the phenomenon described as "leakage". Other tissues may accumulate fluorescein, even if there is no vascular damage, and this phenomenon is then generally referred to as "staining". Both phenomena can be seen as an area of hyperfluorescence on FFA, whereby it is assumed to be a leakage if this area shows a growth over time. In MacTel, FFA shows four pathologic signs. All of those are always found in the temporal parafovea, [25, 32] but also extend to the nasal parafovea.

- Perifoveal ectatic capillaries (telangiectatic vessels)
- Capillaries with larger calibre and seemingly "abrupt" blunt ending - those are called right-angled vessels because they are dipping into the depths of the retina at this point.
- Staining (e.g., around intraretinal pigment plaques and of fibrotic neovascular tissue)
- Leakage in the late phase of the angiogram. This leakage is one of the diagnostic criteria for MacTel. It can be just a small area temporal to the fovea,

but can extend to an oval shaped area centred on the fovea, of approximately 5×10 degrees ($Height \times Width$).

1.4.3 Optical coherence tomography (OCT)

OCT has revolutionised diagnostics in ophthalmology. A relatively new technology, first described in 1991, [34] it has found its way into clinical practice in 1995. [35] Thus, OCT images have been available within the MacTel study from early times on. The physical principle underlying OCT is Michelson interferometry, meaning that the interference of a scanning laser with a reference laser is used to calculate the location of reflection. [34] It allows visualisation of the retinal layers on a near cellular level. In order to understand current visualisation, we need to understand the terminology of A-scan, B-scan and C-scan, which are taken from ultrasound terminology. Like ultrasound, an A-scan is a single measurement and can be represented by a single wave.

A B-scan is a series of spatially related A-scans (e.g., resulting in a horizontal line of A-scans across the posterior pole). This is usually represented by attributing density values to the A-scan wave forms, resulting in two-dimensional images, and this is the most commonly employed type of visualisation (both for ultrasound and OCT). It's very intuitive to understand those images. C-scans are spatially related B-scans, i.e., actual three-dimensional representations of the scanned object / tissue. It is difficult to understand C-scans when they are visualised in two dimensions (on a computer screen or on paper). New technologies such as virtual reality deployments help, [36] but they are still quite experimental and unfortunately not widely available. C-scans can be visualised as cross-sectional images (B-scan equivalents) or "en face" - imaging looking at all B-scans from the top (or bottom) - which makes it possible to measure areas of lesions. Naturally, one can dissect the C-scan and look at specific layers.

MacTel shows very characteristic changes on OCT. It has been proposed that the earliest visible changes might be slight foveal asymmetry. Typically, the foveal pit shows strong symmetry, but in very early MacTel stages, the point with the thinnest retina lies slightly temporal to the anatomical foveal center (as defined by

the foveal vasculature). [37] Less ambiguous signs in early stages of MacTel are found in the inner retinal layers of the fovea. These impose as cystoid spaces, i.e. hypo-reflective ("empty") areas. Importantly, those spaces can look like fluid accumulation in the retinal tissue, i.e., intraretinal edema, but they are of different nature. The retina is typically not thickened, suggesting rather a void of tissue rather than a surplus of fluid. [32] This is important regarding differential diagnostics, as certain types of intraretinal edema currently may be treated with intravitreal injections of antibodies against the vascular endothelial growth factor (anti-VEGF), a therapy which has been introduced in humans in 2004. [38]

In later stages, the outer retinal layers become increasingly disrupted. First, the marked, hyper-reflective band called *ellipsoid zone* (EZ) seems to be interrupted or "lost". This area of this ellipsoid zone loss, or better, *disruption* can be measured on *en face* images, and it has been shown to correlate very well with visual dysfunction, but not necessarily complete loss of function. [39–41] It is very important to keep in mind that a loss of reflectivity on OCT does not mean that the structure is actually lost (therefore quotation marks were used), it is simply a change of reflectivity - either due to true loss or due to a change of alignment and/or changes on molecular level resulting in an altered refractive index (thus a different scatter behaviour). With further progression of the condition, the band corresponding to the retinal outer nuclear layer (ONL) gets thinner and disappears. This corresponds to areas of photoreceptor loss (i.e., atrophy), leading to a functional blind spot (scotoma) in this location. [42]

Other signs on OCT include hyper-reflective dots in the innermost retinal layers, corresponding to crystalline deposits, increased hyper-reflectivity in the inner layers especially in earlier disease stages, and most pronounced temporally, as well as so called "outer retinal hyper-reflectivity", a feature which recently has received increased attention due to its presumptive importance as a predictive factor for clinical trial outcomes. [43, 44]

1.4.4 Fundus autofluorescence

Fundus autofluorescence is also a moderately new technology and has been described first in 1995 as an imaging method of the living human eye. [45] There are several structures of the retina which have fluorescent properties, but the main fluorophore is lipofuscin which is a metabolic product of the visual cycle accumulating over time in the retinal pigment epithelium (RPE). [46] It can be excited by a broad range of wavelengths predominantly in the blue wavelength spectrum. Autofluorescence can give important clues to the integrity of the RPE. For example, it can uncover a loss of RPE which would impose as complete loss of autofluorescence.

The graphical representation of autofluorescence is usually a two-dimensional map, the fluorescence intensity being coded as colour or grey values. Although this suggests intuitive understanding of those images, it is in fact daunting to interpret autofluorescence images correctly because of the three-dimensional nature of retinal tissue which is projected onto a two-dimensional map. In other words, although the majority of fluorescence is derived from the outmost retinal layer, the inner retinal layers contribute to the resulting image because there are structures that scatter and absorb light waves. Changes in the inner retinal layers thus can lead to relatively reduced or increased fluorescence, and without more information about the retinal layers (e.g., with OCT imaging), one is not able to tell what causes the fluorescence to be lower or higher. E.g., intraretinal pigment in MacTel blocks fluorescence, thus seems darker (if not black). This could also be due to loss of RPE in this area. Or, the rhodopsin in photoreceptor outer segments also absorbs blue light around 500nm, [47] thus a loss of photoreceptors leads to a relative increase of autofluorescence. But it could also be increased accumulation of lipofuscin.

Normal autofluorescence includes the central foveal reduction of autofluorescence due to blue light absorption by macular pigment (see subsection 1.4.5). First changes in autofluorescence include temporally increased autofluorescence due to reduced presence of macular pigment. In fact, as with other retinal imaging modalities, the temporal fovea always shows more marked changes than the nasal parafovea - this can be used as a diagnostic marker for MacTel. [48] Other

typical changes include reduced autofluorescence due to intraretinal pigment migration or neovascular membranes, or increased autofluorescence due to photoreceptor loss. [48, 49]

1.4.5 Macular pigment density measurement

Macular pigment accumulates in the human and primate macula - in fact the macula was named after its yellow appearance. [50] It is a mix of carotenoids that humans are not able to naturally synthesise - it has to be added with the diet. Its biological meaning is still contentious, its physical properties luckily less so. [51, 52] Macular pigment has an absorption maximum at 460nm. [52] This property can be exploited when using two wavelengths - green (528nm) and blue (488nm) - for excitation of lipofuscin. In the blue wavelength, macular pigment absorbs the light and thus less fluorescence is detected. This is much less so when using green light autofluorescence. The difference between both can then be used to calculate the optical density of macular pigment. [53]

The distribution of macular pigment is altered in MacTel to very distinctive pattern. [54–56] There is evidence that it is not actually a loss, but rather a redistribution of macular pigment. [57] Although it is still unclear as to what causes this redistribution, it is so characteristic that it is considered pathognomonic, and therefore, in the author's own view, diagnostic of MacTel. Relative loss of macular pigment optical density has been correlated with visual function in many ways, however it remains to be elucidated if the visual function change is indeed due to the lack of macular pigment, or if this is rather a sign of the disease, *also* represented by the macular pigment optical density loss. There is currently only sparse data of progression of macular pigment loss, but the pattern of loss generally seems fairly stable over time and also of prognostic importance for disease progression. [54, 58]

1.4.6 Confocal Blue Light reflectance

Confocal blue light reflectance (BLR) with a scanning laser ophthalmoscope is a measurement of how much blue light is scattered back from the retinal tissues. Healthy retinas usually show a regularly and smoothly decreasing BLR. It was

first shown in 2008 that eyes with MacTel show a central increase of BLR which very closely resembles the loss of macular pigment optical density, in size and shape. [56, 59] Despite this similarity, it is still debated whether the increased BLR is indeed caused by lack of macular pigment, or if it is a sign of a different, underlying disease process. [12, 60] Regardless, its presence is also considered very indicative of MacTel. BLR imaging is prone to artefacts, and optical opacities - e.g., in the lens (cataract) or in the vitreous (floaters) - can impede the signal quality substantially. In addition, the sign is volatile in nature, and it has been shown to be less intense after a small time of bleaching. [12] Given good quality images, simple red free fundus photography can be equally effective to detect the increased reflectivity for blue light. [61] This is of advantage because of the widespread availability of fundus photography: There is hardly any ophthalmology unit without a fundus camera, but confocal imaging might not always be available.

1.5 Function

The eye is a sense organ providing visual perception of our environment. In fact it can be argued that this is the sole purpose of our eyes. Its function is of primordial importance, and without visual function the eye is essentially useless. Thus, it is of central importance to know about the impact of any ocular disease on visual function. Until this herein presented research project, knowledge about retinal function in MacTel was limited to few studies on visual acuity, reading and microperimetry. Those finding are summarised in the following sections.

1.5.1 Best corrected visual acuity

Visual acuity is the central functional measure in ophthalmology. If only one test is chosen to test visual function, then it will be visual acuity. This is the ability to discriminate two points. By convention, the unit of reference is the minute of arc, i.e. $\frac{1}{60}$ of a degree, or $\frac{1}{60\times360} = \frac{1}{21600}$ of a turn (around the observer). Visual acuity is measured with *optotypes*, usually high contrast black on white numbers or letters, with or without background illumination. Commonly used charts for adults in clinical setting are Snellen charts, Sloan charts or ETDRS charts. [62, 63] Those

charts result in different units (Snellen fraction, logMAR and ETDRS letters) which are interconvertible. There has been and still is considerable effort to standardise visual acuity measurement. One of the most successful attempts is the standardised protocol which was specifically designed for the Early treatment of diabetic retinopathy (ETDRS) study. [27, 64] Mathematically and statistically, it is safest to use logMAR, as you can easily calculate (arithmetic) means. [65] Therefore, in this thesis, visual acuities will be converted to logMAR, even if the tests resulted in a different notation, mostly ETDRS letters. As visual acuity hugely depends on the refraction of the eye, for best possible comparison between individuals, the refraction error should be corrected best possible. The visual acuity under best refraction is called *best-corrected visual acuity*, and best corrected visual acuity was used in the studies underlying this thesis, only if explicitly stated differently.

Visual acuity is affected by MacTel, and the severity of impairment is correlated with the disease stage. [66] However, visual acuity loss has been shown to progress only slowly when compared to other functional deficits (see also subsection 1.5.3). [42] In fact, visual acuity is correlated to the position and size of the central scotoma, which can be explained by ability of the central retina to discriminate points which is decreasing with increasing distance from the very center of vision. [67] In other words, the more the scotoma encroaches on the central fovea, the lower becomes visual acuity. [42]

1.5.2 Reading performance

Reading is a very important visual task, and it is physiologically quite complex. [68] It requires not only a certain mental capacity, but is also depending on the ocular physiology, in particular retinal and optical integrity. Impaired central vision can affect reading detrimentally. Plenty of reading tests have been developed, [68, 69] and they can test a variety of functions. Typically, reading speed is tested, i.e. how many words are read per minute, *reading acuity* and *critical print size*. In a clinical setting the Jaeger charts are still widely used for quick and more general evaluation of reading. For more precise and more reproducible measurements required for clinical studies, the more commonly used are the *IREST* and *MNREAD*. [68, 69]

It has been demonstrated that reading ability in MacTel is disproportionally affected when compared with the fairly good and stable visual acuity. [70] It affects all measures like reading acuity, reading speed and critical print size. This may be explained by the position of the scotoma in the central 5 degrees of the visual field required for reading. [71]

1.5.3 Microperimetry

Microperimetry is the semi-colloquial term for fundus-controlled perimetry. It is different from conventional perimetry in a way that the stimulus is directly projected onto the retina and not onto a screen or field in front of or around the observer. Fundus-control is achieved by tracking the retina with a camera and adjusting the position of the stimulus according to the movements of the eye. Although microperimetric devices have been available for a few decades now, the more successful devices started with the use of scanning laser ophthalmoscopy (SLO) cameras for fundus tracking, first commercially available since 2003. [72] Although it is a highly interesting technology, it has not yet found widespread use in clinical practice, possibly due to the costs of the device, and the relative longer duration of examination when compared to conventional perimetry due to lack of fast testing algorithms, and possibly the still missing standardisation of testing protocols which is widely available for more conventional perimetry. [72]

In MacTel, microperimetry is particularly useful to detect and monitor loss of central visual function. In fact it seems superior to visual acuity measurement for this purpose. [42] and and showed the presence of a characteristic scotoma originating in the temporal parafovea. [73] The emergence of a scotoma is prognostically a dire sign. Once the scotoma emerges, it will grow in a near linear fashion by slowly encroaching onto the central fovea, ultimately resulting in loss of central vision. [42] Only when the scotoma reaches the foveal center, visual acuity will be severely affected. Until then, visual acuity remains fairly stable for a long time during disease progression, making it less suitable as a marker for disease progression. Scotoma size and location have been shown to correlate very well with structural changes on OCT imaging, in particular the loss or disruption of the ellipsoid zone. [40, 41]

It has been assumed that the characteristic location of the scotoma would result in particularly marked impairment of reading function when compared with other functional markers. [70]

1.6 Purpose of this study

Knowledge of visual impairment in MacTel was limited to few studies on visual acuity, reading performance, and microperimetry. This lack of knowledge about visual dysfunction and, more importantly, its progression, was relevant for the choice of rather unsuitable outcome measures in early investigational trials with ciliary neurotrophic factor (CNTF). [74] A more thorough characterisation of visual dysfunction and its progression would not only be relevant for patient counselling, but help establish more pertinent study outcome measures. In a previous study, Heeren et al. were able to begin characterisation of progression of functional loss, preparing the ground for the herein presented work. [42]

Chapter 2

Contrast Sensitivity is reduced in MacTel

2.1 Principles of contrast sensitivity

In a metaphysical way, one could argue that without contrast, "things" would be not be perceptible at all. Similarly, in vision, "contrast sensitivity defines the threshold between the visible and invisible". [75] Contrast in vision is defined as the difference of luminance of a stimulus when compared with the background luminance, whereby luminance is the amount of light emitted by a certain area into a specific direction (angle). Contrast can be expressed as the fraction of object luminance versus background luminance $\frac{L_{max}-L_{min}}{L_{background}}$. This is the contrast threshold. The reciprocal of the contrast threshold is called contrast sensitivity. Various methods have been used in history to measure contrast sensitivity. [75] In clinical setting, time and resources for testing patients are limited, therefore the need for easy and quick, yet reliable tests is high. Pelli and Robson have developed charts that fulfil those criteria. [76, 77] They were used to identify contrast sensitivity problems in retinal conditions such as diabetes or age-related macular degeneration. [75] From a theoretical perspective, one could expect reduced contrast sensitivity in MacTel based on recent studies which showed an association of contrast sensitivity with the presence of macular pigment. [52, 78, 79] The idea is that macular pigment reduces light scatter and glare, thus increasing contrasts, and eyes with MacTel have areas

of reduced macular pigment. However, contrast sensitivity has never been formally investigated in MacTel. The hypothesis of the following chapter was that contrast sensitivity and low light visual acuity would be impaired in MacTel, and that it might correlate to the loss of macular pigment.

2.2 Methods

2.2.1 Patients and staging

This study was performed in collaboration with the University Eye Hospital Bonn, Bonn, Germany. Patients of the MacTel Study were enrolled into this pilot study. Participants were selected consecutively, either as part of their registration visit, or on one of their follow up in clinic visits. The study was conducted in accordance with the Declaration of Helsinki, institutional review board (IRB) approval had been obtained, and informed consent was obtained from all participants.

2.2.2 Morphological classification

Eyes were divided into eyes with and those without visible morphological changes in any imaging modality. The latter were designated *stage 0*. To classify an eye as *stage 0* required the presence of a definite MacTel diagnosis in the fellow eye. This also is based on the presumption that MacTel is a bilateral disease. Age-matched controls were recruited from the retinal outpatient department, mostly patients who had unilateral conditions, such as retinal detachments or epiretinal membranes, or non-related people accompanying the study participants.

2.2.3 Contrast sensitivity testing

Contrast sensitivity was tested monocularly on both eyes with Pelli Robson Letter charts at a test distance of one meter with added correction for near distance according to the manufacturer's instructions. Testing was performed under both photopic and mesopic light conditions. Photopic means the mean room illumination was 110 lux, and mesopic means the room illumination was at 1.0 lux. Mean illumination was calculated by taking several measurements on different locations in the testing room, using a calibrated lux meter (Light Meter Lux 840021, Sper Scientific,

Scottsdale, USA). Individuals underwent 10 minutes of adaptation to the ambient lighting for both photopic and mesopic condition prior to testing. In order to reduce memorisation effects, two different test charts were used alternatingly, and mesopic testing was conducted prior to photopic testing. Contrast sensitivity was calculated based on the original suggestion by Pelli and Robson. [76] The chart consists of six letters per row, and each three letters are of the same contrast. Thus, for each group of three, a score of 0.15 log units was given. A group was considered correct, when two of three letters were recognized. Thus, the score resulted in log unit steps of 0.15. If measured under mesopic condition, the results are presented as "low light contrast sensitivity" as opposed to just "contrast sensitivity" when measured under photopic conditions. The difference between contrast sensitivity and low light contrast sensitivity is referred to as "low luminance deficit of contrast sensitivity".

2.2.4 Visual acuity testing

Best corrected visual acuity and low luminance visual acuity were measured in both eyes separately at a test distance of four meters following the original Early Treatment of Diabetic Retinopathy Study (ETDRS) protocol. [27] In order to test low luminance visual acuity, the suggestion of Sunness et al. was followed, [80] by placing a 2.0-log unit neutral density filter placed in front of each eye. For each testing, the ETDRS charts were alternated to reduce memorising effects. Low luminance deficit of visual acuity was defined as the difference between low luminance visual acuity and best corrected visual acuity. The ETDRS values were converted to logMAR using the *eye* package for R. [81]

2.2.5 Macular pigment optical density

Macular pigment optical density (MPOD) was measured using the dual wavelength autofluorescence method originally described by Delori et al. [53] with a commercially available device HRA Spectralis (Heidelberg Engineering, Heidelberg, Germany). Green and blue autofluorescence were obtained simultaneously in a four second long illumination and recording. MPOD was calculated with the manufacturer's software (HEYEX, version 1.9.10.0, HRA/Spectralis Viewing Module

6.0.13.0), resulting in a two-dimensional density map of grey values, highest optical density being coded as white, and absent optical density being black. Loss of MPOD was graded into three classes of increasing MPOD loss. [54] Class 1 showed MPOD loss limited to the temporal macula, with remaining foveal macular pigment. Class 2 was additionally showing loss of foveal macular pigment, and with or without extension into the nasal parafoveal region. Class 3 was defined as a complete MPOD loss with or without a ring of increased MPOD at 5 to 7 eccentricity.

2.2.6 Statistical analysis

Statistical significance was assessed with linear mixed models generated with the *nlme* package, version 3.1.149, [82] for the statistical software R, version 4.0.3. [83] Each model included a random intercept to take into account the correlation within subject observations as well as a fixed term to take into account potential differences between right and left eyes. All statistical analyses were performed with R. All statistical results from the linear mixed model are presented by showing the fixed effect term 'b' which indicates the mean increment in the studied phenomenon for a unit change in the the condition of interest. A p-value < 0.05 was considered significant. The 2D-density contour-plots were generated by 2D-kernel density estimation with the *MASS* package, version 7.3.53. [84]

2.3 Results

2.3.1 Patients and staging

A total of 52 patients (mean age 62.9, SD 10.2, range 35-77) were enrolled into this study. The control cohort consisted of 34 eyes of 17 controls (mean age 65.2, SD 7.4, range 53-78).

2.3.2 Contrast sensitivity testing

One eye of a MacTel patient was excluded from contrast sensitivity and visual acuity analysis because of a non-plausible test result (increase of contrast sensitivity under mesopic conditions). Table 2.1 summarises the results of contrast sensitivity and visual acuity testing.

	ctr	pat
n	34	103
Best corrected visual acuity (mean (SD))	-0.04 (0.08)	0.25 (0.28)
Low luminance visual acuity (mean (SD))	0.16 (0.12)	0.51 (0.26)
Photopic contrast sensitivity (mean (SD))	1.87 (0.13)	1.64 (0.22)
Mesopic contrast sensitivity (mean (SD))	1.59 (0.13)	1.21 (0.19)
Visual acuity low luminance deficit (mean (SD))	0.20 (0.07)	0.26 (0.11)
Contrast sensitivity mesopic deficit (mean (SD))	0.29 (0.11)	0.42 (0.18)

Table 2.1: Results from contrast sensitivity testing. Contrast sensitivity is shown in logarithm of contrast sensitivity (logCS, reciprocal of the so called contrast threshold), and visual acuity in logarithm of minimal angle of resolution (logMAR).

The remaining 103 eyes with MacTel had significantly impaired photopic and mesopic contrast sensitivity when compared to controls (b=–0.237, p-value<0.001 and b=–0.373, p-value<0.001). This impairment was higher in mesopic condition when compared with photopic conditions (b=-0.136, p-value=0.003), shown in Figure 2.1. Eyes with higher or normal photopic contrast sensitivity had a pronounced and significantly higher impairment of contrast sensitivity in mesopic conditions when compared with controls (b=–0.259, p-value<0.001). The six eyes with *stage 0* were within this group (Figure 2.1). Figure 2.2 demonstrates that laterality does not seem to play a role in those findings - the same distribution can be found in right and left eyes when looked at them separately.

2.3.3 Visual acuity

MacTel eyes showed significantly decreased BCVA (b=0.2801, p-value<0.001) and low luminance visual acuity (0.346, p-value<0.001). Visual acuity deficit under low luminance was significantly higher in MacTel eyes when compared with controls (b=0.065, p-value=0.006). However, the absolute differences were not very pronounced, see Figure 2.3. This can be better visualised by comparing the normalised loss of function under low light/ low luminance conditions for both contrast sensitivity and visual acuity (Figure 2.5). Figure 2.4 demonstrates that laterality does not seem to play a role in those findings - the same distribution can be found in right

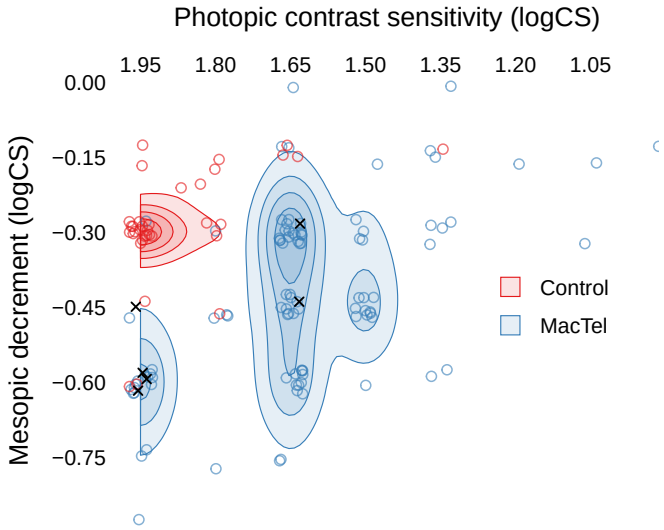

Figure 2.1: Contrast sensitivity in photopic and mesopic conditions. Each circle represents one eye. The crosses represent eyes with *stage 0*, see also subsection 2.2.2. logCS: logarithm of contrast sensitivity. logMAR: logarithm of minimum angle of resolution

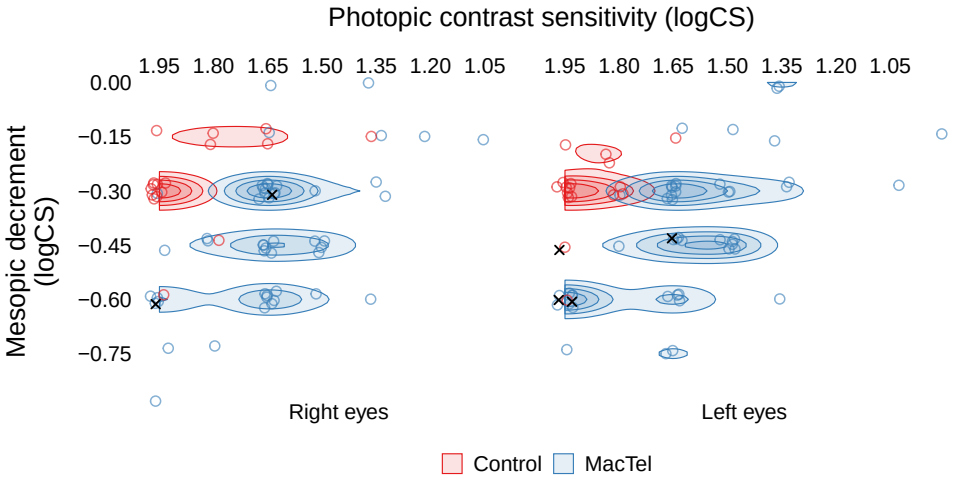

Figure 2.2: Contrast sensitivity in photopic and mesopic conditions in right and left eyes. Each circle represents one eye. The crosses represent eyes with *stage 0*, see also subsection 2.2.2. logCS: logarithm of contrast sensitivity. logMAR: logarithm of minimum angle of resolution

and left eyes when looked at them separately.

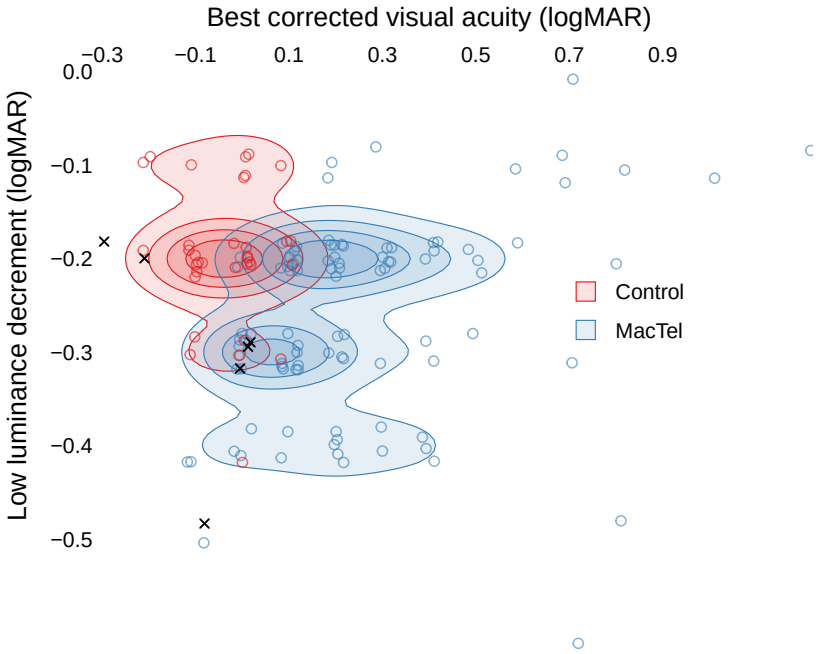

Figure 2.3: Best corrected visual acuity and low luminance deficit. Each circle represents one eye. The crosses represent eyes with *stage 0*, see also subsection 2.2.2. logMAR: logarithm of minimum angle of resolution

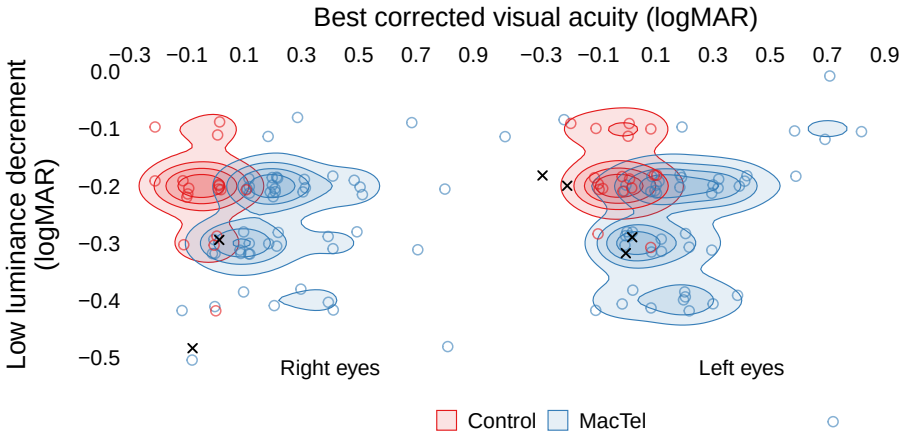

Figure 2.4: Best corrected visual acuity and low luminance deficit in right and left eyes. Each circle represents one eye. The crosses represent eyes with *stage 0*, see also subsection 2.2.2. logMAR: logarithm of minimum angle of resolution

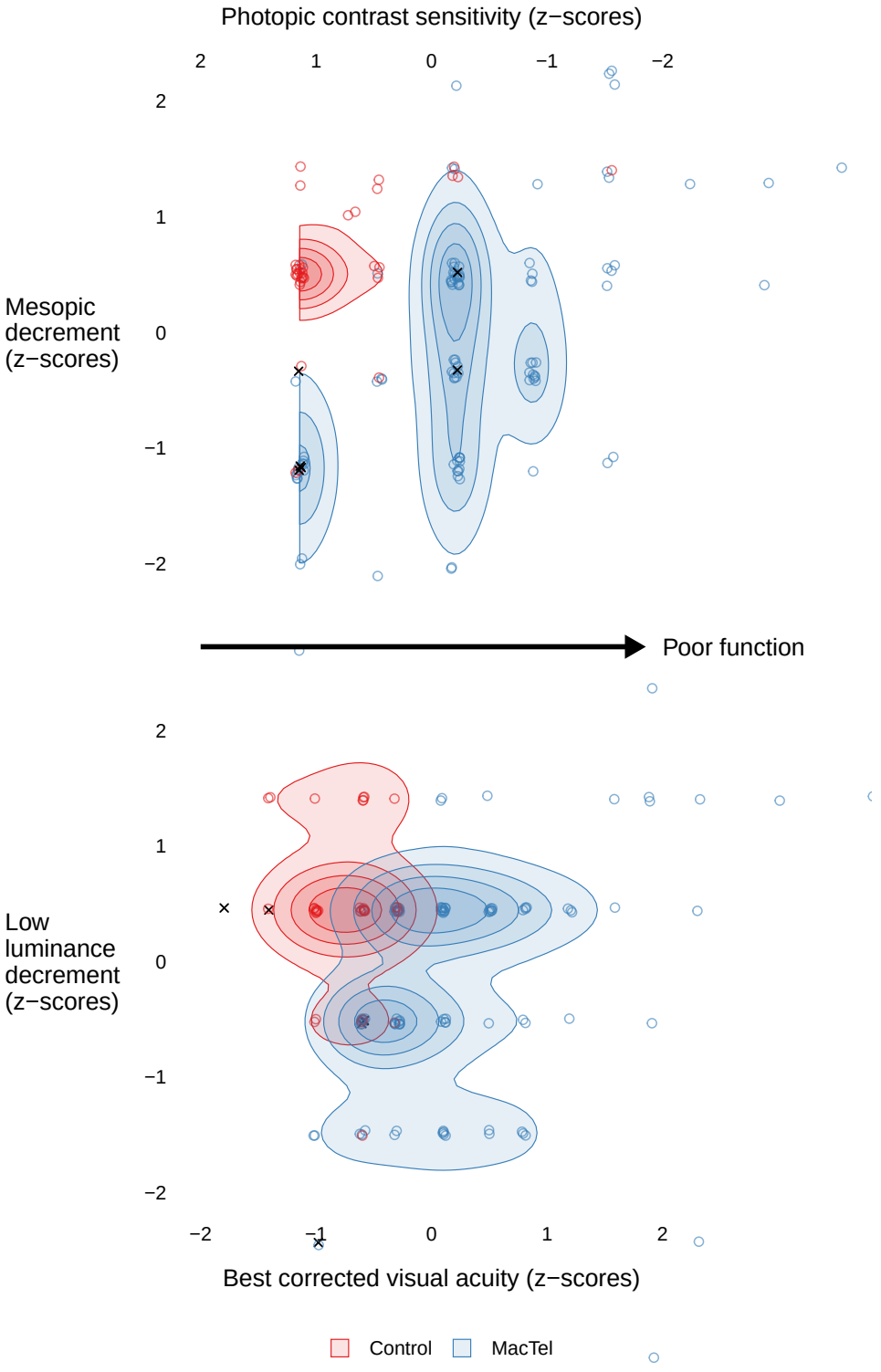

Figure 2.5: Function changing in low light conditions - z-scores are shown, scaled to mean and standard deviation of the entire sample. Each circle represents one eye. The crosses represent eyes with *stage 0*, see also subsection 2.2.2.

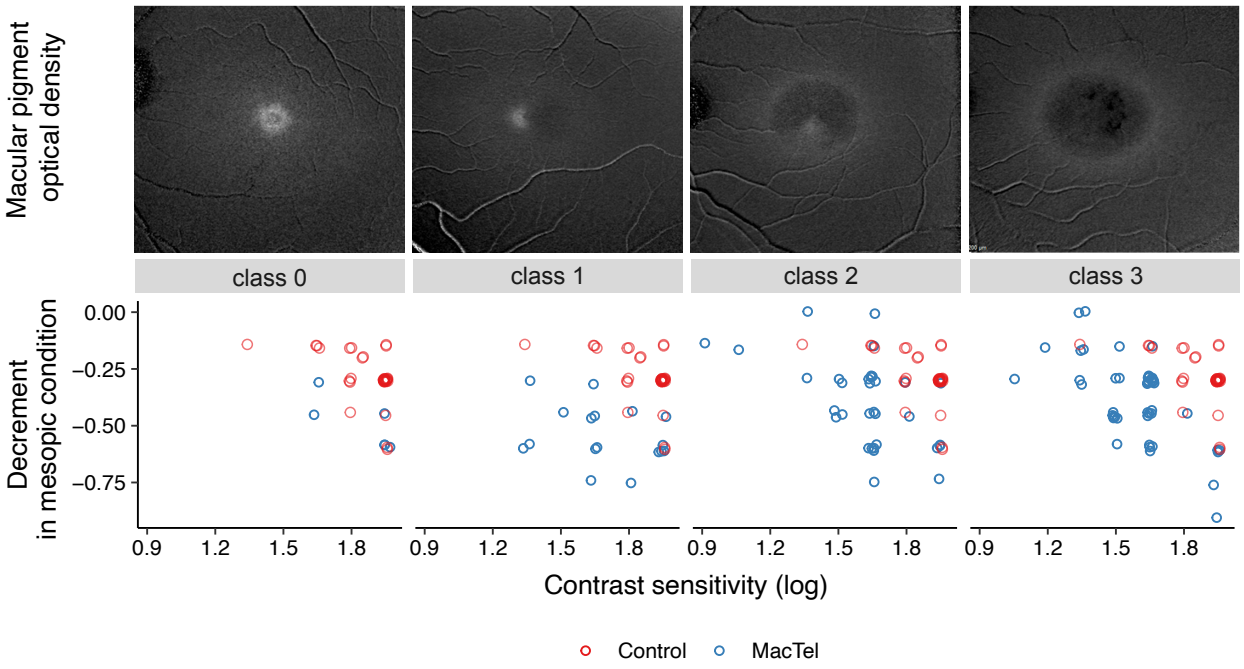

Figure 2.6: Contrast sensitivity and macular pigment optical density (MPOD). The controls are plotted for each panels. Each circle represents one eye.

2.3.4 Macular pigment optical density

MPOD measurement was discarded in two eyes due to poor quality MPOD images. Of the remaining 102 eyes, 6 eyes (6%) were classified as MPOD class 0, lacking any visible MPOD reduction. 17 eyes (17%) as class 1, 33 eyes (32%) as class 2 and 46 eyes (45%) as class 3. Figure 2.6 shows the contrast sensitivity of eyes with different classes of macular pigment loss. Mesopic contrast sensitivity was similarly impaired in all eyes. Photopic contrast sensitivity decreased with higher MPOD classes: We found a significant decrement in contrast sensitivity in photopic condition for each unit increment in MPOD class (b=-0.068, p-value<0.001). Although present, this decrement was not significant in mesopic light condition (b=-0.025, p-value=0.196). Importantly, significance of MPOD classes on contrast sensitivity vanished completely when correcting for BCVA indicating that the effect of MPOD on contrast sensitivity in photopic condition might be connected to its correlation with BCVA.

Summarising the above results, eyes with MacTel showed a generalised impairment of contrast sensitivity which increased in low light conditions. This was

found in eyes without detected morphological changes, and in eyes with normal BCVA and no absolute scotoma in microperimetry testing. A similar, but markedly less pronounced effect was found with visual acuity testing.

2.4 Discussion

Low light conditions have a detrimental effect on visual function in MacTel. Eyes with MacTel show a higher decrement of contrast sensitivity and visual acuity when compared with healthy eyes. This effect seems most pronounced in early disease stages. A possible explanation for this is that visual function in dim light conditions might be affected earlier, when visual function is still unaffected in brighter light conditions. In our sample, mesopic contrast sensitivity was generally reduced, in eyes with both early and late disease stages. Eyes with earlier disease stages have near-normal photopic BCVA and contrast sensitivity. Thus, in our sample, eyes with earlier stages are found rather in the bottom left of the graphs (good photopic function, poor mesopic function), whereas eyes with late stages are more towards the top right (poor photopic and mesopic function with less difference between the two). An increased decrement of contrast sensitivity under mesopic conditions has been shown in other macular diseases including AMD and diabetic retinopathy, as well as in neurological disorders such as Parkinson disease and multiple sclerosis. [75]

Interestingly, all eyes with *stage 0* showed an unexpected decrement of mesopic contrast sensitivity. There is of course the possibility of a sample bias. However, a real functional difference is possible. Impaired contrast sensitivity without morphological changes was also found in patients with diabetes. [85]. There is increasing evidence that there is metabolic imbalance in patients with MacTel. For example, patients with MacTel seem to have increased prevalence of diabetes, and recently an association with an impaired serine-/glycine amino acid metabolism has been shown. [7,86–88] This might lead to stress on a micro-cellular level that might result in structural changes, and ultimately, in cell atrophy.

Another possible explanation might be a functional difference resulting from

structural changes that are to small to detect with more conventional imaging technology. Charbel Issa and Heeren have recently shown that those eyes revealed a reduced "Stiles-Crawford-effect", which could be explained by a slight cone misalignment. [37] Eckmiller hypothesised that cone misalignment might result in metabolic stress [89] and metabolic changes might impair contrast sensitivity. [90] Another possibility might be that the misaligned cones might lead to reduced phototransduction. The latter makes it difficult to explain why photopic function would still be normal in eyes with early disease stages.

The difference between MacTel eyes and controls was less pronounced in low luminance visual acuity testing, and in fact, both groups showed a marked overlap. Visual acuity, a high contrast test of visual function, might therefore not be as useful in order to discriminate early affected eyes from healthy eyes. A possible explanation for the lower decrement in low light condition in visual acuity testing might be the use of high contrasts (>85%) and increasing spatial frequencies. Even when the luminance of both background and stimuli are reduced, those letters still yield a rather high contrast, and therefore the effect of visual impairment might not be so pronounced.

The spatial range of Pelli-Robson letters overlaps with the range of maximum rod contrast sensitivity. [91] Thus, a preceding loss of rod function might also contribute to impaired contrast sensitivity in mesopic condition in our study. [92] It would be interesting to study further spatial frequencies in order to provide evidence for or against the latter.

An additional effect might result from the altered macular pigment distribution. In our sample, we could show a correlation between the degree of central MPOD loss and the impairment of contrast sensitivity. A longitudinal study would be preferable to demonstrate a causal association between both - alas, this is very challenging. Firstly, MacTel is a very slowly progressing disease, and there is currently not much data available about the long-term natural history of macular pigment density. Secondly, supplementation with Lutein and Zeaxanthin showed no change of central accumulation in two independent studies. [54, 93]

2.4.1 Limitations

A limitation of this study is the limited number of available Pelli-Robson charts which might have led to a memorizing effect. We tried to reduce this bias by alternating and testing first under mesopic and then under photopic conditions. Also, the finding in eyes with no or only very early changes might be of mere anecdotal nature. Only further studies will help reveal if the effect is indeed reproducible. Unfortunately, not many of those cases have been identified yet.

Another important limitation is that I have not adjusted for possible bias inducing factors such as sex or the presence of comorbidity, most notably of diabetes. A recent study suggested a possible association of MacTel with sex hormones, thus a possible role of sex as a confounding factor should ideally be acknowledged. [94] As already mentioned in the introduction, it is known that diabetes can affect contrast sensitivity and this might thus have influenced the results. For future studies, sex and diabetic status should be recorded and accounted for by creating a control group which are also matched in sex and diabetic status.

2.5 Conclusion

Overall, our results underscore the importance of background light levels for the visual performance in patients with MacTel. Their contrast perception is impaired, and even more so in low light levels. The impairment of contrast vision under reduced light conditions might be correlated to loss of macular pigment optical density as a pathognomonic finding in MacTel. Our results suggest that even eyes without impairment in visual acuity testing and/or without morphological changes might already show impaired contrast sensitivity. Although we were not able to pinpoint the functional loss to a particular structural or cellular dysfunction, the applied tests have the advantage to be well established, cost-effective, quick and easy to perform. They would, therefore, qualify to be used as additional functional assessments both in clinical routine and potentially as outcome measures in future interventional clinical trials.

Chapter 3

Scotoma characteristics

3.1 Background

3.1.1 Relevance of scotomas

Functional impairment in MacTel typically starts in the fifth or sixth decade of life with reading problems or, less frequently, metamorphopsia as first symptoms. [95] Visual dysfunction in earlier stages is dominated by the occurrence of a paracentral visual field loss ("scotoma") rather than loss of visual acuity. It is assumed that best-corrected visual acuity decreases drastically once the scotoma reaches the foveal center. [42, 73] It was suggested that the presence of paracentral scotomas gives rise to prefixational blindness when occurring bilaterally, affecting the central four degrees of the visual field, which is required to sufficiently process words and perform adequate eye movements for efficient reading. [71] Loss of parafoveal sensitivity thus has a detrimental effect on reading performance when best-corrected visual acuity might be relatively preserved until late disease stages. Reading performance thus was suggested to better reflect visual performance in MacTel. [42, 70] There seems to be usually only one scotoma per eye, and the scotoma always seems to affect the temporal parafoveal area, supporting the idea of predilection of this particular zone. The scotoma seems to have fairly steep borders [40, 42, 73] Once an absolute scotoma emerges, it is very likely to grow. [42] There is evidence that the scotoma may not exceed the so-called “MacTel area,” an oval-shaped area of 2 disc diameters centered on the foveola. However, there was no systematic analysis

to corroborate evidence for such an endpoint of scotoma growth. To have defined borders of a scotoma is important in order to use scotoma growth as an outcome measure for investigational trials - the steeper the scotoma is, the more reliable will the measurement be. Steep borders mean that there is only a narrow space between normal and strongly impaired, if not absent retinal sensitivity.

3.1.2 Measuring scotomas

Parafoveal sensitivity can be measured by fundus controlled perimetry (so called "microperimetry"), [73, 96]. Microperimetry has been performed systematically in five of the MacTel study centres. One major advantage of microperimetry is that it allows for point-to-point comparison with spectral-domain optical coherence tomography images. Loss of retinal sensitivity in MP correlates with loss of structural integrity in spectral-domain optical coherence tomography, in particular areas of outer retinal alterations. [97] Relative scotomas correlate with ellipsoid zone disruption, whereas absolute scotomas correlate with loss of outer nuclear layer (and associated pigment plaques). [40, 42] Only limited correlation was found between retinal sensitivity and total retinal thickness or changes in the inner retina. [97]

3.2 Methods

3.2.1 Participants

Patients were selected from the five centres of the MacTel Study which systematically performed mesopic microperimetry under standard conditions. This was the Jules Stein Eye Institute in Los Angeles, CA, USA, the Moorfields Eye Hospital in London, United Kingdom, the St. Franziskus Hospital in Münster, Germany, the Save Sight Institute in Sydney, Australia, and the University Eye Hospital in Bonn, Germany. For the retrospective analysis of scotoma characteristics, eyes with at least one gradable microperimetry examination were included. For the longitudinal structure function correlation analysis, inclusion criteria were stricter - only eyes with a minimum follow up of two years were included, and they had to have both microperimetry and high quality spectral-domain OCT scan on the same study visit. Further, microperimetry tests had to include testing points that were no more than

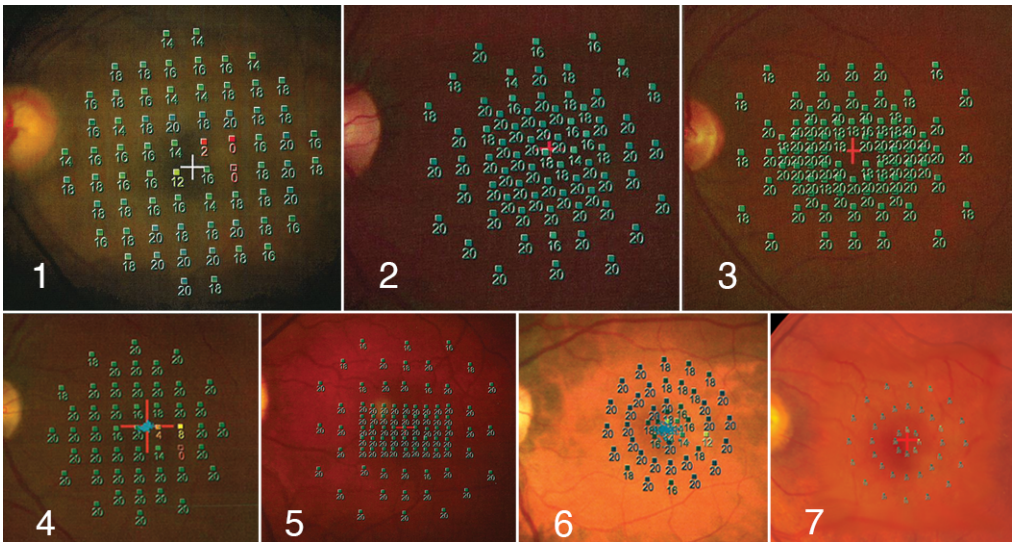

Figure 3.1: Microperimetry testing grids. This figure shows the different microperimetry testing grids used in the different sites.)

one degree apart.

3.2.2 Fundus-controlled perimetry (microperimetry)

Fundus controlled perimetry was performed with direct visualization of the stimulation of the fundus using the MP1 microperimeter (Nidek, Gamagori, Japan). The test was performed after pupillary dilatation. As fixation targets, a red cross of two degrees width was used. In subjects with very poor fixation, the cross had five degrees width. We used the device standard examinations settings (white background at 4 apostilb, Goldman III stimulus with 100ms projection time, 4-2 staircase strategy). Patients underwent five minutes of mesopic light adaptation before the test was started. Seven different grids were used, as shown in Figure 3.1.

Testing protocol details are listed in Table 3.1. In most cases, the testing grid was fixed, and the test followed the 4-2 strategy, with a fixed testing grid. One site employed a slightly different testing protocol, though: The test was finished with a dense grid (Figure 3.1, "grid 5") and a 4-2 threshold strategy. After finishing, additional stimuli were placed at the border of the dense grid to outline the scotoma area, if the last dense stimulus of the dense grid was touched by a dense scotoma. The duration of the test was graded in 5-minute intervals (i.e., 0 minute to 5 minutes,

Grid	n	Number of testpoints	Width	Typical duration	Tests with absolute scotoma
Grid 1	17 (3%)	68	18	15-20	50%
Grid 2	109 (19%)	69	16	10-15	57%
Grid 3	53 (13%)	86	16	15-20	49%
Grid 4	51 (9%)	49	16	5-10	41%
Grid 5	178 (32%)	83-100	16	10-15	46%
Grid 6	45 (8%)	45	12	10-15	46%
Grid 7	112 (20%)	40	10	5-10	52%

Table 3.1: Microperimetry testing grids used in the MacTel Study

5 minutes to 10 minutes, etc.).

Printouts of the tests were sent to the Moorfields Eye Hospital Reading Centre, London, UK. As this was a retrospective study, there were a variety of different testing patterns, because each site adhered to slightly different testing protocols - most importantly different testing patterns. Thus, comparability between those tests was limited. Three parameter were examined that we considered independent of the use of different testing patterns:

- The number of independently developing scotomas (scotoma foci) in each eye. One scotoma focus was defined as contiguous scotoma test points without healthy retina in between. Healthy retinal sensitivity was considered at a sensitivity of 14 dB and higher. The rationale for this definition was based on the results of previously reported test-retest measurements in this device. [98]

- The size of the scotoma was estimated with a simple thresholding strategy, by counting the number of testing points with relative and absolute sensitivity loss. Thresholding has been shown to give comparable results to analysis of scotoma volume (aggregate sensitivity loss). [39] An absolute scotoma was defined as a retinal location on which the brightest test stimulus could not be seen. In the MP1, this is a functional loss of at least 20dB (2 log units) when compared with a healthy retina. Functional impairment was defined as the location at which a stimulus of 12dB or lower was not seen. equivalent to a

sensitivity loss of 8db (0.8 log units) or more. Further, the number of points with 10dB or 8dB and lower was counted. This is demonstrated in Figure 3.2

- The steepness of the scotoma was estimated by calculating the ratio of test points with relative and absolute scotoma, i.e.

  $$Steepness = \frac{Number\ of\ relative\ scotoma\ testpoints}{Number\ of\ absolute\ scotoma\ testpoints}.$$

  A ratio of one would suggest a maximum steep scotoma, and an increasing ratio would would suggest an increasing border of relative scotomas around the actual absolute scotoma, thus less "steepness".

- For the longitudinal structure function correlation, the number of testing points with absolute and relative scotoma was counted. Previous work has shown that functional loss and structural loss correspond well, [40, 41] thus we forewent the exact alignment and simply counted the numbers of scotoma test points, which we compared with the area of ellipsoid zone loss as measured by spectral domain OCT (see there).

3.2.3 Measurement of the ellipsoid zone loss

Spectral domain OCT was performed with Spectralis HRA+OCT (Heidelberg Engineering, Heidelberg, Germany). A high density SD-OCT so called "volume scan" was recorded covering 15 degrees horizontally and 10 degrees vertically with 97 B-scans with a space of 30µm in between. These volume scans were used to generate *en face* images (C-scan), based on which the ellipsoid zone loss was measured, as following:

- The set of OCT-volume scans were automatically segmented into 'all layers' using the manufacturer's software (Heidelberg Eye Explorer, version 6.0.13.0, Heidelberg Engineering, Heidelberg, Germany).

- erroneous segmentation was manually corrected. If a layer was not present, e.g., when the outer nuclear layer or the ellipsoid zone layer was not visible, the segment followed the assumed projection in an otherwise normal retina.

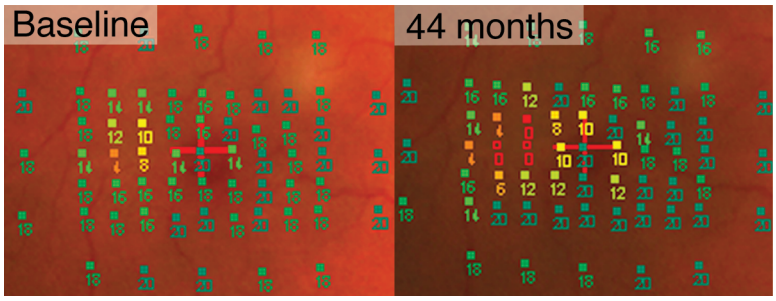

Figure 3.2: Scotoma development detected by microperimetry. Each square represents one test stimulus; the number below the point shows the retinal sensitivity in decibel (dB). Normal values: 20 dB to 14 dB. Relative scotoma: 12 dB to 0 dB (filled square). Absolute scotoma: 0 dB (empty square). At baseline, the patient shows a relative scotoma temporal to the foveal center. Different thresholds were chosen for scotoma counting (*thresholding*). Four stimuli are 12 dB and lower, three 10 dB and lower, and only two 8 dB and lower. No absolute scotoma is seen. After 44 months, the relative scotoma has deepened into a small absolute scotoma (2 stimuli). The area of relative scotoma has increased markedly. Fourteen stimuli are under 12 dB, 10 under 10 dB, and seven under 8 dB.)

- manual correction was limited to the segment of interest, called "PR1" (photoreceptor 1) in the manufacturer's software.
- afterwards, the scan was viewed in so called "transverse display", resulting in *en face* visualisation of the volume scan, i.e., a C-scan.
- The PR1 was set as reference for the en face view and the distance to a second line was set to 0, resulting in a thickness of the layer of one pixel.
- The color table for the OCT image was set to 'White on Black' which resulted in a darker area for ellipsoid zone loss.
- The 'draw region' tool in the same software was used to draw an outlay around the darker area of suspected ellipsoid zone loss within the *en face* panel.
- The position of the overlay was checked in each B-scan (where the edge of

the overlay was shown). If the edge of the overlay did not correspond with the edge of ellipsoid zone loss, the correct position of ellipsoid loss was marked within the en face image.

- Only areas with complete absence of ellipsoid zone on the B-scan were taken into account.
- A new overlay was drawn following the markings within the image.
- The last two procedures were repeated until a satisfactory correspondence between the ellipsoid zone loss border and the overlay was achieved. Usually, not more than two runs were necessary.
- If an eye had multiple areas of ellipsoid zone loss, they were added together to a single value.

3.2.4 Modelling growth of ellipsoid zone loss

- In the following section, the term "growth" is used as a shorthand for *growth of ellipsoid zone loss*.
- Eyes with no growth (one eye) and eyes with negative growth (four eyes) and eyes with no ellipsoid zone loss at follow up time (four eyes) and eyes with large neovascular membranes (one eye) were removed for this exploratory analysis, with 46 eyes of 29 patients remaining
- The Eyes were arranged by increasing size of ellipsoid zone loss at baseline.
- The growth rate per day of ellipsoid zone loss was estimated for each eye separately based on the difference between follow up and baseline, assuming a linear growth during that time.
- Eyes were binned into arbitrary steps of baseline ellipsoid zone loss and the mean rate of growth was calculated for each bin.
- The number of days until reaching the baseline ellipsoid zone loss from the next eye was estimated based on this average rate.

- The resulting days were added cumulatively to the days calculated for the previous eyes.

- Ellipsoid zone loss was then plotted as a function of cumulative days (Figure 3.8).

Based on the expectation of MacTel having a natural "growth saturation", we can assume a logistic growth. Logistic growth can be expressed with the four-parameter model

$f(x) = \frac{Maximum\ ellipsoid\ zone\ loss}{1+e^{-k(x-x_0)}}$, where x_0 is the midpoint of the sigmoid (the point of fastest growth), and k is the logistic growth rate or steepness of the curve. The *nls* function from the *stats* package in R was used to fit this non-linear logistic growth model to the data obtained in the steps outlined above.

Both progression of ellipsoid zone loss and scotoma progression were defined as continuous variables, in numbers of pixels (ellipsoid zone loss) converted to square millimetre with a scaling factor of 1 pixel = 30 μm^2, and number of test points for scotomas. Progression of absolute scotomas or areas of functional impairment was defined as increase in number of test points $\leq$12dB or <0dB in microperimetry, indicating a deterioration in the retinal function. Decrease in best-corrected visual acuity was expressed as numbers of letters loss. Intrarater variability between two ellipsoid zone loss measurements on the same OCT volume scans was approximately 1000 pixel (approximately 0.03mm^2).

3.2.5 Statistical analysis

Statistical analysis was done with R. [83] Intrarater agreement was estimated with the Pearson correlation coefficient. Correlation between growth of ellipsoid zone loss and increased area of functional impairment was assessed with linear mixed models using the *nlme* package. [82] Each model included a random intercept for subjects and a fixed term for eyes. The results from those models are presented by showing the fixed effect term b which indicates the mean increment in the studied phenomenon for a unit change in the the condition of interest. A p-value < 0.05 was considered as significant.

3.3 Results

3.3.1 Participants and baseline characteristics

Data was received from 628 eyes of 316 participants (age 61.1 ± 9.1 years, 59% females). Of those, 559 eyes of 294 patients had at least one gradable test for scotoma characterisation. A total of 56 eyes of 31 participants fulfilled inclusion criteria for the longitudinal structure-function analysis (mean follow-up time was 4.5 years (SD 1.2 years, range 2.3 - 7.6 years). One eye was excluded due to the development of a large neovascular membrane. At baseline, absolute scotomas had a mean size of 3.3 testpoints (SD 6.1, range 0-33), and mean area of functional impairment was 8.9 test points (SD 11.1, range 0 - 55). Mean area of ellipsoid zone loss was 18600 pixel, (SD 25339, range 0 - 124243), approximately equivalent to 0.6 mm^2 (SD 0.8, range 0 - 3.7).

3.3.2 Scotoma characteristics

Scotomas were present in 239 eyes (43%). The scotoma affected the four quadrants around the foveal center as follows: Temporal field: 233 (97%), inferior field: 103 (43%), superior field: 76 (32%), and nasal field: 37 (15%). Only one eye (0.4%) with scotoma showed two scotoma foci, rather than only one. This means, that practically all scotomas were unifocal and were affecting the temporal parafovea. Scotomas did not exceed an area of five times eight degrees of the central retina, thus limiting growth of absolute scotomas to an area of approximately 40 square degrees.

MacTel scotomas are steeply sloped. Although transition from functionally unimpaired retina to absolute scotomas was generally steeply sloped, larger scotomas were comparatively steeper than smaller scotomas. Figure 3.3 demonstrates how the area of functional impairment is comparatively much larger than the area of absolute scotomas, when looking at small scotomas. With increasing size of absolute scotoma, this size difference becomes relatively smaller, approximating the same size when reaching an absolute scotoma size of 30. This suggests that the area of absolute scotoma "catches up" with the area of functional impairment.

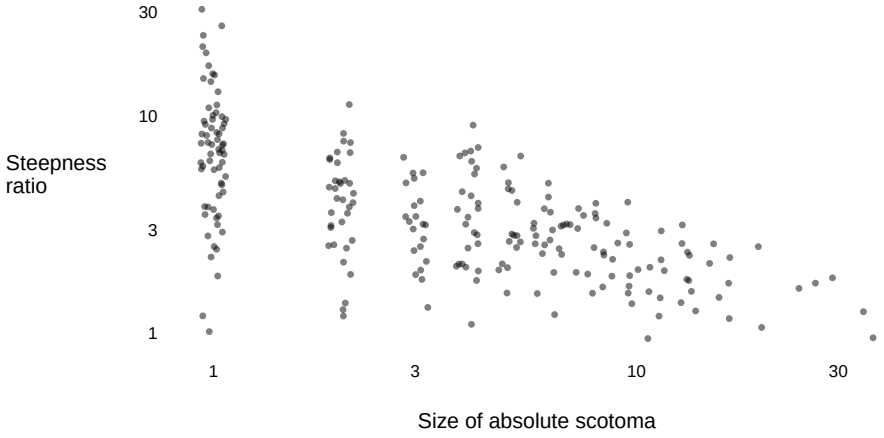

Figure 3.3: Steepness ratio was calculated by dividing the number of stimuli with impaired retinal sensitivity by the number of test points with absolute scotoma, a ratio of one meaning the same area.

Thus, MacTel scotomas seem not only to grow (up to a saturation point), but also to "deepen".

Those scotoma features were consistent throughout a large MacTel cohort with different disease stages. The temporal quadrant was always almost affected, however advanced the disorder, contrary to the nasal parafovea which was often spared.

Figure 3.4 shows the empirical cumulative distribution function of scotoma sizes in a subgroup of 169 eyes with the densest grids (Grids 2, 3, 5 and 6) that allowed calculation of affected retinal area.

The majority of eyes (approximately 80%) had scotomas of less than 10 test points in size, and the vast majority (95%) had scotomas not exceeding 15 test points. there was no scotoma with more than 40 test points in the entire sample, independent of the grid used. This supports the hypothesis of a limitation of scotoma growth to an area of 40 square degrees, equivalent to the central five times eight degree of the "MacTel area" (chapter 6).

3.3.3 Progression of ellipsoid zone loss versus scotomas

There was high inter- and intrarater agreement for ellipsoid zone loss measurements. Figure 3.5 shows the plotted scaled values, demonstrating the high agreement.

Progression of ellipsoid zone loss correlated well with relative and absolute

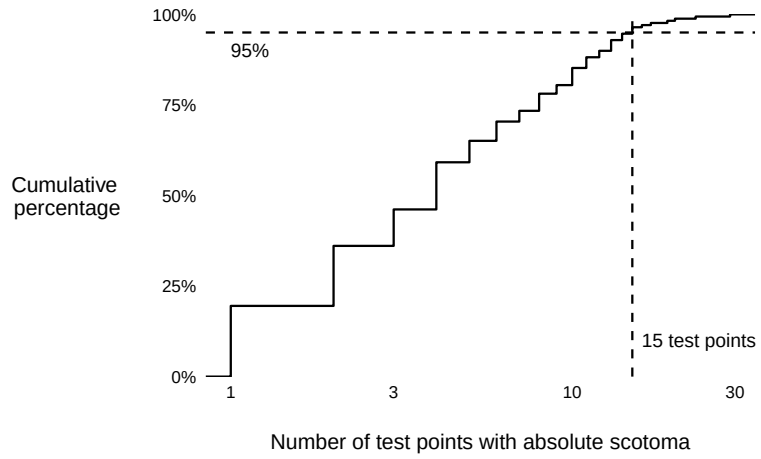

Figure 3.4: This is the empirical cumulative distribution of the number of test points with absolute scotomas in eyes tested with a dense central grid. The majority of eyes (95%) had scotomas of less than 15 test points in size

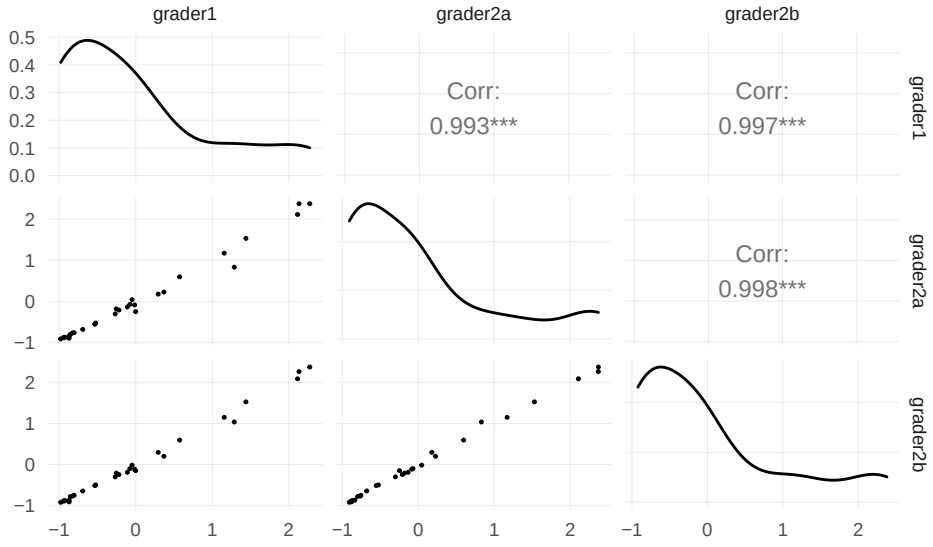

Figure 3.5: Demonstrating scaled values (z-scores). The upper right panels show the Pearson correlation coefficient, diagonale middle panels show density distribution of measurement values, lower panels show values plotted against one another. Asterisks indicate statistical significance p<0.001

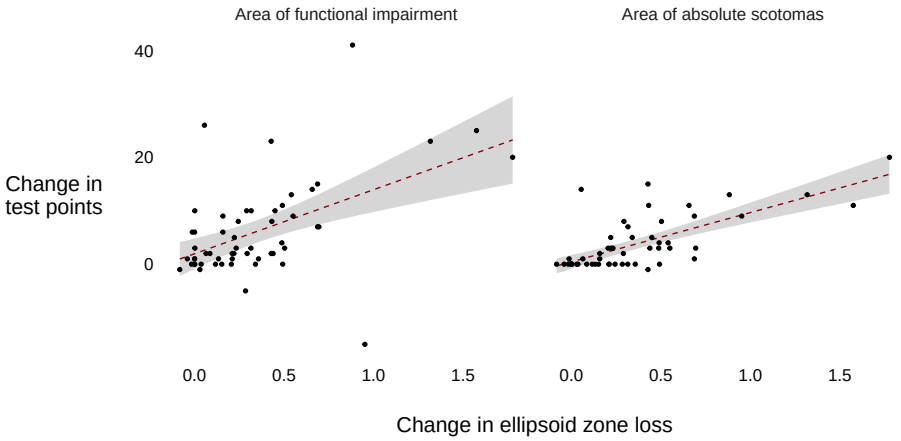

Figure 3.6: Scotoma growth as a function of ellipsoid zone loss

scotoma progression (Figure 3.6).

For each unit increase of ellipsoid zone loss there were approximately nine more scotoma test points (b = 8.9, p-value < 0.001). This correlation was confirmed when comparing the location of scotoma and ellipsoid zone loss topographically (Figure 3.7). Here, ellipsoid zone loss corresponds rather to a generally impaired retinal function than absolute loss of functions - the area of impaired function increases and corresponds to the area of ellipsoid zone loss, whereas the number of absolute scotomas changes less. In the case of Figure 3.7, best corrected visual acuity remained stable at a Snellen fraction of 6/15. Figure 3.7 also shows a small area of ellipsoid zone loss regression. This might be due to a real improvement, but might be resulting from structural changes with influence on OCT reflectivity. B-scans of baseline and month 44 area show an irregularity in the ellipsoid zone layer at this position and an overall thicker retina, maybe due to minor retinal edema, which favours the idea of a structural alteration rather than a real improvement, which could in turn influence the strength of the ellipsoid zone signal.

3.3.4 Model estimating ellipsoid zone loss:

The "model disease projection" was estimated as $f(x) = \frac{3.58}{1+e^{-11.6(x-18)}}$. The predicted disease mid point would be around 18 years, where speed of scotoma growth is at its maximum (Figure 3.8, left panel). The asymptote, or growth saturation, can be better visualised on a logarithmic scale (Figure 3.8, right panel) - maximum of

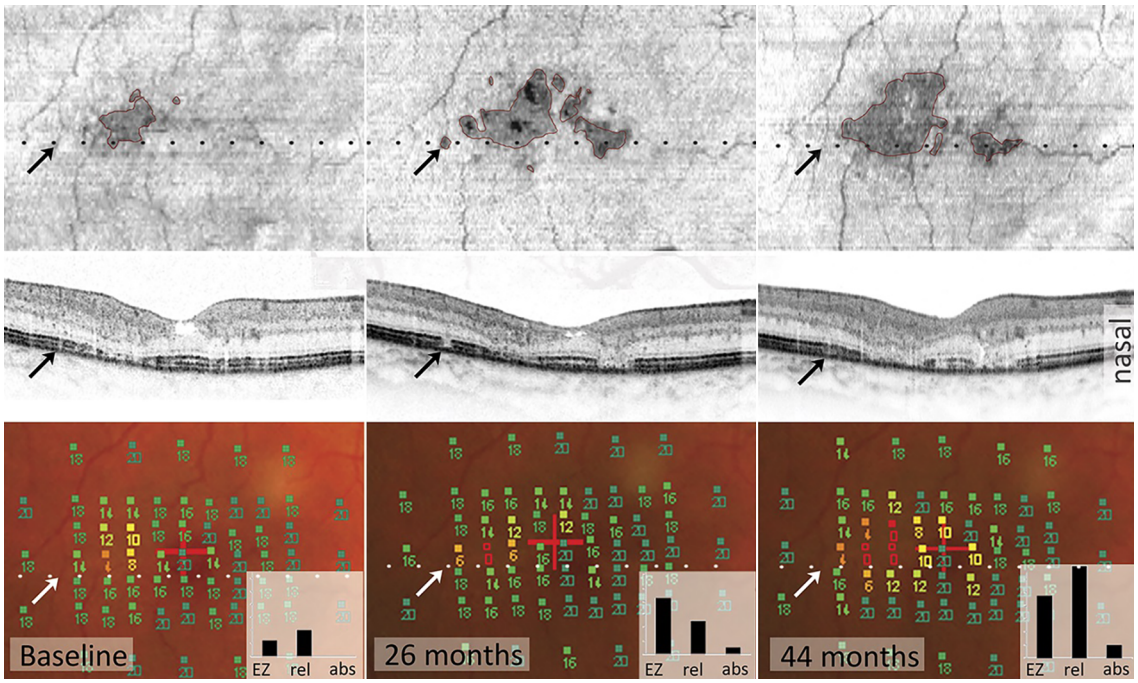

Figure 3.7: Topographical correlation of functional loss and ellipsoid zone loss. Disease progression of Macular Telangiectasia type 2 seen on spectral domain optical coherence tomography (OCT, first and second row) and microperimetry (*bottom row*). Areas of ellipsoid zone (ellipsoid zone) loss appear dark in en face images (outlined in purple, showing the outline as created in the Heyex viewer, Heidelberg Engineering, Heidelberg, Germany). The dotted black and white lines show the position of the B-scan (middle row). Each square in MP images represents one test point, shown with the respective retinal sensitivity in dB next to it (normal sensitivity:14-20dB, impaired sensitivity: 0-12dB, absolute scotoma (empty square): <0dB. The graph inlets show the estimated affected retinal area in square degree, based on ellipsoid zone loss (ellipsoid zone), number of test points with impaired function (rel) or absolute (abs) scotoma. The black and white arrows point to an area of ellipsoid zone loss which seems to fluctuate over time.

ellipsoid zone area loss was estimated at approximately 3.6 mm^2.

3.4 Discussion

There is only one scotoma per eye which slowly grows. The analysis of this large cohort confirmed findings from a previous study on a subgroup of this cohort. [42] This scotoma is very near to always found temporally to the fovea, corroborating the notion of MacTel being a disease with temporal epicenter. [73] This is such a characteristic feature that it might indeed be suggested as a diagnostic criterion for MacTel. No eye showed two separate absolute scotomas with completely healthy retina in between. However, rarely, an area of relative scotoma can show two dips into absolute scotoma, usually one dip being temporal and the other nasal of the fovea. The temporal predilection is not fully understood, and vascular asymmetry has been suggested, maybe something akin to a "watershed area".

Scotomas in MacTel are not only limited to a specific area, but they also have steep borders, and this steepness is related to the size. Large scotomas are steeper edged than smaller scotomas. A possible explanation for this observation might be that relative impairment precedes absolute functional loss and might delineate diseased areas time before it fully deteriorates. Thus, in earlier stages, when there is larger areas of relative functional impairment and only little absolute scotoma, the ratio between both is large, and the scotoma border less steep (Figure 3.3). In later stages, the absolute functional loss fills the potentially diseased area more, leaving less area of only relatively impaired retina, thus the ratio is decreased, and the scotoma edge is steeper.

Both ellipsoid zone loss and scotoma growth seem to be suitable parameters to monitor disease progression in MacTel. Both show a slow progression in most eyes and they are both reasonably well correlated. It has already been shown that best-corrected visual acuity is only limited useful to monitor disease progression, as it is slower and more granular when compared with scotoma monitoring. [42] Moreover, visual acuity is impaired only late in the disease course, mainly due to the disease epicentre temporal to the fovea. In fact, nearly all eyes with a scotoma

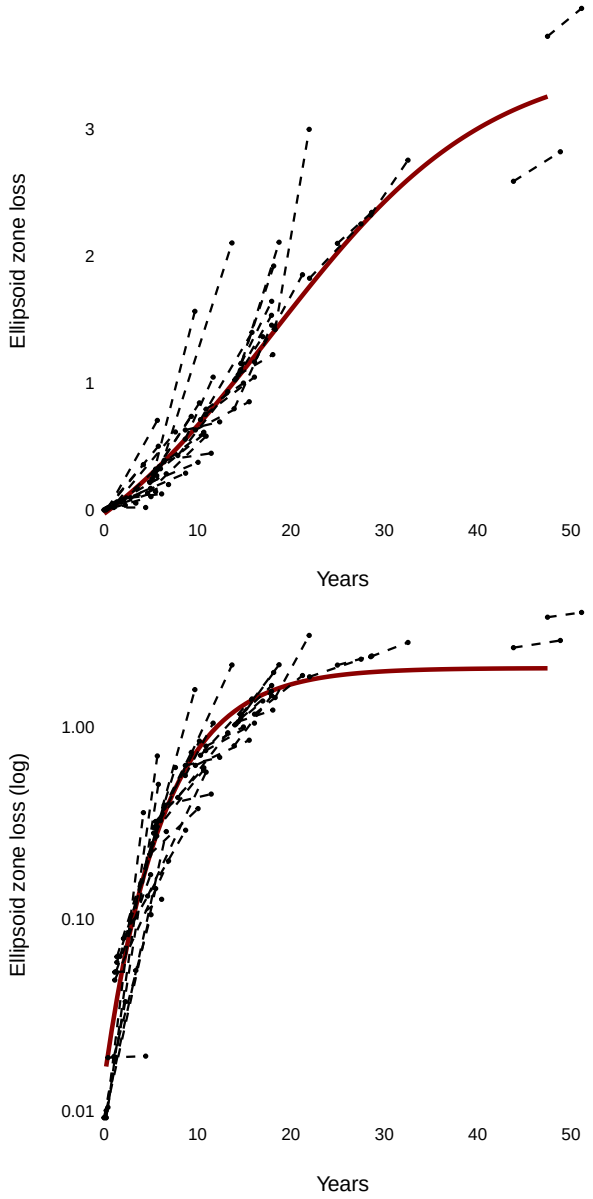

Figure 3.8: Model fit for growth of ellipsoid zone (EZ) loss. Upper graph: Non-transformed data, with a four-parameter logistic growth model. Lower panel: Log-transformed data with an asymptotic growth model. Each dot pair of dots that are linked with a dashed line represent the baseline and last follow up measurement of EZ loss over time in one eye. The x position for a baseline measurement M was determined by estimating the time it would take from the eye with the nearest lower (baseline) EZ loss to reach the EZ loss M with an average growth rate of EZ loss that was calculated for arbitrary bins of baseline EZ loss (bin size 0.5mm^2).

showed functional loss temporal to the fovea, whereas the majority of eyes did not show nasal impairment.

Comparing microperimetry results with published reports is challenging because of the variety of different test protocols used, e.g., different machines, different testing grids, and of course different statistical methods which can be quite daunting in visual field analysis due to the extensive autocorrelations. Thresholding seems a fairly simple approach where the challenges of autocorrelation are reduced (because we obtain only a single value per eye), and a comparison with other studies with similar parameters seems reasonable. The overall cohort showed a similar rate of scotoma growth as a previously published cohort. [42] This smaller cohort was part of the overall cohort, but it is reassuring that this subgroup did not show different growth rates. The growth rate approximates one new scotoma test point per year, equivalent to approximately one square degree of retinal area.

Results of ellipsoid zone loss can be more easily compared with results from other studies, because the methodology used is more reproducible - less of the "psycho" part of the psychophysical test method here, and one would expect more "objective". Challenges in comparing results of ellipsoid zone loss arise from different machines and software used, which employ different scalings of their data. The progression of ellipsoid zone loss in this study ($0.08mm^2$) was overall not as marked as suggested by Sallo et al. in a previous study ($0.14mm^2$). [40, 41] This difference might have arisen merely from a different constant for pixel-to-area conversion, but it might be due to the different inclusion criteria: Sallo et al. included only eyes that already showed ellipsoid zone loss at baseline whereas this study included all eyes regardless of presence of ellipsoid zone loss. Including eyes with no ellipsoid zone at baseline might therefore lower the overall mean - the arithmetical average is quite dependent on extreme values.

One eye in our sample showed a clear reduction of ellipsoid zone loss. In a recent study with adaptive optics imaging technology, an reduction of the ellipsoid zone loss has been demonstrated. More importantly, this study demonstrated the presence of photoreceptors in areas where spectral domain OCT showed ellipsoid

zone loss. [99–101] Ellipsoid zone loss does not reflect presence of photoreceptors but rather seems to reflect an altered reflectivity, e.g., due to a sort of misalignment. This might be a structural change within the photoreceptors (most likely of the cones) altering the directionality of the light guidance which could change the optical OCT signal. This also might explain presence of visual function in areas of ellipsoid zone loss, albeit impaired. [99] It is unclear whether rod or cone function is more impaired in areas of ellipsoid zone alteration, as this would require single photoreceptor testing which is not possible with rods as of yet. However, earlier studies showing more pronounced loss of rod function than cone function, and a striking correlation of ellipsoid zone loss with rod photoreceptor loss hint to more advanced rod loss in areas of impaired ellipsoid zone. [92, 102–104] An overall decrease of ellipsoid zone loss, however, occurs only in a relatively small percentage of cases and the effect might be negligible. The good longitudinal correlation of ellipsoid zone loss with functional loss in microperimetry suggests that ellipsoid zone loss appears to be reliable and reproducible as an objective measure of disease progression. The results indicate that ellipsoid zone loss might even detect disease progression more precisely than microperimetry because smaller changes are identified, which might justify ellipsoid zone as a potential surrogate outcome measure in investigational trials.

Chapter 4

Binocular inhibition of reading

4.1 Background

Reading is an important part of our lives. It facilitates participation in social activities, allows for education, and increases the availability of information. Most technical tasks require at least a minimal ability to read. Reading is a complex physiological event which requires intact retinal and cerebral function. For fluent reading, an intact central visual field of approximately five degrees is required. [71] More importantly, the location of visual field defects has an impact on reading function as well. [105] In MacTel, scotomas develop, that are mainly located temporally to the fovea (chapter 3), affecting reading function more than best corrected visual acuity testing would suggest. [70] Further, paracentral scotomas were shown to be associated with impaired stereoscopic vision. [10] As detailed in chapter 3, scotomas can be measured and visualised with microperimetry. Reading performance is associated with the presence of scotomas. [70] This has been shown by testing each eye separately. However, most people do not shut one eye when reading, i.e., reading is in general a binocular activity. Binocular reading performance has not yet been systematically investigated in MacTel. This is relevant, because visual performance can differ when performed with only one eye or with two eyes. Commonly, binocular function is compared with monocular function of the better seeing eye, and the difference is called binocular gain. [106] If binocular function is better than monocular function, binocular gain is positive and may also be called binocular

summation, or else it is negative and may be called binocular inhibition. Binocular summation is a well-known phenomenon in visual acuity testing, [107] but there is currently no compelling evidence for binocular summation in reading. [108–110] Scotomas in MacTel are typically non-homonymous (i.e., they don't correspond in their location in the visual field). With non-homonymous scotomas, one might expect binocular summation, because the missing information from one eye should be mutually compensated by the other eye. Interestingly, patients with MacTel frequently report that reading is easier with one eye closed (unpublished personal observation). This might arise from so called *binocular rivalry*, where the missing information from one eye interferes negatively with the other eye. This study was performed to investigate the presence of binocular inhibition in MacTel.

4.2 Methods

4.2.1 Participants

Patients were recruited from a single center of the MacTel study (University Eye Hospital Bonn, Bonn, Germany). They were consecutively recruited from the participants enrolling in the study, and those coming in for their annual visit. Exclusion criteria were extra-foveal or unstable fixation (as defined by fewer than 75 percent of fixation points falling within a 4-degree circle in microperimetry) and dyslexia. Best corrected visual acuity was measured with the ETDRS protocol, reading acuity and reading speed were tested monocularly and binocularly. Macular retinal sensitivity was examined with microperimetry. Scotomas were quantified by their size, their depth, and their proximity to the fovea.

4.2.2 Testing reading function

Reading acuity and reading speed were assessed monocularly and binocularly with Radner reading charts. Standard Radner reading charts were used at a test distance of 40 cm and with best-corrected refraction for this distance. We used three different charts in order to test binocular reading, followed by monocular reading with the right eye and then with the left eye. The test sentences were covered with cardboard, and the investigator asked the patients to read each sentence aloud and

without interruptions or corrections as soon as it was uncovered. Reading time was measured, and reading speed in words per minute (wpm) was calculated according to the manufacturer's instructions. Reading acuity was determined as the smallest print size at which the patient was able to read the sentence in less than 20 seconds, factoring in reading errors as proposed by the manufacturer. It was measured as logarithm of reading acuity determination (logRAD). Reading speed between two eyes of one patient was defined as different when they were more than 25 words per minute apart, and reading acuity when more than 0.1 logRAD apart, corresponding to the reference range of test-retest variability. [111]

4.2.3 Microperimetry and scotoma quantification

Macular sensitivity was assessed in each eye separately with the MP1 microperimeter (Nidek Technologies, Padua, Italy). In short, the test was conducted under mesopic light conditions with dilated pupils with a test grid of 83 test stimuli (Goldmann size III, 4-2 strategy, $1.27\frac{cd}{m^2}$ background illumination, stimulation time 100ms) within the central eight degrees of fixation. In particular, the central four by eight degrees were covered by a grid of five rows of nine test points per row, each row and point being one degree apart, thus resulting in a regular grid of 45 test points with the central row going through the foveal center. The stimulus intensity ranged from 0 to 20dB. A fixation target (red cross, two degrees in size) was provided and fixation stability was monitored. Importantly, the device allowed for placement of additional stimuli after finishing the examination with the above specified grid. In case a scotoma reached the margin of the central dense grid, we added further testing points (approximately one degree apart) around the scotoma. This procedure was repeated until we were able to outline the scotoma with a fringe of normal retinal sensitivity, allowing to define the full extension of the scotoma and to limit the analysis of testing points to the central grid (Figure 4.1).

Scotoma size was defined as the largest horizontal diameter of the scotoma. It was obtained by counting the number of scotomatous points in the central row of the testing grid – thus reflecting the maximum horizontal diameter in retinal degrees as each testing point was one degree apart (Figure 4.1). The largest horizontal diameter

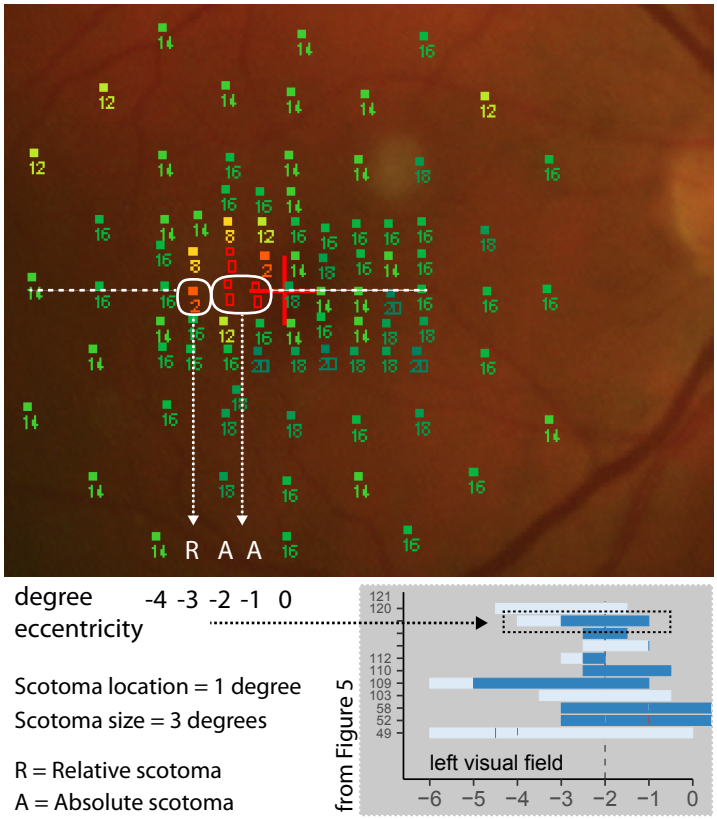

Figure 4.1: Method for scotoma quantification. Additional testing points were added to the custom testing grid if the scotoma abutted the margin of the central dense testing grid. Scotoma depth was defined by the testing point with the lowest sensitivity. In this case, the eye was graded as "absolute scotoma".

was found in the central row of testing points in most cases and we assumed it was suitable as a scotoma measure, because in MacTel, scotomas are typically monofocal and continuous (see chapter 3). Relative and absolute scotomas (see below) were considered equal for quantification of scotoma location and size. *Scotoma location* was defined as the retinal location in degree of the nearest scotomatous point to the foveal center (Figure 4.1). *Scotoma depth* was graded in three categories based on the lowest sensitivity value encountered in the exam, instead of using sensitivity as a continuous variable. This means, an eye with a single test location with an absolute scotoma would be graded as 'absolute scotoma' for the analysis, by virtue of this single test location. For linear regression, those categories were dummy coded (no scotoma = 1, relative = 2, absolute = 3). This approach was cho-

sen due to the reduced dynamic range of the MP1 device, resulting in both strong ceiling and floor effects. Moreover, there is a 97% chance that pointwise sensitivity would fall in a range of 6 dB at retest. [98] The grading of presence of relative versus absolute scotomas was similar to a "local defect classification", comparing the tested sensitivity with a normal sensitivity range. [98] A relative scotoma was defined as retinal sensitivity lower than two standard deviations (SD) from an average sensitivity in healthy observers. We used previously published normal values (mean 18.62 dB, SD 3.1 dB) creating a cut-off value for relative scotomas of 12 dB and lower. [112] An absolute scotoma was defined as a test location where the brightest stimulus of the device was not perceived by the observer.

4.2.4 Statistical analysis

Statistical analysis was performed using R. [83] Paired t-tests were used for comparison of function of the better eye and binocular function. P-values were corrected for multiple testing using Bonferroni correction. To test the hypothesis that the magnitude of binocular gain might be correlated to the functional difference between eyes, we used simple linear regression models with binocular gain as dependent variable and difference between eyes as independent variable. Magnitude of binocular gain was defined as binocular functional performance minus monocular performance in the better eye. Multiple linear regression models were fitted to the data for exploration of the effect of scotoma characteristics on monocular and binocular visual performance. Model fits were compared with analysis of variance testing and based on the Bayesian information criterion. P-values of 0.05 and lower were considered statistically significant.

4.3 Results

4.3.1 Participants

Seventy-two participants were examined. Four people did not meet the inclusion criteria and were excluded from analysis. Thus, 68 participants were analysed (32 males, 36 females, mean age 62.7 years, SD 6.3; range: 52-78 years).

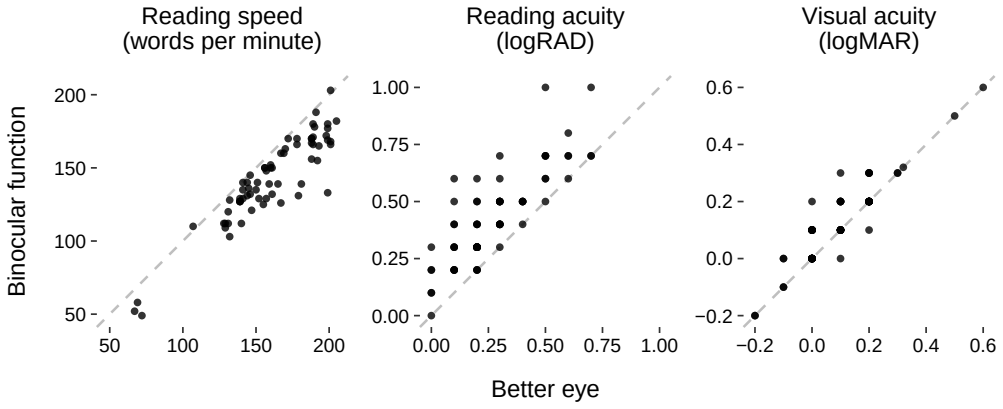

Figure 4.2: Binocular gain for Reading Speed, Reading Acuity and Best Corrected Visual Acuity. Reading performance was almost always better when performed with the functionally better eye than when performed binocularly. Visual acuity is not always worse when binocular function was tested

4.3.2 Reading function

Monocular reading speed of the better eye (mean 159.79 wpm, SD 31.07) was faster than binocular reading speed (mean 142.13 wpm, SD 29.58, $p < 0.001$; Figure 4.2, left graph). Likewise, the better eye had higher monocular reading acuity (mean 0.28 logRAD, SD 0.19) and best corrected visual acuity (mean 0.09 logMAR, SD 0.14) compared to binocular testing (mean 0.43 logRAD, SD 0.2, $p < 0.001$; mean 0.12 logMAR, SD 0.14, $p < 0.001$; Figure 4.2, middle and right graph). Although this indicated the presence of binocular inhibition (negative binocular gain) in all tested functional parameters, the difference was small for reading acuity (0.15 log units) and very small for BCVA (only 0.03 log units) and thus not clinically relevant for those measures.

The magnitude of binocular inhibition of reading speed was correlated to the interocular difference of reading speed (R^2=0.6, p<0.001; Figure 4.3, left graph). Binocular gain of reading acuity and visual acuity were not correlated to interocular differences ($R^2 = 0$ and $R^2 = 0.03$; respectively, Figure 4.3, middle and right graph). This indicated binocular rivalry as possible mechanism for binocular inhibition in reading speed, but not in reading acuity and visual acuity.

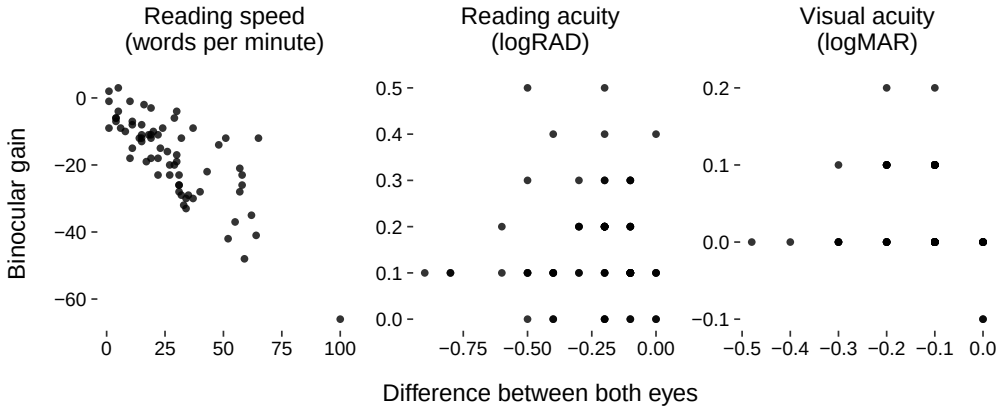

Figure 4.3: The functional difference between both eyes (interocular difference) was predictive of binocular gain in reading speed – the bigger the difference, the more negative was binocular gain – i.e. the stronger was binocular inhibition. There was no similar correlation for reading acuity or visual acuity.

4.3.3 Relation of reading function and scotomas

We therefore focused on reading speed in our exploratory analysis on the correlation of scotoma measures with binocular inhibition. Monocular reading speed in the right eye was correlated with scotoma size (p<0.001) and scotoma depth (p=0.008). This changed when including BCVA as a covariate: in this case, scotoma depth was not a significant predictor in the model. Scotoma location was not a significant predictor for monocular reading speed of right eyes in the explored linear models. Monocular reading speed in the left eye was correlated with scotoma size ($p < 0.001$) and scotoma depth ($p < 0.001$). This did not change when including BCVA as a covariate. Scotoma location was not a significant predictor for monocular reading speed of left eyes, after adjusting for scotoma size and depth and BCVA. Binocular reading speed was correlated to scotoma size and depth in the left eye, but not to scotoma parameters of the right eye, when adjusting for BCVA in both eyes (*adjusted* $R^2 = 0.81$, $p < 0.001$). The fit of regression models with and without inclusion of scotoma parameters in the right eye was not significantly different between both models. Scotoma size in the right eye was a significant predictor in the model when excluding BCVA as a covariate, but the overall model fit decreased drastically in this case. Binocular reading speed plummeted to very low values in

Figure 4.4: Binocular reading speed does not correlate with scotoma size in the right eyes in general, but there is a statistical interaction of scotoma size in the right eye and scotoma presence in the left eye - reading speed is dependent on scotoma size in the right eye only in patients with a scotoma in the left eye (left graph). Binocular reading speed correlates with scotoma size in the left eye (right graph). The dashed lines show the regression line from a simple linear regression model.

eyes where the scotoma affected the foveal center (the three dots in the bottom left of the left graph in Figure 4.2, and the bottom three lines in Figure 4.5), but scotoma location was not a significant predictor in linear regression models. Binocular gain on the other hand did not show such a strong linear correlation with scotoma measures (*adjusted* $R^2 = 0.35$, $p < 0.001$). The best model fit was achieved when including scotoma size of both eyes and, interestingly, an interaction term of scotoma size in the right eye with presence of scotoma in the left eye. This means that binocular reading speed was always correlated with scotoma presence in the left eye (Figure 4.4, right graph), regardless of presence of scotoma in the right eye. However, binocular reading speed was only correlated to scotoma size in the right eye in patients who also had a scotoma in the left eye (Figure 4.4, left graph). Scotoma location, scotoma depth, BCVA of each eye and interocular BCVA difference were tested as independent variables and discarded as non-significant.

In order to visualise the effect of scotoma measures on binocular reading speed, we plotted the horizontal scotoma size and location of both eyes on one horizontal

line for each patient and then sorted the patients along the y-axis according to their reading speed, with the fastest reading speed on top (Figure 4.5). There is an evident continuous increase of scotoma size in the left eye, but a more random distribution of scotoma sizes in the right eye.

Figures 4.6 and 4.7 shows another visualisation of the effect of scotoma measures on binocular reading speed (and binocular gain).

We created subgroups based on scotoma distribution in both eyes and ordered those groups along the x-axis according to their reading speed, the group with best reading speed being to the left. It might be possible to draw several conclusions based on this figure: (1) Decline in reading speed may correlate with the emergence of deep scotomas. Best reading speed was achieved by the person without scotoma (group 1), and reading speed fell with the emergence of absolute scotomas (groups 5 to 7). (2) Scotomas in the left eyes may have a stronger negative effect on binocular reading speed than scotomas in the right eyes (compare groups 2 with 3 and groups 5 with 6). (3) The highest degree of binocular inhibition was found in people who had a scotoma in their left, but not in their right eyes (group 3). (5) Visual acuity does not change clinically significantly between the groups (bottom graph). In those groups where scotomas were similar in both eyes (groups 1, 4 and 7), the better reading eye was almost exclusively the right eye (Figure 4.7).

4.4 Discussion

We provide evidence for the presence of binocular inhibition of reading performance in MacTel, likely due to binocular rivalry. This may result from the characteristic paracentral scotomas in non-corresponding retinal fields and, in particular, a disruptive projection of scotomas in reading direction arising from the left eyes. Patients may benefit from occluding one eye whilst reading. In this study, we observed a significantly worse outcome for binocular reading speed, reading acuity and visual acuity compared to monocular reading speed in patients with MacTel, suggesting the presence of binocular inhibition. Although statistically significant, the effect in BCVA and reading acuity were clinically negligible. The finding that

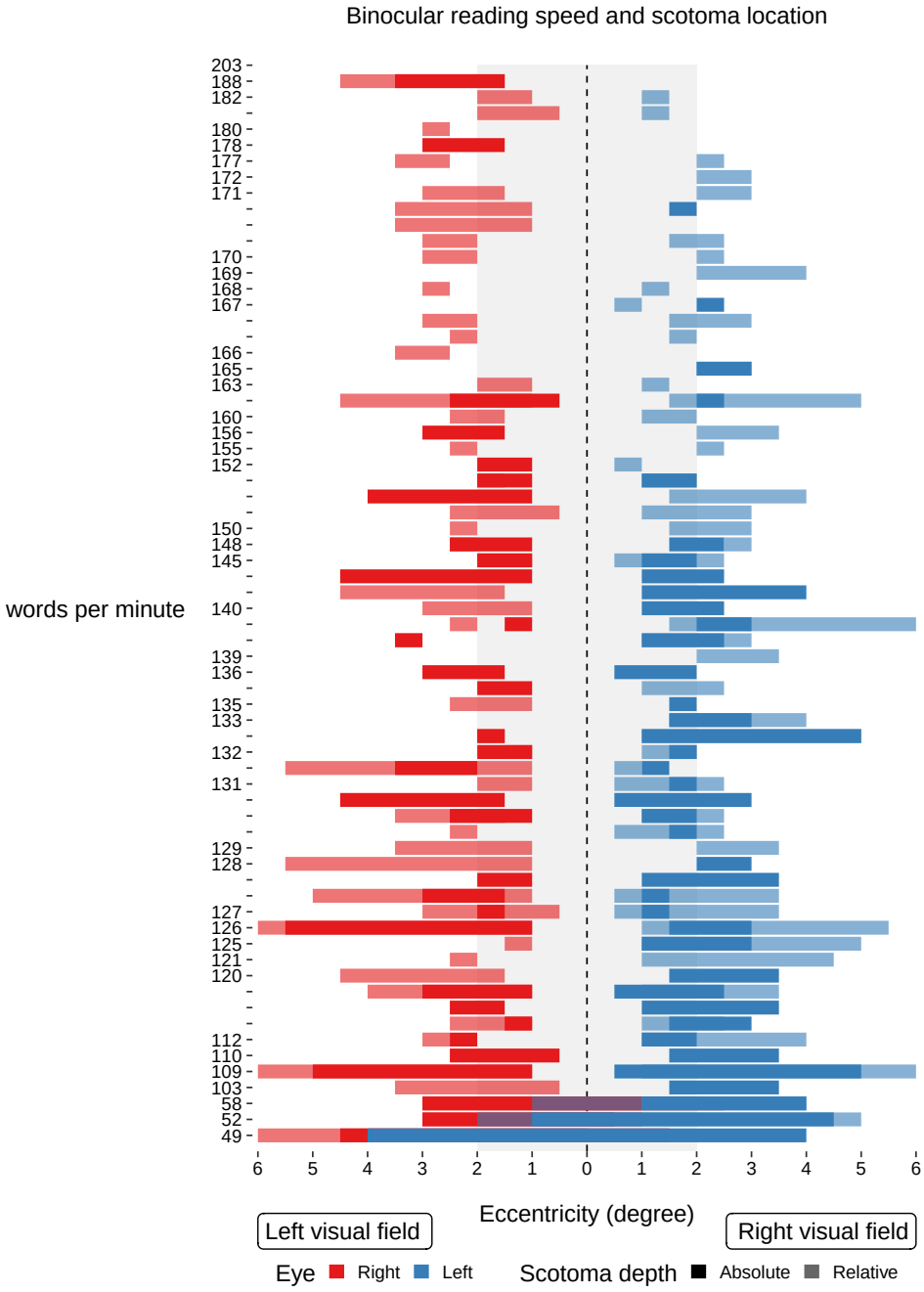

Figure 4.5: Horizontal scotoma size and location in both eyes of one patient were plotted on one horizontal line for each patient. The patients were sorted along the y-axis according to their binocular reading speed, with the highest reading speed on top. The axis does not scale to the values - axis ticks without labels have the same reading speed as the nearest lower label. Patients with the same reading speed were ranked randomly. The dashed line at 0 degree represents the location of fixation. The grey shaded area delineates the minimum visual field required for fluent reading.

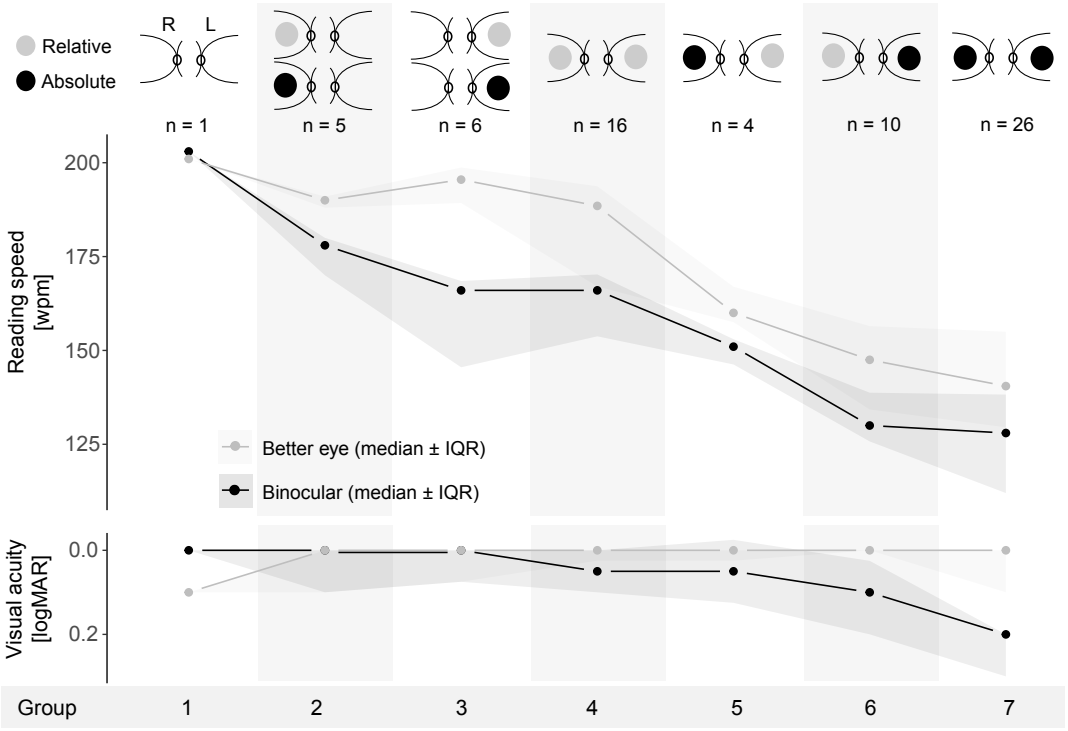

Figure 4.6: Binocular reading speed and scotoma presence. Subgroups were created based on the presence of relative or absolute scotomas in eyes. Decreasing binocular reading speed (arranged from left to right) was associated with more severe scotomas. The occurrence of absolute scotomas seemed to correlate with a drop in reading speed. E.g., group 5 shows a markedly lower reading speed than group 4. Groups with more pronounced scotoma in the left eye seemed to have generally worse function (compare groups 2 with 3 and groups 5 with 6). The difference between grey and black lines indicates the magnitude of binocular inhibition. This was most pronounced in patients with a scotoma in their left, but without scotoma in their right eyes (group 3). Visual acuity in the better eye was similar across groups, and there was no clinically significant binocular inhibition. R = right eye, L = left eye.

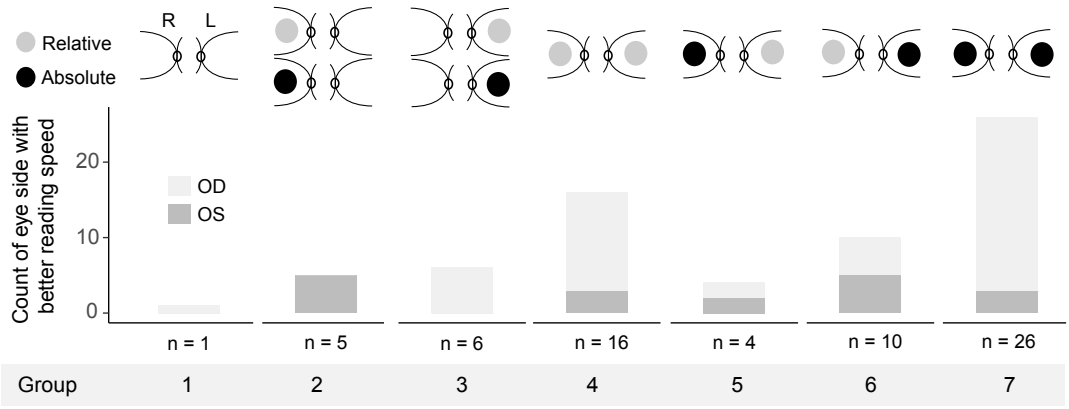

Figure 4.7: Distribution of the better eyes in each of the groups shown in main figure 4.6. In most cases, the better reading eye is the right eye. This becomes most apparent in those patients who have similar scotomas in both eyes (Groups 1, 4 and 7).

the magnitude of binocular inhibition of reading correlated with interocular differences in reading speed is suggestive of binocular rivalry. Our exploratory analysis supports the hypothesis that in MacTel, this binocular rivalry might be related to the presence and characteristics of the typical paracentral scotomas. Although the statistical modelling proved to be quite challenging due to the abundance of predictive measures and the presence of collinearity and also statistical interactions, the association of scotoma size with binocular reading speed and binocular gain was consistently present in all models. Our data strongly suggested in multiple ways that scotomas in the left eye had a stronger effect on binocular reading speed than scotomas in the right eyes. Moreover, our data suggested that the magnitude of binocular inhibition was associated with scotoma measures in left eyes, but not with scotoma measures in right eyes. An increase in scotoma size resulted in increased binocular inhibition, regardless of the presence of a scotoma in the other eye. A similar effect was not found for scotomas in the right eyes. One explanation for this could be the observation that the right eye was more frequently the better reading eye and thus binocular gain would more often depend on the reading speed in the right eye – i.e. a lower reading speed in the right eye due to the presence of a scotoma would leave less room for impact of the scotoma in the left eye to make binocular gain. On the other hand, there seems to be a larger observed effect size

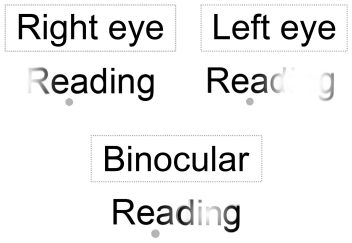

Figure 4.8: Simulation of possible monocular and binocular reading in eyes with macular telangiectasia type 2. The grey dots denote the fixation location, and can also be used as an aid for fusion of both images. The contemplator of this figure might get an impression of binocular reading vision of people with binasal paracentral scotoma due to MacTel. In the left eye, the scotoma projects in reading direction. The scotoma in the right eye is not impairing the reading field, but may impede finding the next line. The binasal scotoma results in a pre-fixational scotoma which might interfere with fusion and result in the phenomenon of 'dancing' or 'lost' letters which is often described by patients, thus challenging fluent reading.

of left eye scotomas than of right eye scotomas on binocular reading speed in patients with unilateral scotoma. This is generally in line with the concept of left eye scotomas having more impact on reading function than scotomas of right eyes.

A potential explanation for the different effect of scotomas in right and left eyes might be the relative location of the scotomas in the visual field (Figures 4.5 and 4.7). For fluent reading, a perceptual span of approximately 5° in reading direction is required in order to guide the next saccade to the following text location and organize the switch between fixation and saccades during the reading process. [71] When reading from left to right, the visual field to the right direction appears to be of higher importance for reading performance than the visual field to the left side. [113] Scotomas of the left eye are projected on the right side of the fixated letter/ word and hence in reading direction, thus interrupting the perceptual span required for reading (Figures 4.5 and 4.7). Interestingly, in our sample, left eyes had generally lower reading speed than right eyes, which would be in keeping with this idea (Figure 4.7). Accordingly, Sunness et al. have found a trend to

higher reading speed in patients with AMD when they were fixating to the right of their scotoma (resulting in a free visual field to the right). [105] Scotoma presence and size might not be the only relevant factors for binocular reading speed and binocular inhibition in MacTel. In a previous study, Kabanarou and Rubin were unable to provide evidence for binocular gain (summation or inhibition) in eyes with scotomas due to age-related macular degeneration (AMD). [114] It is not trivial to explain this difference between AMD and MacTel. A possible explanation might be the non-homonymous, bi-nasal projection of the scotomas in MacTel, whereas scotomas in AMD might generally be more homonymously or randomly distributed. Bi-nasal visual field defects result in a pre-fixational scotoma, which might interfere more with binocular vision than defects in more corresponding or more randomly distributed retinal areas. Our previous finding of an early impaired stereoscopic vision in MacTel would be in keeping with this concept. [10] Impairment of binocular fusion might also partly explain the phenomenon of 'dancing' or 'lost' letters, which is frequently reported by patients with MacTel (unpublished observation). Figure 4.7 attempts to simulate impaired monocular reading and impaired binocular fusion when reading. Another possible explanation of the difference between AMD and MacTel might also be different methodology in the studies. For example, sampling of a wider range of different scotomas in AMD might have obscured relevant effects in similar subgroups to MacTel. Furthermore, Kabanarou and Rubin have performed a comparison of the better eye with binocular function, but have not compared interocular differences with the magnitude of binocular gain and have not quantified scotomas. Fixed testing order or eye dominance might possibly have influenced our results. In a test-retest analysis of the applied reading test, [111] there was no evidence for a learning effect in reading speed, whereas there was a trend to mildly increased reading acuity at the retest. In our study, the right eye (test 2) consistently performed better than the left eye (test 3) and also consistently better than binocular function (test 1). If testing order were a confounder, this would have to be a combination of both learning effect (from test 1 to test 2) as well as a fatigue effect (from test 2 to test 3). This is of course not impossible, but we believe

that it is rather unlikely to have occurred consistently in most observers. Several studies have failed to provide compelling evidence for effects of eye dominance on reading performance in healthy observers. [108–110] Nevertheless, the fixed testing order remains a potential limitation of our study. It would be an interesting proof of concept and further evidence for our hypothesis, if the effect was reversed when reading from right to left. That is, a similar study for example in Israel, where text is read from right to left, would be predicted to show that scotoma measures in right eyes were more relevant for binocular reading than scotomas in left eyes.

4.5 Conclusion

We provide evidence for the presence of binocular inhibition of reading performance in MacTel. The magnitude of binocular inhibition correlated with the difference in reading speed between eyes, possibly due to the characteristic paracentral scotomas in non-corresponding retinal fields and a disruptive projection of scotomas in reading direction mainly arising from the left eyes. People with MacTel may improve their visual symptoms by occluding their worse eye whilst reading.

Chapter 5

Scotopic microperimetry

5.1 Background

Previous findings indicated more functional impairment in low light conditions (chapter 2). In eyes with very early structural disease manifestation, no functional loss was found on visual acuity and mesopic microperimetry testing. [37] In eyes with more advanced disease, areas adjacent to the deep and sharply demarcated scotomas on mesopic microperimetry testing show mild rod dysfunction. [92] Low light conditions have an overly negative effect on contrast sensitivity and visual acuity in MacTel patients compared to controls (chapter 2). Recently, a two-color dark-adapted microperimetry device was introduced which combines the advantage of microperimetry with the possibility of retinal sensitivity testing under light and dark-adapted conditions (*scotopic microperimetry*). [115, 116] In microperimetry, as opposed to conventional perimetry, stimuli are directly projected onto the retina which allows creating precise retinal sensitivity maps. There is evidence that the use of two different wavelengths may allow separating cone from rod function. [115–117] The hypothesis of this study was that scotopic microperimetry might be able to uncover functional impairment in early disease stages and that dark-adapted cyan sensitivity would be more impaired as sign of more severe rod dysfunction.

5.2 Methods

5.2.1 Participants

Patients of the MacTel Natural History Observation Registry (NHOR) study and age-matched healthy controls were examined in the Department of Ophthalmology, University of Bonn, Germany. The study was conducted in accordance with the Declaration of Helsinki and informed consent was obtained from all participants. The participants underwent retinal imaging including dual wavelength autofluorescence macular pigment optical density (MPOD) measurement. Retinal sensitivity was assessed with scotopic microperimetry using cyan (505 nm) and red (627 nm). Disease was graded into classes of MPOD loss (0 to 3). For perimetry analysis, the differences of the mean sensitivities (MacTel minus controls) were compared at each test location and the results were aggregated to global indices.

5.2.2 Two-wavelength dark-adapted microperimetry

After pupil dilation with phenylephrine 2.5% eye drops and tropicamide 1% eye drops, participants underwent scotopic two-color microperimetry. First, participants underwent testing under mesopic conditions with white stimuli on white background (the results of which are not presented in this study). Thereafter, they were dark-adapted for 30 minutes before being tested with red (627 nm) and cyan stimuli (505 nm) on a dark background. A perimetry grid with 49 concentrically arranged stimuli was used (Figure 5.1).

The S-MAIA device is calibrated based on the CIE 1951 scotopic luminosity function or $V'(\lambda)$ which shows (in terms of radiance) roughly a 20 dB lower rod threshold for cyan than for red stimuli for healthy observers. This means that the actual radiance of a stimulus at a measured sensitivity value of '0 dB' is approximately 20 dB brighter for red than for cyan stimuli. A healthy retinal area with normal rod and cone function would therefore yield a cyan-red difference of 0 dB for eccentricities > 2°. [18] The central fovea, including the rod-free zone with a diameter of approximately 1-1.25 degree, does not contain many rods or S-cones, so the sensitivity for cyan stimuli is very low and can reach absolute scotoma levels

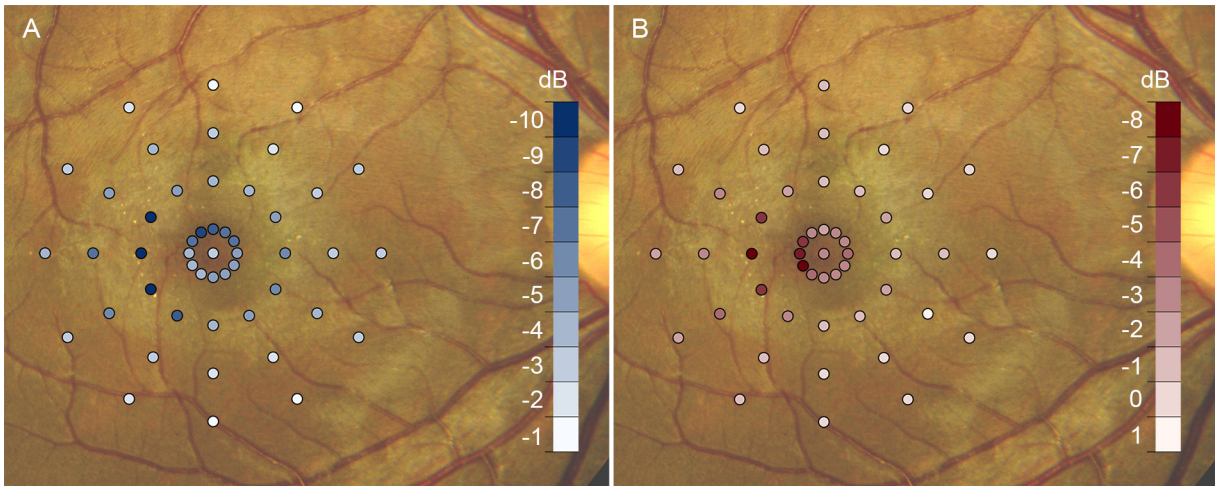

Figure 5.1: Difference of the means (MacTel minus control) for dark-adapted cyan (A) and red (B) sensitivity at each stimulus location. The fundus image shows an example of an eye with MacTel (here with greying, crystals, and blunted venules). The rings of the grid are at 1-, 3-, 5-, and 7-degree eccentricity from the fovea. The dots show the actual size of a Goldmann 3 stimulus on the retina. Cyan impairment seems more generally reduced (all points below zero) and obtains generally lower values than red sensitivity (explaining the different scales used) and shows deep loss of retinal function in a larger area, with a predominance in the temporal retinal sector.

even in the healthy retina. Cone and rod sensitivities for long wavelengths (red) are at similar luminance levels in darkness. [118] Thus, an isolated loss of rod function will lead to a relatively stronger loss of cyan sensitivity, yielding negative cyan-red difference scores. If both photoreceptor systems are similarly impaired, the cyan-red difference would become 0dB again. Table 5.1 gives an overview about those patterns of sensitivity loss and how we suggest their interpretation.

5.2.3 Macular Pigment Optical Density

We graded the disease into four different classes of MPOD loss, using a mildly modified version of a previously suggested classification. [54] MPOD class 1 was defined as temporal loss of macular pigment with remaining foveal macular pigment. Additional foveal loss of MPOD defined class 2. Class 3 was defined as MPOD loss in the entire *MacTel area*. Eyes without MPOD loss were defined as

Cyan-Red Difference	Cyan	Red	Interpretation
0 dB	Normal	Normal	Normal dark-adapted, rod-mediated vision
0 dB	Reduced	Reduced	Equally impaired rod and cone function
< 0dB	Reduced	Normal or mildly reduced	Impaired rod function with normal or comparatively less impaired cone function, i.e. selective rod dysfunction

Table 5.1: Aid to interpret patterns of sensitivity loss for two wavelengths

stage 0. Those eyes did not show any evidence of MacTel on any of the imaging modalities used in this study and were therefore considered *seemingly unaffected*. It has been shown in an earlier study that those seemingly non-affected eyes may show functional deficits in low light conditions and show a reduced Stiles-Crawford effect. [37]

5.2.4 Global perimetry indices

Mean deviation (MD) is the average of all deviations from normal sensitivity across all test locations, adjusted by the local normal variance. Pattern Standard Deviation (PSD) measures irregularity of visual field losses. This is obtained by summation of a local defect at all test locations. In this case, local defect is the difference between the measured value and the average field sensitivity (defined as normal sensitivity plus mean deviation) at this location. If the PSD is 0, then the visual field either can be normal at every point, or it may be uniformly reduced across all test points. MD and PSD were calculated with the following equations: [119]

$$MD = \left[\frac{1}{m}\sum_{i=1}^{m}\frac{(Tested - Normal\ sensitivity)_i}{\sigma^2}\right] : \left[\frac{1}{m}\sum_{i=1}^{m}\frac{1}{\sigma^2}\right] \tag{5.1}$$

$$PSD = \sqrt{\left[\frac{1}{m}\sum_{i=1}^{m}\sigma^2\right] \times \left[\frac{1}{m-1}\sum_{i=1}^{m}\frac{((Tested - Normal\ sensitivity)_i - MD)^2}{\sigma^2}\right]} \tag{5.2}$$

In equations 5.1 and 5.2, σ^2 is the normal variance at location i and m is the number of tested locations.

5.2.5 Statistical Analysis

All statistical analyses were performed using R. [83] Only eyes with a complete test set with mesopic and dark-adapted microperimetry were used for final analysis. Mixed linear models were fitted with the *lme4* package. [120] For testing the effect of MacTel on retinal sensitivity, participant category (control versus MacTel) was considered fixed effect, with subject and eye as random intercepts. To test the effect of eccentricity, retinal eccentricity was added as fixed effect to the previous model. When testing the global indices, only a random intercept for the subject was included. Random term inclusion was tested using likelihood ratio tests. Significance of fixed effect terms were tested using Wald test. A p-value < 0.05 was considered as significant.

5.3 Results

5.3.1 Participants

Thirty-four eyes of 19 patients (mean age 62.2, range 35-76) were compared with 25 eyes of 25 controls (mean age 61.5, range 38-80). Thirty-one eyes presented MPOD and OCT pattern typical of MacTel (class 1: 7 eyes, class 2: 9 eyes, class 3: 15 eyes). Three eyes did not show any typical characteristics of MacTel on multimodal imaging (MPOD class 0), but had clinical and imaging features consistent with MacTel in the fellow eye. Both cyan and red sensitivity were lower in MacTel. This was more pronounced at one and three degree eccentricity. Eyes with MPOD class 0 did not exhibit a functional deficit. Class 1 had impaired cyan, but normal red sensitivity. Class 2 and 3 behaved similarly and had impaired cyan and red sensitivity with a relatively higher cyan impairment.

5.3.2 Two-wavelength dark-adapted microperimetry

In two color dark-adapted microperimetry, mean retinal sensitivity for both cyan and red was lower in eyes with MacTel when compared to controls. The effect size was larger for cyan than for red (-4.75dB vs. -2.26dB) resulting in a negative cyan red difference (Table 5.2).

MacTel was associated with a higher reduction of cyan than red sensitivity

	Cyan			Red			Cyan-red difference		
Predictors	*Estimates*	*CI*	*p*	*Estimates*	*CI*	*p*	*Estimates*	*CI*	*p*
Control (Intercept)	10.27	9.50 – 11.05	**<0.001**	11.94	11.03 – 12.85	**<0.001**	-1.66	-2.54 – -0.79	**<0.001**
Mactel	-4.75	-5.88 – -3.62	**<0.001**	-2.26	-3.57 – -0.95	**0.001**	-2.52	-3.75 – -1.29	**<0.001**
Observations	2696			2696			2696		

Table 5.2: Effects of MacTel on retinal sensitivity for two colors in dark-adapted microperimetry. The intercept represents the mean sensitivity of the control eyes. The effect of having MacTel can be interpreted as the difference to this intercept. Fixed effect: Presence of MacTel. Random effects: Subject and eye. MacTel was associated with lower cyan and red sensitivity. CI: 95% confidence intervals, p: p-value

when compared with controls at each eccentricity, resulting in a negative cyan-red difference at each eccentricity. In MacTel, the largest reduction of both cyan and red sensitivity compared with controls was found at 1 and 3 degree eccentricity (Table 5.3). The largest reduction of the cyan-red difference was found at 3 degree, possibly indicating stronger rod than cone impairment in this area. We observed that sensitivity loss seemed more pronounced in the temporal when compared with the nasal retinal sector (Figures 5.1 and 5.2).

5.3.3 Macular Pigment Optical Density

MPOD class was a relevant predictor of retinal sensitivity (Table 5.4, Figure 5.3). MPOD class 0 was not associated with a change of cyan and red sensitivity. MPOD class 1 was associated with reduced cyan sensitivity, but not with a change in red sensitivity. MPOD class 2/3 were associated with both reduced cyan and red sensitivity. The effect of MPOD class 2/3 for cyan was more pronounced than for red sensitivity (higher loss), but MPOD classes 2/3 had a similar effect for each color (Table 5.4).

MacTel patients showed a lower mean deviation (MD) and higher pattern standard deviation (PSD) for both cyan and red. For MD, the effect was more pronounced (more loss) for cyan, but for PSD, the effect was similarly large for both colors (Tables 5.5 and 5.6).

In Figure 5.4, this can be seen as a shift towards lower MD values for cyan –

		cyan			red		cyan red difference		
Predictors	*Estimates*	*CI*	*p*	*Estimates*	*CI*	*p*	*Estimates*	*CI*	*p*
0 degree (fovea)									
Control (Intercept)	2.08	0.60 – 3.56	**0.006**	11.96	10.68 – 13.24	**<0.001**	-9.88	-11.64 – -8.12	**<0.001**
Mactel	-2.82	-5.06 – -0.58	**0.014**	-2.98	-4.70 – -1.26	**0.001**	0.17	-2.14 – 2.49	0.883
Observations	59			59			59		
1 degree									
Control (Intercept)	5.71	4.96 – 6.45	**<0.001**	13.66	12.35 – 14.98	**<0.001**	-7.96	-9.37 – -6.55	**<0.001**
Mactel	-5.84	-6.82 – -4.86	**<0.001**	-4.01	-5.88 – -2.14	**<0.001**	-1.80	-3.79 – 0.18	0.075
Observations	708			708			708		
3 degrees									
Control (Intercept)	11.76	10.63 – 12.89	**<0.001**	12.50	11.53 – 13.47	**<0.001**	-0.74	-1.86 – 0.38	0.194
Mactel	-6.45	-8.18 – -4.72	**<0.001**	-2.78	-4.21 – -1.35	**<0.001**	-3.67	-5.33 – -2.01	**<0.001**
Observations	612			612			612		
5 degrees									
Control (Intercept)	12.25	11.37 – 13.13	**<0.001**	11.20	10.40 – 12.00	**<0.001**	1.05	0.34 – 1.76	**0.004**
Mactel	-3.61	-4.98 – -2.24	**<0.001**	-1.34	-2.56 – -0.13	**0.031**	-2.32	-3.34 – -1.30	**<0.001**
Observations	612			612			612		
7 degrees									
Control (Intercept)	12.05	11.23 – 12.87	**<0.001**	10.38	9.59 – 11.16	**<0.001**	1.68	1.04 – 2.31	**<0.001**
Mactel	-2.30	-3.49 – -1.11	**<0.001**	-0.87	-2.02 – 0.29	0.141	-1.48	-2.36 – -0.59	**0.001**
Observations	705			705			705		

Table 5.3: Effects of MacTel on retinal sensitivity for two colors in dark-adapted microperimetry, **for each retinal eccentricity**. The intercept represents the mean sensitivity of the control eyes. The effect of having MacTel can be interpreted as the difference to this intercept. Fixed effect: Presence of MacTel. Random effects: Subject and eye. When controlling for eccentricity, MacTel is associated with an impaired cyan and red sensitivity. There is an interaction of eccentricity with MacTel. MacTel was associated with lower cyan sensitivity at 1 and 3 degree. CI: 95% confidence interval, p: p-value

		cyan			red		cyan red difference		
Predictors	*Estimates*	*CI*	*p*	*Estimates*	*CI*	*p*	*Estimates*	*CI*	*p*
Control (Intercept)	10.27	9.58 – 10.96	**<0.001**	11.94	11.13 – 12.74	**<0.001**	-1.66	-2.46 – -0.87	**<0.001**
MPOD class 0	-1.52	-3.15 – 0.11	0.068	0.00	-2.18 – 2.18	1.000	-1.33	-3.54 – 0.88	0.237
MPOD class 1	-6.00	-7.52 – -4.48	**<0.001**	-0.47	-2.40 – 1.46	0.636	-5.45	-7.40 – -3.50	**<0.001**
MPOD class 2	-4.98	-6.21 – -3.76	**<0.001**	-3.44	-4.91 – -1.97	**<0.001**	-1.61	-3.08 – -0.15	**0.031**
MPOD class 3	-4.95	-6.18 – -3.72	**<0.001**	-2.45	-3.89 – -1.01	**0.001**	-2.50	-3.93 – -1.07	**0.001**
Observations	2696			2696			2696		

Table 5.4: Effects of macular pigment optical density class on retinal sensitivities. CI: 95% confidence intervals

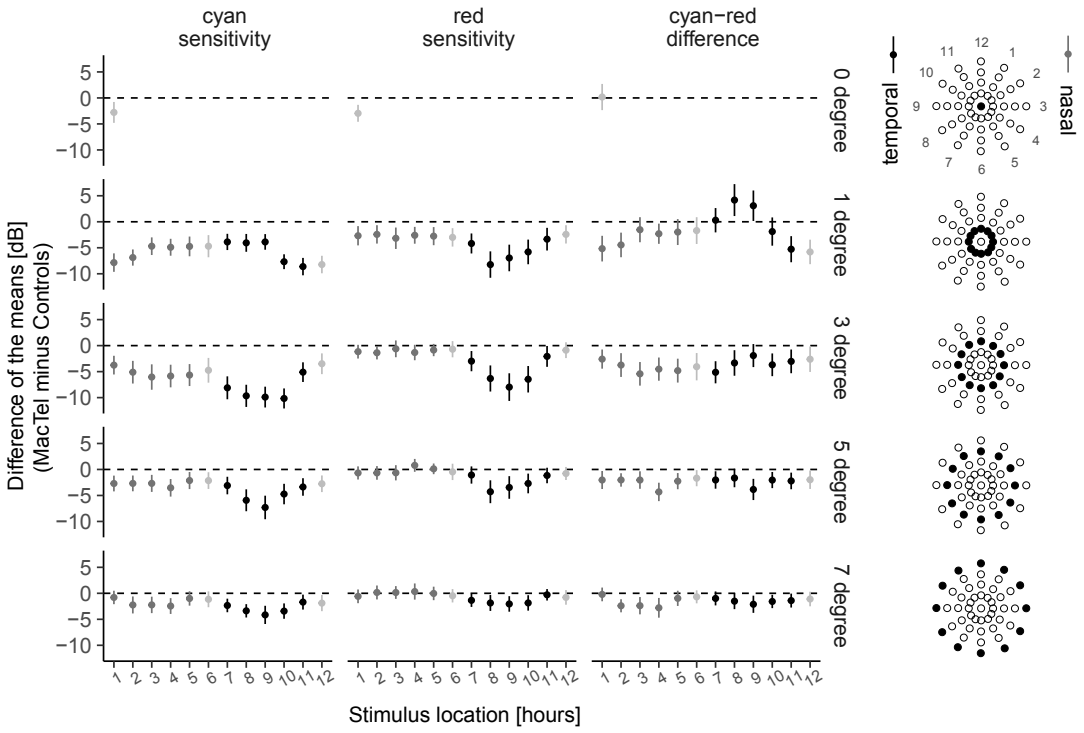

Figure 5.2: Difference of the means (MacTel minus control) of dark-adapted cyan and red sensitivities and for their differences for each stimulus location. The error bars show the 95% confidence intervals. Temporal locations show higher differences than nasal locations, and the differences are stronger for cyan than for red. The highest differences are found at 1- and 3-degree eccentricity

		cyan			**red**	
Predictors	*Estimates*	*CI*	*p*	*Estimates*	*CI*	*p*
Control (Intercept)	-0.00	-0.78 – 0.78	1.000	-0.00	-0.85 – 0.85	1.000
Mactel	-3.85	-4.99 – -2.70	**<0.001**	-1.86	-3.08 – -0.63	**0.003**
Observations	60			59		
Marginal R^2 / Conditional R^2	0.476 / 0.822			0.155 / 0.660		

Table 5.5: Effects of MacTel on mean deviation (MD) for two colors in dark-adapted microperimetry. The intercept represents the mean MD of the control eyes. The effect of having MacTel can be interpreted as the difference to this intercept. Fixed effect: Presence of MacTel. Random effects: Subject and eye. MacTel was associated with lower MD in both cyan and red. CI: 95% confidence intervals, p: p-value

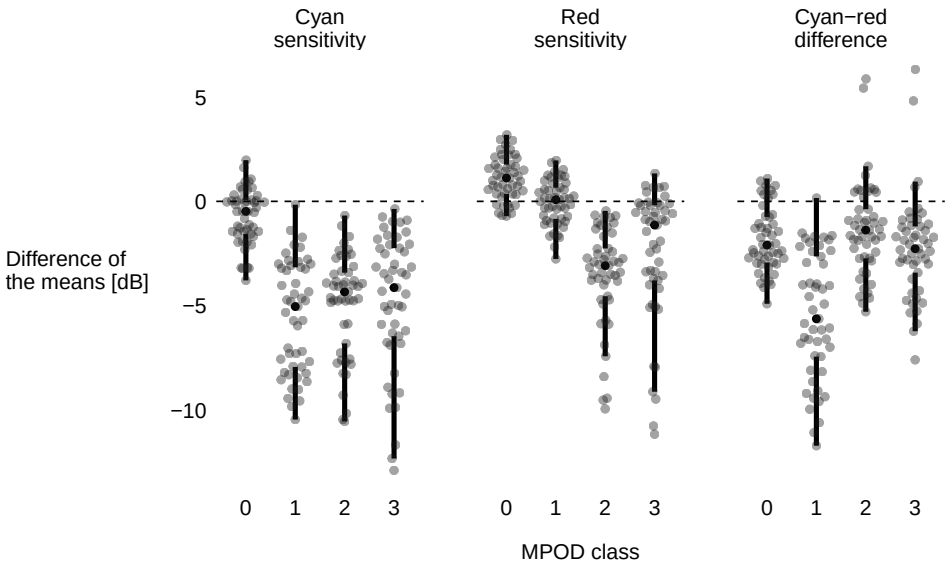

Figure 5.3: Difference of the means (MacTel minus control) of dark-adapted cyan and red sensitivities and for their differences on each test location by MPOD class. MPOD class 0 is basically not different from controls. MPOD class 1 shows reduced cyan and normal red sensitivity. MPOD classes 2/3 show reduced cyan and red sensitivity

		cyan			**red**	
Predictors	*Estimates*	*CI*	*p*	*Estimates*	*CI*	*p*
Control (Intercept)	2.25	1.90 – 2.60	**<0.001**	1.68	1.30 – 2.07	**<0.001**
Mactel	1.36	0.86 – 1.86	**<0.001**	1.38	0.81 – 1.94	**<0.001**
Observations	60			60		
Marginal R^2 / Conditional R^2	0.357 / 0.607			0.318 / 0.691		

Table 5.6: Effects of MacTel on pattern standard deviation (PSD) for two colors in dark-adapted microperimetry. The intercept represents the mean PSD of the control eyes. The effect of having MacTel can be interpreted as the difference to this intercept. Fixed effect: Presence of MacTel. Random effects: Subject and eye. MacTel was associated with higher PSD in both cyan and red. CI: 95% confidence intervals, p: p-value

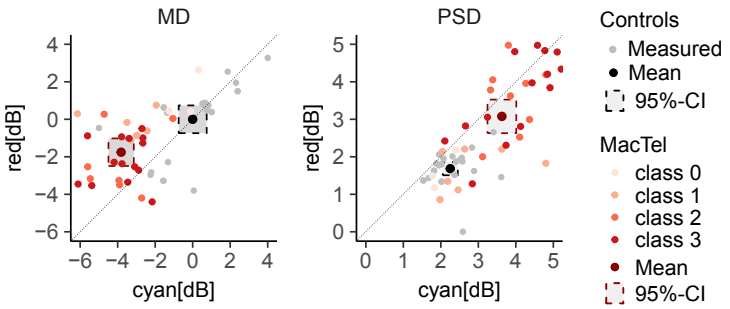

Figure 5.4: MD and PSD for the two colors. The gray line represents the line of equality. Eyes with MacTel have a lower MD than healthy eyes (generally reduced function), with a shift toward the left part of the graph, showing stronger loss for cyan. The PSD is higher in MacTel (indicating a larger focal loss). Both MacTel and healthy eyes have a mild and similar bias of the PSD toward cyan (being to the right of the line of equality), possibly due to the natural absence of rods in the fovea.

a shift towards the left side of the line of equality. For PSD, there is a mild bias towards higher values for cyan for both control and MacTel –possibly due to the naturally lower cyan sensitivity in the fovea, as higher PSD values reflect more focal sensitivity losses.

Figure 5.5 shows the cumulative defect curves for all eyes with MacTel (upper panel) and for each MPOD class (lower panel). The total of eyes showed a global sensitivity reduction in the cumulative defect curve for cyan color, and a more focal loss for red sensitivity. Eyes with MPOD class 0 had normative cumulative defect curves for both cyan and red. Eyes with MPOD class 1 showed a globally reduced cyan sensitivity, but a quasi-normative red sensitivity. Eyes with class 2 and 3 showed similar curves to one another, with a global deficit for cyan, and a more focal deficit for red color.

5.4 Discussion

The results suggest characteristic sensitivity changes for the two tested colors in a dark-adapted state. Sensitivity loss was more pronounced for cyan, and this was strongest at 1- and 3-degree eccentricity from the fovea. This pattern of sensitivity

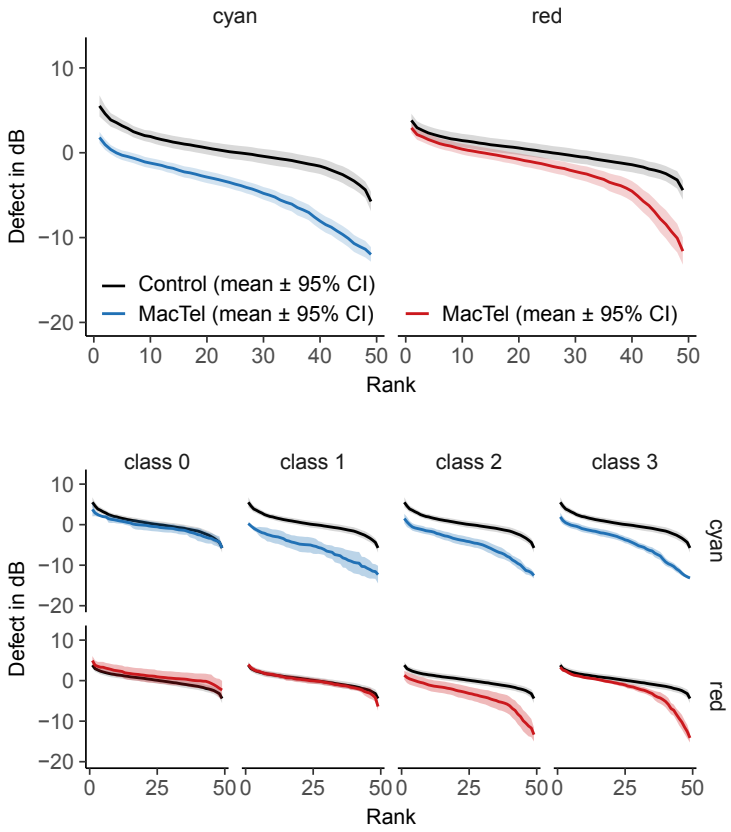

Figure 5.5: Cumulative defect curves for all eyes (top) and for each MPOD class. The figure shows a ranking of "local defects" (sensitivity at this point minus the mean of all sensitivities of healthy eyes). A general downshift of the curve denotes a more general sensitivity loss. A downshift only to the right side of the graph represents more focal sensitivity losses. MPOD class 0 shows normal cyan and red curves. MPOD class 1 shows a general cyan impairment, but normal red sensitivity. Eyes with classes 2/3 show a general cyan impairment and a more focal impairment of red sensitivity.

loss is suggestive of more pronounced rod impairment, which could be explained by photoreceptor absence or dysfunction on a cellular level. The lower rod density in the central macula might be one explanation for the latter, [18] maybe due to an increased susceptibility of those rods, or a lack of redundancy. [121] Cones might also partially contribute to cyan responses and using only two wavelengths might not be enough to reliably separate cone from rod function. [122] Moreover, the device used in the study shows both floor and ceiling effect for cyan and red stimuli, challenging the distinction between cone and rod function, especially when reaching brighter cyan levels (i.e., more severe rod dysfunction, or natural absence of rods in the fovea). However, previous studies provided evidence that selective loss of cyan function indeed reflects more pronounced loss of rod-mediated vision. [115–117] A revised version of the device with an improved dynamic range might be able to quantify severe degrees of rod dysfunction more reliably. [123] The results presented here therefore constitute rather conservative estimates for the degree of photoreceptor dysfunction.

Although there remains a degree of uncertainty of which photoreceptor class is actually responding and the device does not fully replace more elaborate psychophysical methods, we uncovered relevant and marked differences between different classes of macular pigment loss, regardless of the responding photoreceptor type. Eyes with preserved macular pigment (MPOD class 0) did not show functional deficits in this study. This finding is interesting and important, because we were previously able to show a marked loss of the Stiles-Crawford effect and an impairment of low luminance contrast sensitivity in those eyes of the same observers. [37] The impaired contrast sensitivity (chapter 2) as opposed to the unimpaired microperimetry sensitivity in those eyes might be indicative of a rather postreceptorally impaired cone system, e.g., in the bipolar or horizontal cells, which would also be in keeping with recent electrophysiological findings in MacTel suggesting an inner retinal dysfunction. [13] Eyes with only minor MPOD loss (class 1) showed a general loss of cyan sensitivity but normal red sensitivity, whereas eyes with more pronounced MPOD loss (classes 2 and 3) showed focal loss of red sen-

sitivity and (more pronounced) loss of cyan function (Figure 5.5). As this might reflect stronger rod impairment, our results were in accordance with previous studies of scotopic function in patients with MacTel, which showed a more pronounced loss of scotopic than photopic sensitivity. [92] Another explanation for the effect of MPOD class on retinal sensitivity might also be a type of adaptation mechanism to longstanding absence of macular pigment, maybe on photoreceptor level, making the retina less sensitive to blue light (macular pigment has its absorption maximum in the blue spectrum). [52] This idea would fit our observation that the loss of cyan sensitivity affected the central one degree in a rather concentric manner, possibly correlating to a loss of foveal MPOD, and also fit our observation that eyes with MPOD class 0 did not show impaired cyan sensitivity. Figures 5.3 and 5.5 show how eyes with MPOD classes 2 and 3 had markedly worse function than eyes with MPOD classes 0 and 1. This correlation suggests that MPOD loss might also be useful as an adjunct parameter for the assessment of disease progression; however, classes 2 and 3 were showing similar results in our study and it might be useful from a functional perspective to reduce them to a single category. The localised retinal dysfunction in MacTel with its temporal predominance represents a peculiar phenomenon. Electrophysiological studies showed normal morphology and retinal function in the retinal periphery of MacTel. [13], in keeping with the concept of the *MacTel area* - see also chapter 6 The MacTel area seems to be anatomically congruent with the area containing Henle's fibers (unpublished observation from histology studies by one of the coauthors [MF]), which corresponds to the rod-free area before the centripetal photoreceptor migration during embryogenesis. [28,29] It is conceivable that the photoreceptors in this area might behave differently from "peripheral" photoreceptors, possibly due to differences in metabolism and subsequently higher susceptibility to metabolic dysfunction. [121, 124] Lens opacities might also have influenced the sensitivity for cyan stimuli due to absorption of shorter wavelengths, but one would expect a more global loss of sensitivity and not a focal loss as our results strongly suggested. We therefore decided not to account for cataract as another independent variable lest the linear mixed models contain too many covariates. A

limitation of our study was the small numbers of patients with early and earliest disease stages. The results were therefore more of observational character and the reliability of statistical inference would therefore remain limited. Future studies including more eyes with early disease are required. Those are likely to be identified because of our increasing knowledge about early stages and potential precursors of the condition.

5.5 Conclusion

In summary, we present the first scotopic microperimetry study in eyes with MacTel. Our results corroborated evidence that rod function might be compromised earlier and to a greater extent than cone function. In context with the findings in chapter 2, where eyes with no structural change showed loss of contrast sensitivity (testing primarily cone function in mesopic conditions), the results might point toward an early affection of inner retinal function mainly of the cone system. Categories of macular pigment loss and global perimetry indices might be useful as adjunct measures of functional impairment and thus disease progression. The results are encouraging for further research into retinal function in low light conditions in MacTel, and might help understand the pathophysiology of the disease.

Chapter 6

Visual acuity, disease end stage, and the MacTel area

6.1 Background

The first symptoms in MacTel are usually reading difficulties and, less commonly, metamorphopsia which start in the fifth to seventh decade of life, although the age of onset may vary considerably. [95] A characteristic feature of vision loss is a progressive focal paracentral scotoma resulting from photoreceptor loss that first occurs temporal to the foveal center and that may be mapped using microperimetry testing (see chapter 3 and chapter 4).

Best-corrected visual acuity (BCVA) may remain well preserved over prolonged periods. Several larger case series indicate that a significant drop in BCVA may occur when the scotoma (or a structural surrogate marker) progresses also to involve the foveal center or when the disease course is complicated by the development of a neovascular membrane or macular hole. [42] Overall, however, loss in BCVA is slow, with a documented mean decrease of approximately one letter per year, based on longitudinal data from the MacTel Project with a mean follow-up of 4.2 years (range, one to six years). [15]

The frequency distribution of BCVA levels in people with MacTel has not yet been investigated in detail. Moreover, little is known about the retinal phenotype of those with the worst visual function, representing the natural end point of the

disease. A limitation of functional loss to the central macular area was suggested previously (see also chapter 3), [42] and characteristic findings on advanced imaging such as confocal blue light reflectance or dual-wavelength autofluorescence indicate that structural damage is also limited to a specific oval-shaped area, which may be referred to as the MacTel area. [55, 56, 59, 125] A better characterisation of the topographic dimensions of disease-related alterations in eyes with late-stage disease could strengthen the concept of such a MacTel area to which degeneration would remain limited, even in late disease stages.

6.2 Methods

6.2.1 Participants

The MacTel Natural History Observation Study (NHOS) recruited patients with MacTel from 2005 to 2011, as well as age-matched, not related controls without retinal disease. Participants of the NHOS were followed for at least 5 years. After 2011, new participants were enrolled in the MacTel Natural History Observation Registration Study (NHOR) for a single clinic visit only and then annual telephone review. Patients were identified and recruited at participating study centers, and family members were also invited to be screened for presence of MacTel. The diagnosis of MacTel was confirmed by the Moorfields Eye Hospital Reading Center (MEHRC), based on diagnostic features on multimodal imaging. This initially mainly included color fundus and fluorescein angiography images in accordance with the classification by Gass and Blodi. [24] Later, characteristic findings on optical coherence tomography (OCT) scans and fundus autofluorescence (AF) images were increasingly used for confirming the diagnosis. At database access, 60 centers worldwide were actively recruiting patients. Institutional Review Board (IRB)/ Ethics Committee approval was obtained at each center. The study was conducted in accordance with the Declaration of Helsinki and written informed consent was obtained from all participants. The presence of common phenotypic characteristics of MacTel, such as retinal crystals, retinal 'greying', blunted retinal vessels and pigment plaques, was graded in all eyes by certified graders of the Moorfields Eye

Hospital Reading Center (MEHRC).

6.2.2 Best-corrected visual acuity testing

Best corrected visual acuity (BCVA) was obtained using the standard ETDRS protocol. [27] The clinical databases of both NHOS and NHOR were accessed on 30th May 2019 to extract data of all patients with a confirmed diagnosis of MacTel. BCVA of the last study visit was extracted. Severe vision loss was defined as BCVA $\leq$38 letters, which is approximately equivalent to a Snellen visual acuity of 20/200 - the threshold for legal blindness in the United States. Other BCVA cut-offs were $\leq$68 letters (approximately equivalent to Snellen 20/50) and $\leq$23 letters (approximately equivalent to Snellen $\leq$20/400) – the thresholds for driving and for legal blindness in many European countries, respectively.

6.2.3 Severe vision loss

Eyes with other causes for severe vision loss were excluded from analysis (Figure 6.2 and table 6.1). All eyes with severe vision loss were reviewed for plausibility of the BCVA test result based on the previous ocular and medical history as well as retinal imaging data - stored on MEHRC servers - including color fundus photographs (CF), fluorescein angiography (FFA) and optical coherence tomography scans (OCT).

This included grading of presence of outer retinal atrophy, sub-retinal fibrosis or full thickness macular hole (FTMH) within the foveal area (corresponding to ETDRS field 1). The center of the foveal area was defined as the center of the foveal avascular zone as seen on FFA. In advanced cases or when imaging did not allow for visualisation of foveal capillaries, the location of the foveal center was estimated based on the location of the second- and third-degree retinal vasculature. Whenever the foveal structure or other ocular findings did not sufficiently explain low BCVA in the experience of two retinal specialists (PCI and TFCH), the sites were contacted and asked for data confirmation. A suspected data entry error was confirmed in 106 cases, and the information obtained from database access was updated. 36 queries were not resolved and those eyes were excluded from analysis

Cause	Frequency
Advanced Glaucoma	2
Advanced Glaucoma and DME	2
AION	1
Amblyopia	5
Branch Retinal Vein Occlusion	1
Cataract	7
Central Retinal Vein Occlusion	2
Congenital Scar	1
Cornea - Keratoplasty	1
Corneal Scar	3
Corneal Scar - Herpetic	1
Functional	6
Macular Branch Vein Occlusion	1
Macular Laser With Scarring	2
Ocular Ischemia, CVA, Microvascular Plaques	1
Previous Retinal Detachment With Macula Off	1
Prosthesis	1
Staphyloma	1
Vitrectomy With Membrane Peel	2

Table 6.1: Other causes than MacTel for very poor visual function. DME = diabetic macular edema. AION = anterior ischemic optic neuropathy, CVA = cerebrovascular accident

(Figure 6.2).

Eyes were graded for presence of neovascular changes and full thickness macular holes (FTMH). Neovascular changes included large haemorrhages or fibrotic scars on CF, neovascular membranes on FFA, sub-retinal fibrosis and/or fibrovascular (hyper-reflective) pigment epithelium detachment with or without intraretinal or sub-retinal fluid on OCT.

6.2.4 Asymmetry

As the BCVA data suggested an asymmetry between right and left eyes (see results), we analysed phenotypic asymmetry in patients with very early stages, because subtle differences between eyes in later disease stages may not be as obvious. For this, all eyes that had been labelled as early MacTel by the MEHRC were re-adjudicated (TFCH) in order to group those eyes into two categories: 1) Eyes with no retinal abnormality on any imaging modality used, but where the fellow eye showed typical signs of the condition (apparently unilateral MacTel) and 2) eyes with no changes on CF, no or only very little leakage on FA, and very mild changes on OCT images, such as foveal asymmetry or mild inner retinal hyper-reflectivity (asymmetric MacTel). [37]

6.2.5 Quantification of the MacTel area

The area of any visible changes (staining and leakage) on late phase FFA images of eyes with BCVA $\leq$20/200 was measured using Fiji imaging software by a single grader (TFCH). [126] The maximum horizontal and vertical dimension of the retinal changes was set in relation to the distance between the temporal optic margin and the foveal center as reference (Figure 6.1). The foveal center was defined as described above.

6.2.6 Measurement of retinal thickness based on OCT

Retinal thickness was measured using OCT imaging data obtained with Heidelberg Spectralis devices (Heidelberg Engineering, Heidelberg, Germany). The ETDRS grid was centered on the foveal center, and the average total retinal thickness as provided by the manufacturer's proprietary software (HEYEX) was noted for each ETDRS subfield. Eyes with neovascularisation were excluded. The values were compared with published data from a device- and age-matched normative sample. [127] Right and left eyes were analysed separately.

6.2.7 Statistical Analysis

Analysis was performed with R. [83] A Wilcoxon signed-rank test was used for comparison of visual acuity in right versus left eyes. For analysis of occurrence of

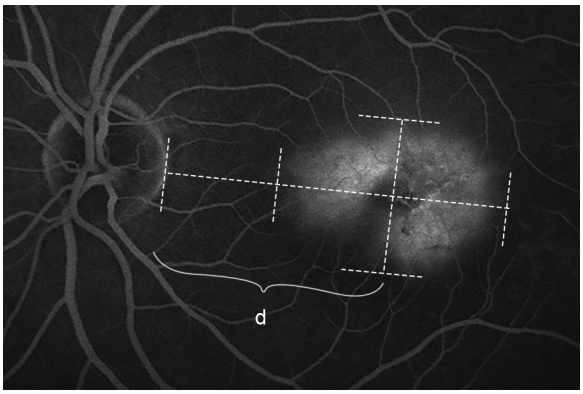

Figure 6.1: Measurement of the MacTel area. Measurement of visible retinal alterations on fluorescein angiographic (FFA) images using Fiji. The measurement was performed from the temporal optic disc margin to the nasal border of the lesion, from there to the foveal center, and from there to the temporal margin of the lesion. The vertical dimension was measured perpendicular to this axis. All measurements were scaled to the distance between the temporal optic disc margin and the foveal center (d).

early stages (asymmetry) in eyes, Fisher's exact test was used. The average retinal thickness of ETDRS fields was compared with unpaired t-tests, for right and left eyes separately, with Bonferroni-correction for multiple testing. Data was visually checked for normality using histograms. Simple linear regression was used to model mean BCVA as predicted by age. Linear logistic regression was used to model the proportion of eyes with severe visual impairment with age as predictor variable, and to model the proportion of eyes with severe vision loss with typical MacTel characteristics as predictor variables. The significance level for all tests was 5%. Data visualisation (figures/ tables) was done with the packages *ggplot2*, *patchwork* and *sjPlot*. [128–130]

6.3 Results

6.3.1 Participants and asymmetry

At database access, 4517 eyes of 2259 patients (Mean age: 62.7 years (SD 9.5), range 21 – 93) were available for analysis (Figure 6.2).

Neovascular changes were present in 439 eyes (9.7%) of 329 patients (bilateral

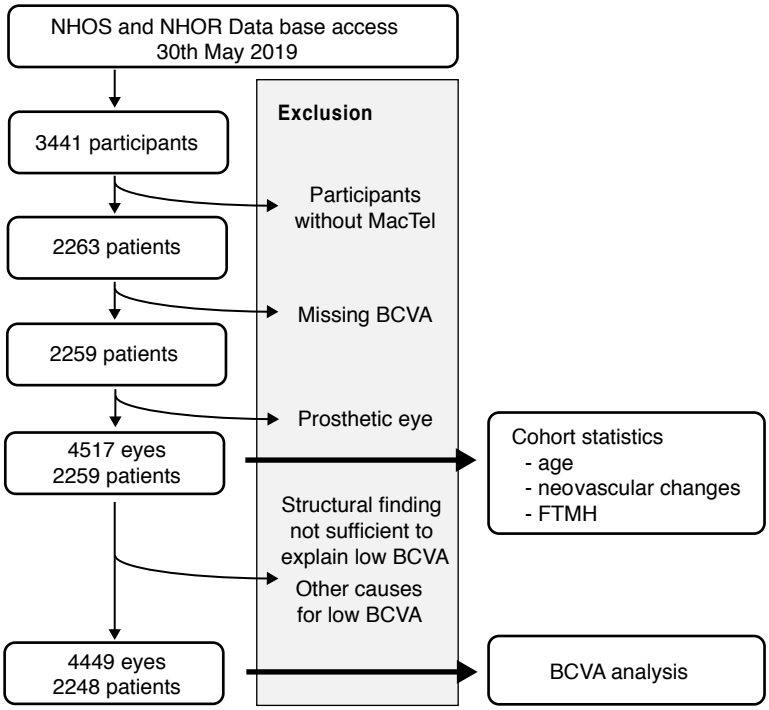

Figure 6.2: Pre-analytical flow chart. MacTel: Macular Telangiectasia Type 2. NHOS: Natural History Observation Study. NHOR: Natural History Observation and Registry Study. Out of the 4517 eyes analysed, 40 eyes with best corrected visual acuity (BCVA) $\leq$20/200 presented with other causes explaining their severe visual impairment (Table S1), and 28 eyes with BCVA $\leq$20/200 remained without obvious explanation for the documented low BCVA (data entry errors possible), resulting in 4449 eyes included in BCVA analysis. FTMH: Full thickness macular hole.

in 110 patients; 33%) and a FTMH was found in 63 eyes (1.4%) of 54 patients (bilateral in 9 patients; 17%). Right eyes more frequently presented with more advanced morphological changes. Table 6.2 summarises the frequency of eyes with neovascularisation or a FTMH, which were more common in right than in left eyes. In contrast, no obvious or a very mild disease manifestation was more common in left eyes of patients with very asymmetric disease where only one eye clearly allowed the diagnosis of MacTel (apparently unilateral disease, n=78, 3.4% of the entire cohort where both eyes were available for grading).

Affected Eye	Apparently unilateral cases	Neovascularisation	Full thickness macular hole
Right eye only	54	130	26
Left eye only	24	89	19
Both	0	110	9
Total	78	329	54

Table 6.2: Asymmetry in MacTel

6.3.2 Best-corrected visual acuity

4449 eyes of 2248 patients were included in the BCVA analysis (Figure 6.2. Median BCVA was 73 letters (Snellen equivalent 20/40). BCVA was $\leq$20/50, $\leq$20/200 and $\leq$20/400 in 37.3%, 3.8% and 0.9% of all eyes, respectively (Figure 6.3). Bilateral BCVA $\leq$20/50 was found in 414 patients (18.4%), $\leq$20/200 in 15 patients (0.7%), and $\leq$20/400 in two patients (0.09%).

Participant age correlated with BCVA, but the effect size was small. If a neovascularisation or macular hole were present, bilateral occurrence was frequent (33% or 17%, respectively), and BCVA was better than 20/200 (79% or 78%, respectively) or 20/50 or better (26% or 13%, respectively). Eyes with advanced disease (BCVA, $\leq$20/200) showed the following characteristics: (1) atrophy of the foveal photoreceptor layer with or without associated sub-retinal fibrosis; (2) an affected area, termed MacTel area, limited to a horizontal diameter not exceeding the distance between the temporal optic disc margin and foveal center, and the vertical diameter not exceeding approximately 0.8 times this distance (exceptions were eyes with large active or inactive neovascular membranes); (3) reduced retinal thickness measures within the MacTel area; and (4) less frequent retinal greying and more frequent hyperpigmentation compared with eyes that have better BCVA.

There was an asymmetry of visual impairment between right and left eyes, with a median BCVA of 71 letters in right eyes and 74 letters in left eyes (p-value<0.0001). BCVA was $\leq$20/50, $\leq$20/200 and $\leq$20/400 in 42.3%, 4.4% and 1.1% of right eyes, as opposed to 32.4%, 3.2% and 0.7% of left eyes (Figure 6.3). In controls and family members enrolled in the study who were not diagnosed

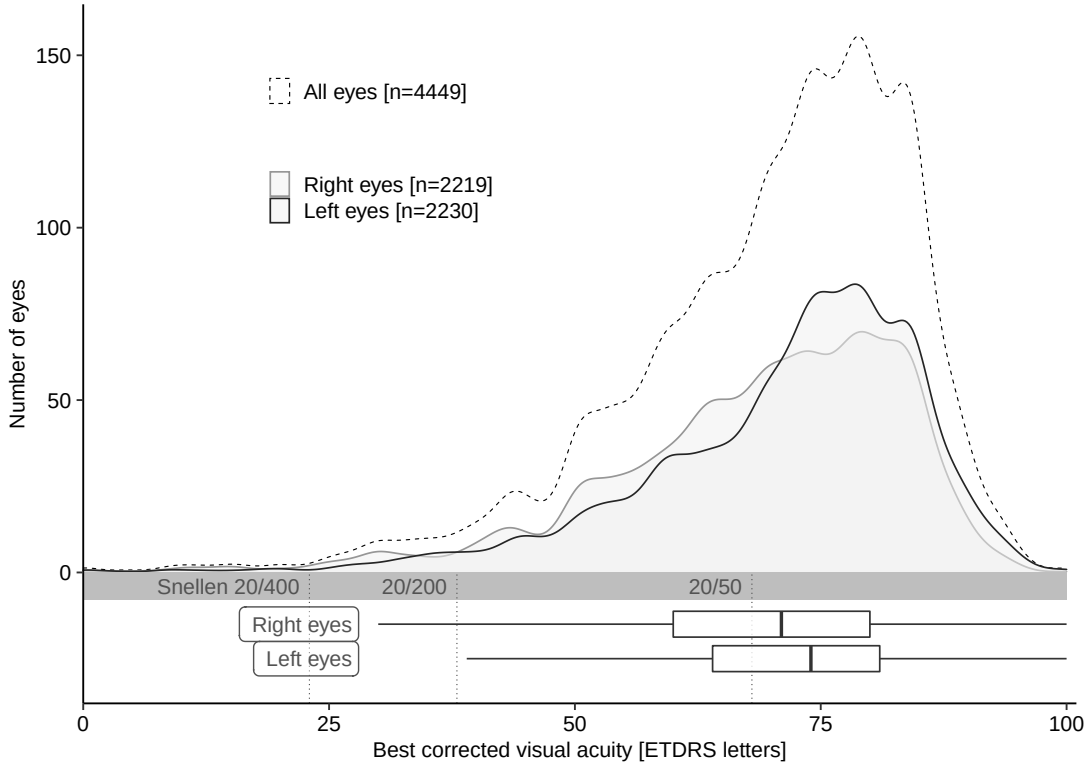

Figure 6.3: Frequency distribution of best corrected visual acuity (BCVA) values for all eyes, and for right and left eyes separately. The vertical dashed lines show Snellen visual acuity cut offs at 20/50 (68 letters) as the threshold for the ability to drive, as well as 20/200 (38 letters) and 20/400 (23 letters) as the limits for legal blindness in the US and many European countries, respectively. Box plots show median (thick line), interquartile range (IQR, box) and data extremes (end of whiskers) at 1.5 times the IQR away from the lower or upper quartile (or upper maximum).

with MacTel, BCVA distribution was not different between right and left eyes (Figure 6.4).

There was a mild effect of age on the relative frequency of severe vision loss (Figure 6.5, upper graph). From an overall risk of 3.8% for severe visual impairment (BCVA $\leq$20/200) in at least one eye, the likelihood is predicted to increase to 5.7% over ten years, equivalent to an increase of the odds ratio of approximately 4% for each year increase in age (Table 6.3).

Age also was a significant predictor for BCVA, although the effect was only

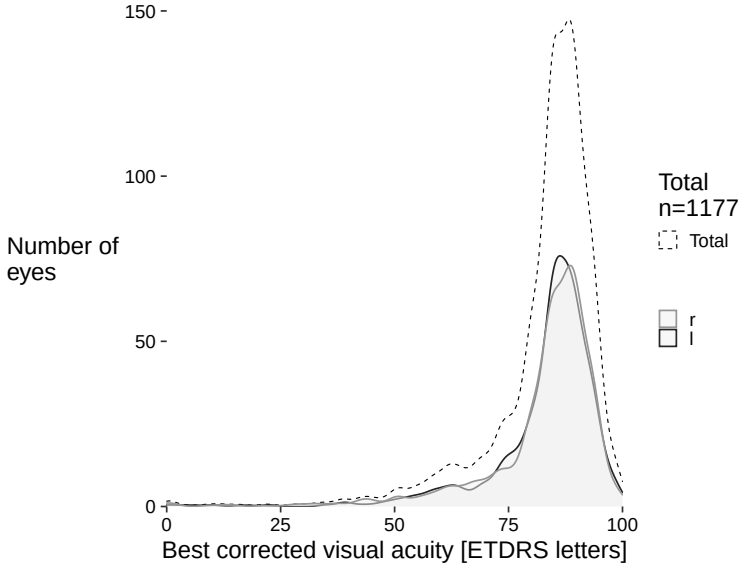

Figure 6.4: Best corrected visual acuity frequency distribution of eyes of participants of the MacTel study without a diagnosis of MacTel.

		low BCVA	
Predictors	*Odds Ratios*	*CI*	*p*
(Intercept)	0.01	0.00 – 0.02	**<0.001**
final_age	1.04	1.02 – 1.06	**<0.001**
Observations	2247		

Table 6.3: Results of logistic regression analysis of proportion of patients with severe vision loss (BCVA $\leq$ 20/200) in at least one eye as dependent variable, and age as independent variable. The effect is significant, but only small in size.

small (Figure 6.5, lower graph). For each decade increase in age, mean BCVA decreased 2.2 letters (95%-confidence interval: 2.9-1.6 letters).

6.3.3 Anatomy of eyes with very poor vision

Eyes with BCVA $\leq$20/200 (168 eyes of 153 patients) were analysed for structural alterations of the macula on OCT images to identify causes for MacTel-related severe vision loss (clinical examples in Figure 6.6).

The majority of these eyes had photoreceptor/outer retinal atrophy involving the fovea, either without (72 eyes, 43%) or with a paracentral (22 eyes, 13 %) or

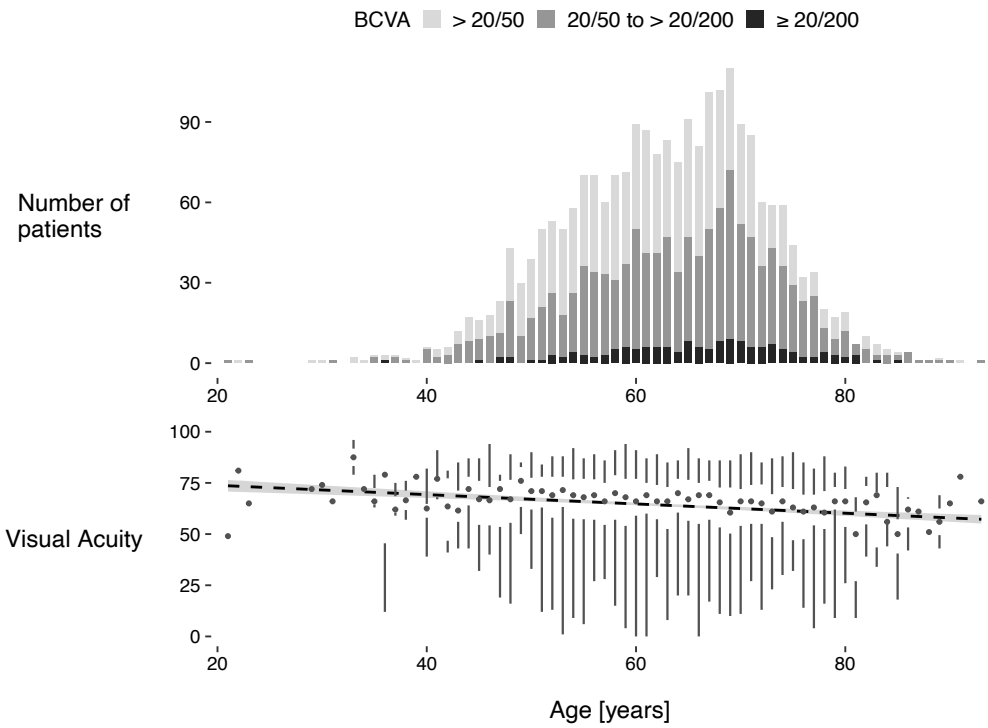

Figure 6.5: Effect of age on best-corrected visual acuity (BCVA) in macular telangiectasia type 2 (MacTel). Upper graph: Frequency of severe vision loss ($\leq$20/200) and BCVA between >20/100 to 20/50. The eye with lower visual acuity was selected for this analysis (n=2247 eyes, as age was not available for one patient of the BCVA analysis group). The upper graph shows the distribution of BCVA ranges of the worse eyes as a function of age. The fraction of patients with severe vision loss ($\leq$20/200, black bars) does not seem to be higher in older patients. Lower graph: Median BCVA (dots) as a function of age. The gap represents the interquartile distance (IQD), and the whiskers extend to the data extremes. The dashed line shows the regression line (with error) from a simple linear regression model.

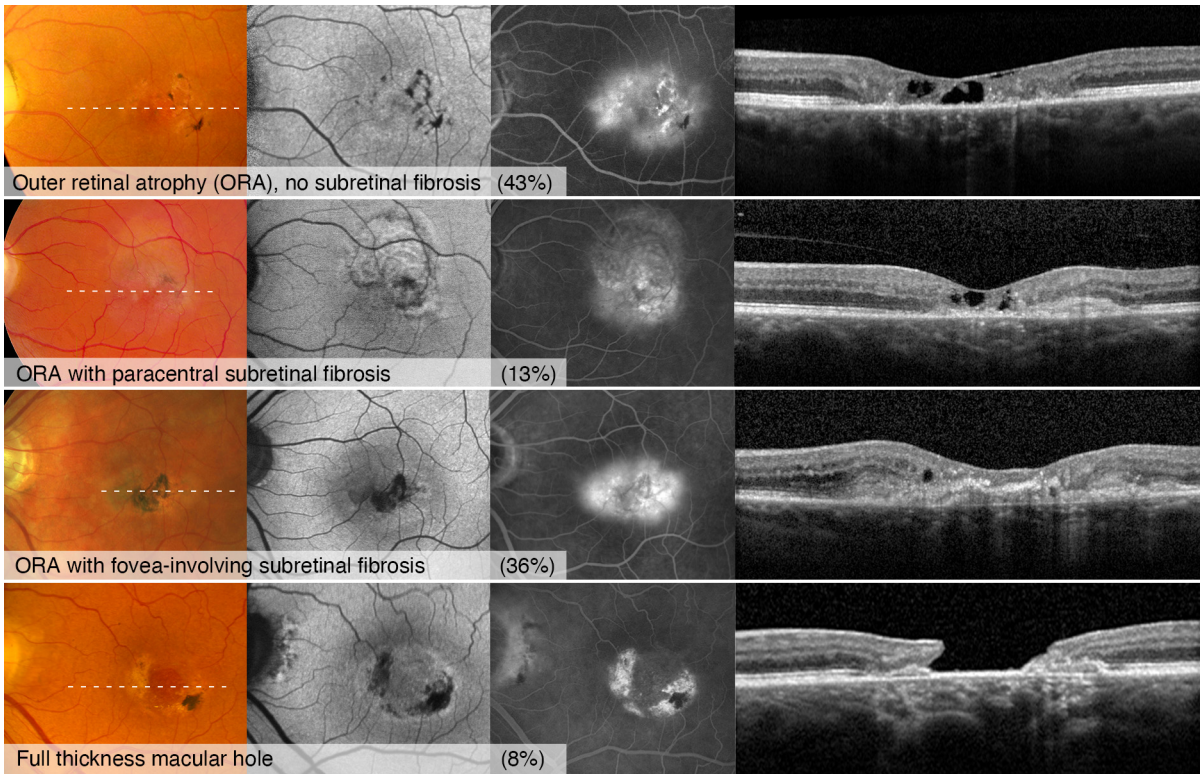

Figure 6.6: Exemplary cases for structural correlates to low visual function (best corrected visual acuity (BCVA) $\leq$ 20/200). Color fundus photographs (first column), fundus autofluorescence (second column), fluorescein angiography (third column) and SD-OCT images (fourth column). Dashed lines in the CF show the position of the SD-OCT scans. The OCT shows regular retinal layers outside the MacTel area in all cases.

fovea-involving (61 eyes, 36%) sub-retinal fibrosis / active NV. Thirteen eyes (8%) had a FTMH. However, NV and FTMH were not necessarily associated with severe visual impairment: BCVA was >20/200 in the majority of eyes with NV (n=345, 79%) and FTMH (n=49, 78%), and $\geq$20/50 in 26% (n=111) and 13% (n=8), respectively (Figures 6.8 and 6.7).

We did not perform a similar analysis in eyes with BCVA >20/200 for presence of photoreceptor atrophy in the absence of a FTMH or NV because this parameter was not part of the original reading center (MEHRC) grading and the relevant structured information was therefore not available for all eyes. Grading of CF images was available for 4005 eyes of 2006 patients. Eyes with severe visual impairment

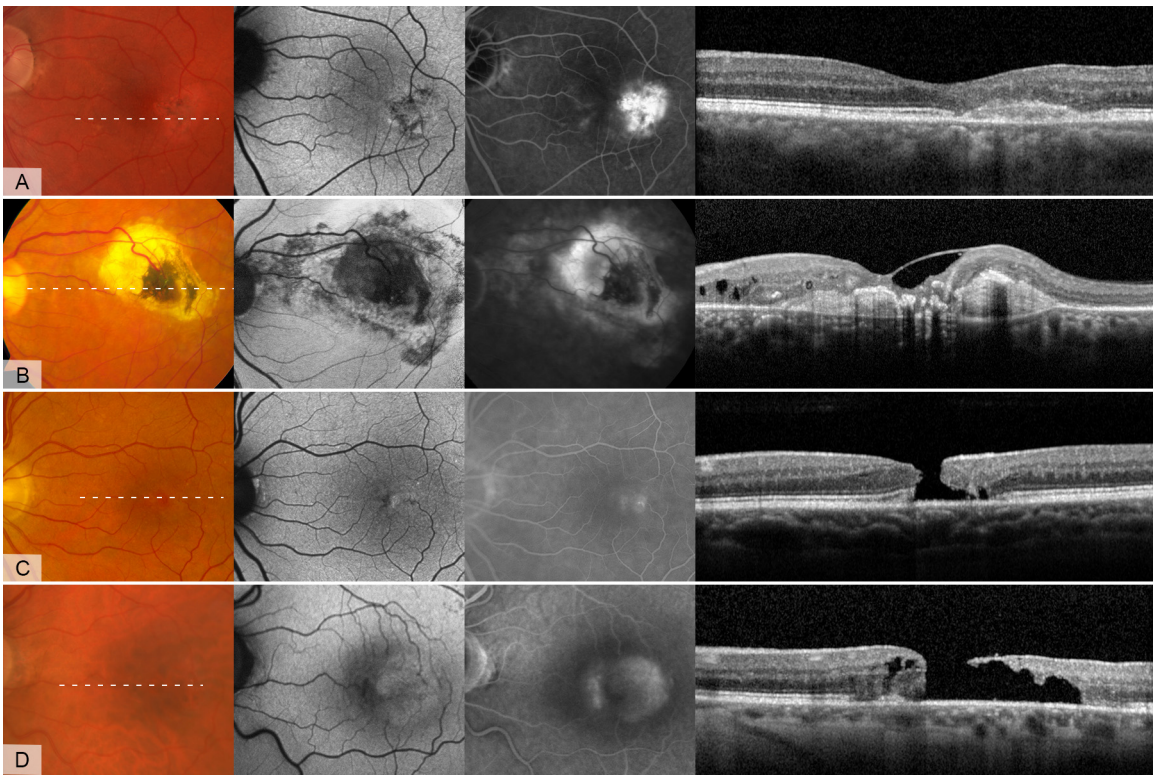

Figure 6.7: Examples for eyes with neovascularisation (NV) or full thickness macular hole (FTMH) with good and poor best-corrected visual acuity, respectively. A) Small sub-retinal fibrosis from previous NV temporal to the foveola with well-preserved BCVA (Snellen 20/25). B) Large scar due to neovascular membrane with poor BCVA (hand movement). The diagnosis of MacTel was made based on historic images. C) Small, slightly paracentral FTMH with well-preserved BCVA (20/25). D) Large FTMH with complete outer retinal atrophy especially in the temporal parafovea with poor BCVA (Snellen 20/320).

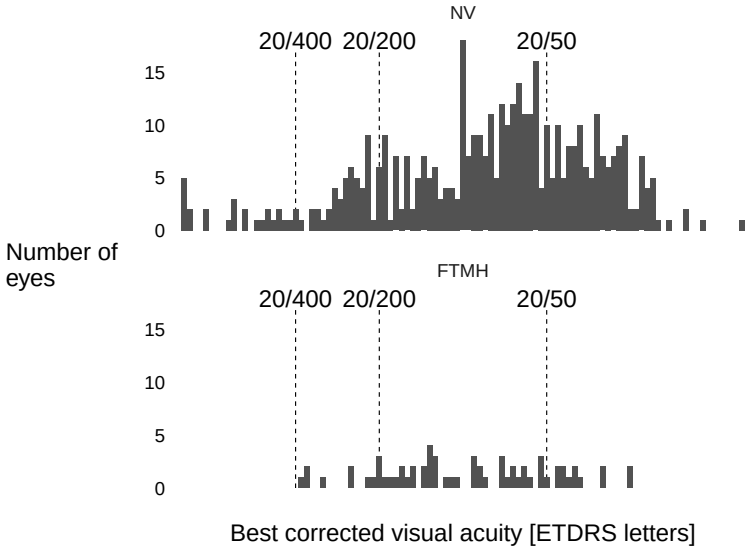

Figure 6.8: Best corrected visual acuity (BCVA) distribution of eyes with neovascular changes (upper graph) and full thickness macular holes (lower graph). The majority of eyes had BCVA >20/200 (38 ETDRS letters)

(BCVA $\leq$20/200) consistently showed hyperpigmentation, but rarely greying. After adjusting for the presence of the other features, BCVA was on average 11 letters lower in eyes with pigment and 3.5 letters higher in eyes with greying. The odds ratio for severe vision loss was significantly increased with the presence of pigment plaques and significantly decreased with the presence of greying, but did not change with the presence of crystals or blunted, right-angled vessels (Figure 6.9 and Table 6.4.

6.3.4 The MacTel area

The maximum size of the retinal area affected by MacTel (i.e., the MacTel area) was investigated in eyes with severe visual impairment (BCVA, $\leq$20/200), which likely represent the phenotypic spectrum of end-stage disease. Measurements were based on FA images, which were available for 134 of 168 eyes with BCVA of 20/200 or worse. The oval retinal area with MacTel-related changes was larger in the horizontal than in the vertical direction. In eyes without neovascular changes, the horizontal width did not exceed the distance between the temporal optic disc margin and foveal center (distance, d), and the vertical height did not exceed approximately 0.8 times

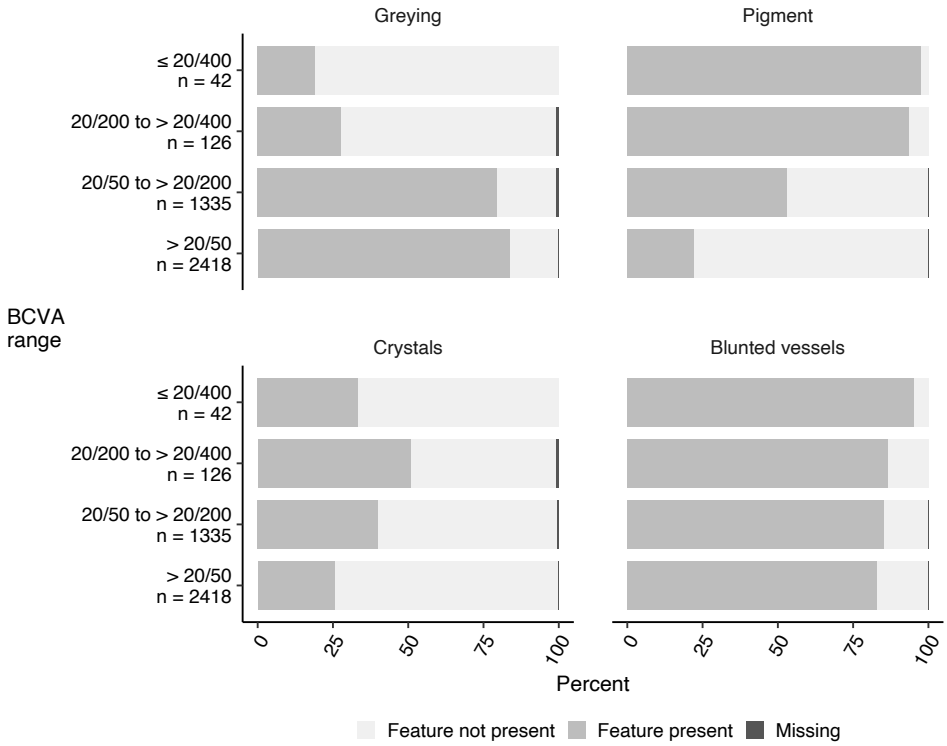

Figure 6.9: Frequency of funduscopic findings characteristic for MacTel, grouped according to different ranges of best corrected visual acuity (BCVA). Missing information (NA) was due to unavailable or ungradable fundus images.

		Low BCVA	
Predictors	*Odds Ratios*	*CI*	*p*
(Intercept)	0.04	0.03 – 0.06	**<0.001**
crystals present	1.23	0.91 – 1.66	0.171
blunted present	0.77	0.53 – 1.12	0.155
pigment present	5.80	4.19 – 8.14	**<0.001**
greying present	0.50	0.36 – 0.69	**<0.001**
Observations	3955		

Table 6.4: Results of logistic regression analysis of proportion of eyes with funduscopic findings characteristic for MacTel as dependent variable, and severe vision impairment as independent variable. p-values printed in bold are significant.CI: confidence interval. BCVA: best corrected visual acuity

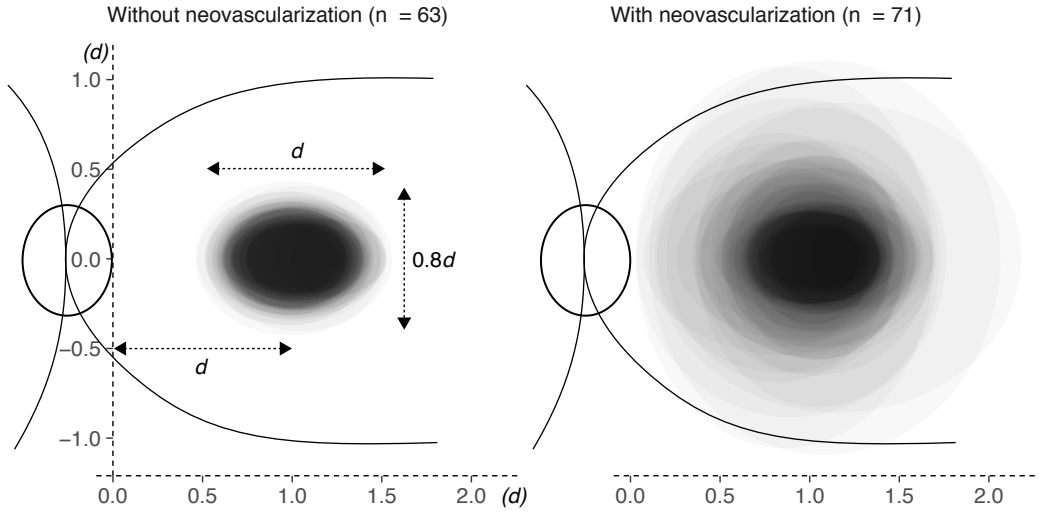

Figure 6.10: Dimensions of the MacTel area. The diagrams showing the extension of macular telangiectasia-related fluorescein-angiographic changes in eyes with severe vision loss (best-corrected visual acuity, $\leq$20/200) (A) without and (B) with neovascular change. Right and Left eyes were considered equally. Gray level represents the cumulative frequency of angiographically visible changes at a given location, plotted for each eye based on horizontal and vertical measures. Darker gray level indicates higher frequency. d = distance between temporal optic disc margin and foveal center.

d (Figure 6.10). Mean width was 0.73 d (SD, 0.15 d), and mean height was 0.53 d (SD, 0.12 d). Eyes with neovascular changes showed a larger affected area exceeding these limits (mean width, 0.91 d [SD, 0.35 d]; mean height, 0.78 d [SD, 0.41 d]).

After exclusion of eyes with neovascularisation, OCT measurements suitable for ETDRS sector analysis were available for 2923 eyes of 1545 patients of the entire cohort and for 60 eyes of 55 patients from the low-vision sample. In the total cohort, retinal thickness was significantly thinner in all 4 sectors of the inner ring and in the foveal center. It was thinner than normal in the nasal outer field of right eyes (difference of the means, 10 microns) and thicker than normal in the temporal outer field in left eyes (difference of the means, 5 microns), but was similar to normal in all other outer ETDRS fields (Table 6.5). In eyes with severe visual impairment, retinal thickness was significantly thinner in all inner ETDRS fields (inner

Eye	Field	n	Mean (SD) (Control)	n	Mean (SD) (MacTel)	p-value
Left	Fovea	108	279 (24)	1472	254 (38)	<0.001
Left	Nasal inner	108	341 (16)	1471	316 (24)	<0.001
Left	Superior inner	108	339 (15)	1453	313 (23)	<0.001
Left	Temporal inner	108	326 (14)	1472	299 (32)	<0.001
Left	Inferior inner	108	336 (15)	1458	306 (23)	<0.001
Left	Nasal outer	108	309 (15)	588	304 (18)	0.008
Left	Superior outer	108	295 (14)	363	294 (17)	0.856
Left	Temporal outer	108	279 (14)	679	284 (18)	<0.001
Left	Inferior outer	108	283 (14)	366	286 (17)	0.077
Right	Fovea	97	279 (20)	1449	251 (38)	<0.001
Right	Nasal inner	97	345 (16)	1449	315 (24)	<0.001
Right	Superior inner	97	343 (16)	1434	312 (22)	<0.001
Right	Temporal inner	97	330 (16)	1449	299 (31)	<0.001
Right	Inferior inner	97	340 (16)	1439	305 (24)	<0.001
Right	Nasal outer	97	314 (15)	539	304 (19)	<0.001
Right	Superior outer	97	301 (19)	349	295 (19)	0.006
Right	Temporal outer	97	283 (14)	683	284 (18)	0.361
Right	Inferior outer	97	287 (14)	357	287 (19)	0.682

Table 6.5: average retinal thickness of ETDRS (Early Treatment of diabetic retinopathy study) fields from all available Spectralis scans of patients with MacTel, compared with a normal age-matched cohort (data from Nieves-Moreno et al. [127]). For this analysis, eyes with neovascular changes were excluded. p-values are shown from unpaired t-tests. After correction for multiple testing with the Bonferroni method, significance was considered at a level of $\frac{0.05}{18} = 0.002$

ring and central subfield), but was similar to normal in all outer fields (Table 6.6).

6.4 Discussion

MacTel only rarely results in legal blindness. The majority of eyes (approximately 60%) in this large cohort retained a visual acuity level of 20/50 or higher and only few patients (0.7%) had developed bilateral severe visual acuity loss (BCVA $\leq$20/200). Approximately 20% of all people had bilateral BCVA below the legal threshold for driving in most countries (Snellen 20/50 in the better eye). Severe vi-

Eye	Field	n	Mean (SD) (Control)	n	Mean (SD) (MacTel)	p-value
Left	Fovea	92	278 (23)	24	219 (49)	<0.001
Left	Nasal inner	92	339 (15)	24	285 (33)	<0.001
Left	Superior inner	92	336 (15)	23	284 (28)	<0.001
Left	Temporal inner	92	324 (14)	24	253 (45)	<0.001
Left	Inferior inner	92	334 (15)	23	272 (30)	<0.001
Left	Nasal outer	92	307 (15)	13	298 (19)	0.130
Left	Superior outer	92	293 (15)	9	284 (19)	0.235
Left	Temporal outer	92	278 (14)	15	267 (18)	0.039
Left	Inferior outer	92	281 (14)	8	280 (19)	0.902
Right	Fovea	72	277 (21)	36	234 (56)	<0.001
Right	Nasal inner	72	343 (17)	36	304 (41)	<0.001
Right	Superior inner	72	340 (15)	34	303 (35)	<0.001
Right	Temporal inner	72	327 (16)	36	273 (46)	<0.001
Right	Inferior inner	72	338 (16)	36	289 (38)	<0.001
Right	Nasal outer	72	312 (14)	17	301 (18)	0.032
Right	Superior outer	72	298 (19)	12	287 (20)	0.098
Right	Temporal outer	72	281 (14)	18	273 (19)	0.115
Right	Inferior outer	72	285 (13)	12	284 (21)	0.866

Table 6.6: average retinal thickness of ETDRS fields from all available Spectralis scans of those patients with best corrected visual acuity ≤ 38 letters and without neovascular changes, compared with a normal age-matched cohort (data from Nieves-Moreno et al. [127]) p-values are shown from unpaired t-tests. After correction for multiple testing with the Bonferroni method, significance was considered at a level of $\frac{0.05}{18} = 0.002$

sion loss was associated with outer retinal atrophy in most cases. The disease seems to be naturally constrained to a macular area with specific dimensions - the "MacTel area". An unexpected finding was the mild inter-ocular asymmetry with significantly worse BCVA and a higher frequency of FTMH or NVs in right eyes, and more frequent early disease stages in left eyes. Hence, MacTel may be an asymmetric disease. Another explanation may be a systematic error due to a learning effect if right eyes were consistently tested first as per study protocol. However, controls without MacTel who underwent BCVA testing following the same protocol did not

show a similar difference between eyes. A third explanation could be that reading the BCVA test chart may be more difficult with right eyes, in which the para-central scotoma is projected to the left of fixation. A fourth possibility is that the study cohort may have been biased by ocular dominance, which is more frequently right-sided. [131] Patients may be more likely to seek help for vision problems in their dominant eye which may explain the more frequently affected right eyes in patients with apparently unilateral disease. The cause and significance of disease asymmetry would need to be further explored. Another unexpected finding was the small effect of age on vision loss. Age was almost normally distributed with an only mild left skew and a mode around 70 years. Although age was a significant predictor for mean BCVA and the frequency of severe vision loss, the effect size was small and clinically negligible. The proportion of people with at least one eye with severe vision loss remains overall on a stable low level across all age groups of this sample. If MacTel is a progressive disorder ultimately leading to vision loss, one would expect the proportion of patients with severe vision loss to increase more with higher age. Possible explanations for this discrepancy include a selection bias due to mistaking late MacTel disease stages for other diseases such as age-related macular degeneration or macular dystrophies. Without a diagnosis of MacTel, patients would not be referred to a MacTel center and would thus not appear in our statistics. Another explanation might also be an increased mortality of patients with more severe types of MacTel, preventing an accumulation of patients with severe vision loss over time. Previous studies which have shown associations of MacTel with systemic morbidities such as obesity and diabetes or neurologic disorders may be supportive of this alternative explanation. [7,66,86,132] The predominant structural alteration in eyes with severe vision loss was atrophy of the foveal photoreceptor layer, detected on OCT images. Such neurodegeneration most frequently occurred without evidence for a sub-retinal NV (46%), or the NV was located slightly eccentric to the foveal atrophic changes (13%) indicating possible independence from the neovascular process. In eyes with sub-foveal NV (36%), photoreceptor degeneration may have developed independently or secondary to the neovascular process. Severe vision loss

in eyes with FTMH may either occur subsequent to the FTMH itself or due to adjacent photoreceptor atrophy involving the foveal center. Photoreceptor atrophy as the most common cause of severe vision loss is in keeping with previous studies on functional loss in patients with MacTel: The structural correlate of the characteristic deep para-central scotomas is atrophy of the photoreceptor layer, and proximity of such scotomas to the foveal center has been found to be associated with loss of visual acuity. [42, 97] Severe vision loss was associated with the presence of pigment proliferation within the MacTel area. This would be in keeping with the assumption that such pigmentation develops subsequently to outer retinal atrophy, thus representing a surrogate marker for photoreceptor degeneration. The pathophysiology of MacTel-related pigment proliferation may reflect observations in a mouse model in which photoreceptor atrophy and approximation of retinal vessels to the retinal pigment epithelium results in intraretinal pigment migration. [133] As a reliable feature, [73] pigmentation may thus serve as one useful criterion in future disease classifications. In contrast, loss of retinal transparency (retinal greying) was a rather rare observation in eyes with severe vision loss. As the exact cause of this characteristic funduscopic feature is not yet well understood, reasons for its absence remain speculative. Retinal greying is also often absent in very early disease and hence, it may represent a particularly dynamic, active phase of the disease. Its loss in late disease stages with severe functional loss might be explained if its presence may depend upon intact Müller cells and/or photoreceptors. In the entire study cohort, eyes with NV often had relatively preserved vision, possibly due to a non-central localisation of the neovascular lesion or due to lack of extensive photoreceptor atrophy of the overlying retina. Whether or not anti-vascular endothelial growth factor (VEGF) therapy has played a role for preservation of visual acuity in eyes with NV cannot be concluded from this dataset. Similarly, a substantial proportion of eyes with a FTMH had a BCVA >20/200. Possible explanations include a small and non-progressive size of MacTel-related FTMHs, or a slightly para-central location. To explore this further, a systematic structure-function analysis and longitudinal data capture would be required. Some MacTel patients may have predisposing factors

for developing NVs or FTMH: Calculated based on our sample prevalence, one would expect bilateral occurrence of NV or FTMH by chance in approximately 4% and 1% of patients with NV or FTMH, respectively. In our cohort, however, bilateral lesions were observed in 33% and 17%, respectively. One of the most striking features of MacTel is the restriction of the disease to an oval shaped area in the macula, which we call the "MacTel area". Its horizontal dimension does not exceed the distance between the temporal optic disc margin and the foveal center and its vertical dimension does not exceed approximately 80 percent of this distance. Even in eyes with the most advanced disease manifestation, angiographic changes and retinal thinning remained limited to this area. Retinal changes beyond this area were either not related to MacTel, or resulted from neovascular complications, including retinal edema, sub-retinal haemorrhages and/or fibrosis. Such limitation of retinal changes to the MacTel area is in agreement with investigations of visual function which have shown that the central scotoma in non-neovascular disease does not exceed a macular area of approximately eight times five fundal degree. Only when retinal thickness was analysed in the entire non-neovascular cohort, a very mild retinal thinning within the nasal outer sector of the ETDRS grid (i.e., outside the MacTel area) was found, which was significant in right eyes. A possible explanation would be a retrograde neurodegeneration of inner retinal neurons secondary to chronic macular photoreceptor degeneration or dysfunction. In contrast, the temporal outer field in left eyes revealed a very mild but significant thickening. The left temporal thickening may be driven by only a small area just outside the inner rings, by those cases where the MacTel area extends just beyond the inner ring. This may correspond to a mild temporal thickening which can sometimes be observed before atrophy develops. [32] Overall, these observations would be in keeping with the generally observed asymmetry with more severe disease in right eyes. Limitations of our study are the cross-sectional nature of the data which would not allow conclusions on individual disease progression. Also, ascertainment bias may have resulted in a disproportionate frequency of certain disease stages or even phenotypes, e.g. when the diagnosis of MacTel is not considered in patients with large

neovascularisations, macular holes or apparently unilateral disease. Moreover, the prevalence estimates for NV were mainly based on color fundus and angiography images and may thus under-estimate the true prevalence of NV in our sample, because those imaging modalities may not always detect a MacTel-related neovascular process. This study is relevant for patient counselling. The majority of MacTel patients will retain a level of vision to perform most daily tasks, although the legal ability to drive may be lost in approximately 20% of cases in countries with a legal limit of Snellen BCVA of 20/50. Previous studies indicate that reading function is increasingly impaired by progression of MacTel (see also chapter 4), but a certain degree of reading function is likely to be maintained even in late disease stages - though special reading aids may be necessary. [70] The findings corroborate previous evidence for a natural endpoint of MacTel which needs to be taken into account when modelling disease progression. Finally, this study indicates an asymmetry between right and left eyes, of which the significance yet needs to determined.

6.5 Conclusions

Severe vision loss is rare in MacTel and is related to photoreceptor atrophy in most people. Results indicate disease asymmetry with slightly worse vision and more advanced disease manifestation in right eyes. MacTel-related neurodegeneration does not spread beyond the limits of the MacTel area.

Chapter 7

Overarching Discussion

7.1 Impact

Visual function is affected in a specific way in MacTel. Although a disease of the macula, visual acuity remains unaffected for a long time, yet quality of life is more impaired than one would expect when comparing with other macular conditions and similar levels of visual acuity. [134] The studies presented in this thesis helped quantifying and providing further details of the character of functional loss. Understanding the specific impact of the condition on affected people will help direct future research in this condition, as it helps focussing research efforts and means on problems and questions that have a more pertinent impact on people affected by the condition.

Especially the knowledge about early functional changes not only helps patient counselling, but also provides important clues to the disease mechanism. For example, the simple advice to improve lighting in the daily environment, in particular when performing common tasks such as reading, can be of life changing importance for the patient. Similarly, encouraging people to try to read only with one eye open can help them reading more fluently and it is quite surprising how often patients have never tried to read in this way or have not dared to cover their eye because they might think it causes harm to do so. The studies presented in this thesis provide some more scientific ground to this commonplace advice, and it helps patients to understand why they might struggle with specific tasks so much.

The affection of contrast sensitivity even in eyes that otherwise seem (structurally) normal indicates that dysfunction might start on a cellular level when our current imaging and scanning methods fail to show changes. It is difficult to specify the specific mechanistic failure though, as contrast sensitivity is a highly complex visual task in which the entire visual pathway is involved. However, given that visual acuity remains quite high until a late stage, it seems plausible that there is rather a dysfunction in the inner retina and the inter-cellular communication rather than only on photoreceptor level. If this is secondary to the presumed Muller cell dysfunction or if it coincides, is difficult to ascertain. This is only seemingly in disagreement with the finding that dark-adapted blue sensitivity is impacted earlier and stronger than dark adapted red sensitivity. Generally people try to explain such finding with rods being more affected than cones. In MacTel, histology in an eye with MacTel confirmed that rods were lost to a greater extent than cones. [102, 103] However, this was an eye with late disease stage and it does not necessarily reflect a mechanism specific for MacTel, as as rods seem generally more vulnerable than cones. [121] Previous functional studies in dark-adapted eyes are well in accordance with the findings from dark adapted microperimetry studies presented in this thesis, and it seems plausible that this results from an affection of the rod pathway. But it does not necessarily mean that it the dysfunction happens primarily on photoreceptor level, but could result from inner retinal dysfunction that starts in the rod-specific pathways which consists of different bipolar, horizontal and ganglion cells than used by cones.

On the other hand, knowledge about late disease stages also has a huge influence on patient counselling. The unfortunately still fairly broadly used disease staging with a neovascular stage as "stage 5" is very suggestive of this stage being the unavoidable end stage in all cases, but evidence is speaking against neovascularisation as a necessary end stage. In contrary, disease end stage is defined by photoreceptor atrophy and neovascularisations seem only a complication that happen only in a minority of cases, although it might be more common than previously assumed. Previous studies of prevalence of neovascularisation were solely based

on more conventional imaging methods such as color fundus photographs and fluorescein angiography, but newer methods such as OCT can reveal even smaller neovascularisation that are undetectable on those previous methods. The study here used a multimodal approach, but also largely relied on disease grading on CF and FFA, thus even in this study the real prevalence of neovascularisation might be underestimated.

One of the key features that differentiates MacTel from other macular conditions is that it is weirdly limited to a very specific area which shows peculiarly consistent dimensions and can be expressed relative to the distance between the optic disc and the fovea. As a matter of fact, this specific affection only of this area is used as a pathognomonic feature diagnostic of MacTel. This can of course lead to a ascertainment bias, as cases with affection beyond that area will not be diagnosed as MacTel, thus maybe artificially removing cases where MacTel features can be found beyond. However, to the best knowledge of the author, there are no reports of cases where MacTel features were found beyond the MacTel area. However, there are reports of cases that show signs of other retinal conditions that might exceed the MacTel area, such as concurrent central serous chorioretinopathy. [135] It is still quite unclear what exactly defines this specific area and what makes it so special, but it is quite plausible that this results from a distinct genetic profile with differences in metabolism and cellular expression that results in increased cellular vulnerability in this area.

The limitation of MacTel to a small area in the central retina has significance to visual prognosis of affected patients. The large data base that collected data on several thousand eyes could confirm that only very few people have functional loss that fulfils criteria of blindness in most countries. In fact the vast majority of people retain visual acuity levels that are high enough for driving in most countries. This knowledge is often very reassuring for patients, although they might not always feel comfortable when driving, given that there are central scotomas and they might struggle to always identify number plates and street signs. In many countries, vision requirement for driving includes an intact binocular central field of vision, and in

later disease stages this might be affected because of overlapping scotomas. So far, there are no studies with binocular visual fields that might help clarify how many people might be affected in that way.

Some of the employed methods presented in this thesis are still fairly young. For example scotopic microperimetry has only recently emerged due to developments of better imaging technology, improved software required for fundus tracking and reactive positioning of the projected stimuli. There is still need to establish standardised methods to analyse the results from this method. [72] The thesis demonstrated that location-independent visual field parameters such as mean deviation can be useful although they are generated against predicted (interpolated) normal sensitivity maps. It is necessary to generate interpolated sensitivity maps because there are currently no existing standards for visual field patterns in microperimetry as they exist in conventional perimetry (e.g., the 24-2 visual field pattern). It would be virtually impossible to create normal maps for every location on the posterior pole that can be in theory tested with microperimetry. Pfau et al. undertook an immense effort by creating the normative data which underlies the calculated visual field indices obtained from the test results in our study. Nonetheless, the use of such parameters is extremely useful for analysis, as they are relatively easy to understand and they summarise complex geographically dependent test results into a single parameter, allowing for simpler and more intuitive statistical analysis.

An important limitation of the presented functional investigations are the rather small numbers to which functional studies are naturally confined. They are very daunting for both examiner and observer, requiring energy and time, the latter of which can be measured economically: time is expensive. This makes it difficult to always appropriately address statistical problems such as symmetry between eyes, and to account for all possible factors which can introduce a bias. In MacTel, those are most notably the sex of the patient and the presence of diabetes, which was both not accounted for in this study. A recent study suggested a possible association of MacTel with sex hormones. [94] Similarly, people with MacTel more often have diabetes [66] and the presence of diabetes can affect visual function - e.g., contrast

sensitivity. Therefore sex and diabetic status might have influenced the results and ideally should have been accounted for.

Slow disease progression is one of the key challenges in the interventional research in neurodegenerative diseases such as MacTel, as changes might not occur in the observation period and differences that are resulting from treatment might not be picked up, or, maybe worse, a treatment effect might be incorrectly suggested by chance alone. It has been demonstrated in several studies that changes on imaging can be valid as relevant markers of disease progression. [2, 40, 41] In MacTel, the disruption of the ellipsoid zone on OCT imaging is a valid surrogate measure for loss of visual function as measured by microperimetry. The advantage of using a structural measure is that it facilitates monitoring and detection of disease progression, and it allows to reduce required sample size in studies because the variance of rather "objective" tests is expected to be much lower than the variance of results from psychophysical tests such as microperimetry. This validation work has prepared the ground for the approval of a structural measure as a surrogate measure for disease progression as an outcome measure in an investigational trial by the federal drug agency (FDA). [136] It is likely that this gives precedence for the use of structural surrogate measures as primary outcome measure for other trials in other conditions that have similarly slow disease progression as MacTel.

Other challenges in research of slow progressing neurodegenerative disease include that early disease stages are rarely picked up, those sampling is biased towards later stages. It seems plausible that any intervention will have more effect when applied rather early in the disease course, so the challenge moves towards early and correct identification of affected people, ideally before they show functional or structural changes. Some of the herein functional methods seem to pick up changes earlier than more conventional measures, but they still analysed mostly patients where a clear diagnosis of MacTel could be made based on structural alterations. Of great interest are those patients that have seemingly unilateral disease affection. A recent study was able to show that cone directionality seems to be lost in the seemingly unaffected eyes in those patients. [37]

As a side project of this work, an R package was developed which will help future eye researchers to handle ophthalmic data in a more streamlined manner. In particular the often quite challenging inter-conversion of visual acuity notations, and other often astonishingly daunting tasks such as counting the number of patients and eyes has been made an easy task with this package. The software was published on the comprehensive R archive network (CRAN) under a Massachusetts Institute of Technology (MIT) licence, a permissive free software license. A detailed description of this package can be found in Appendix A. People who are not proficient in R can use parts of the functionality of this software on www.va-converter.com, which is a website created for the purpose of converting visual acuity notations and is free to use.

7.2 Future directions

Structure function correlations have demonstrated that structural changes are valid. In a recent study, Kihara and Heeren et al. demonstrated that it is possible to predict functional loss based on structural findings on OCT imaging alone, using deep learning. [8] The algorithms were able to accurately predict retinal sensitivity on microperimetry based on OCT B-scans. This allowed for an unprecedented resolution of "retinal sensitivity maps" that cannot be achieved with actual functional tests. The use of deep learning slowly changes the paradigm of research from a hypothesis driven to a data driven approach, were patterns in the data are uncovered that are not visible or detectable to the human mind. Sometimes the results confirm current understanding and hypothesis, such as the study from Kihara and Heeren where the outer retina was confirmed as primordial to predict retinal sensitivity, but there can be also surprising findings, e.g., recently a study showed that artificial intelligence was able to predict sex based on the fundus image, which so far no human was able to do. [137] We will have an increasing amount of data available, as technology allows for easier acquisition and, maybe more importantly, less expensive and easier storage as well as access of data. Thus, data driven research will likely become more and more important.

Fancy algorithms, however, are hardly of any use in absence of data. In functional studies, absence of data mostly results from challenges of data acquisition. It requires time, effort and money from both researcher and study participant, thus data acquisition is often limited to only few subjects and to few functional tests. Extensive characterisations of specific functional tests such as the microperimetry studies published by Pfau et al. are rather exceptional. [115, 116] It would be desirable to deepen the knowledge about visual function in patients with MacTel. For example, contrast sensitivity studies could be extended to a thorough characterisation of the contrast sensitivity functions, or true microperimetry with adaptive optics could help reveal retinal (dys-)function on a cellular level.

Given the paucity of functional data especially of patients with early disease stages, it would furthermore be desirable to validate and reproduce findings made in the herein presented studies, as this might have important implication on our understanding of the disease mechanism. In particular the interesting finding of reduced contrast sensitivity in eyes without structural changes warrants further investigation. It is possible that this is much in keeping with findings of impaired cone directionality, but currently there are two major impediments to further studies of this question - there are no standardised and widely available methods to test directionality and there are only very few subjects where very early disease stages have been identified. However, it is likely that relevant insight will rather be gained from more elaborate methods such as adaptive imaging. Thus, targeted functional testing of single photoreceptors might help answering the question on which cellular levels functional or even structural changes occur first.

Chapter 8

General Conclusions

Visual function is essentially what the eye is made for. Characterising functional loss in a disease is of primordial importance in order to understand disease mechanism and the specific impact of the condition on affected people. The herein presented thesis summarises the result from studies on visual function in patients with macular telangiectasia type 2. The studies demonstrate that functional loss changes in character with disease progression and there are specific functional changes even in eyes that otherwise do not seem to show structural alterations. It was also demonstrated that MacTel is limited to a specific area - *the MacTel area* - and confirmed that visual prognosis is less dire than in other retinal conditions, i.e., MacTel will only rarely result in legal blindness.

As a side project of this thesis, software was developed to aid other vision researchers to deal with their ophthalmic data. This software has been made freely available to be used by future generations.

Appendix A

eye - an R package for analysis of ophthalmic data

A.1 Typical challenges with ophthalmic data

There are quite repetitive tasks when working with ophthalmic data. One of the most commonly encountered challenges is the different visual acuity notations used in clinical and research setting. Although generally inter-convertible, the seemingly easy task can be quite daunting, especially when there is a mix of entries with different notations, e.g. logMAR notation, ETDRS letters, Snellen acuities, and possibly even "qualitative" visual acuity entries such as "counting fingers", "hand movement", or "perception of light". It is an ever recurring question in the world of ophthalmic research how to deal with those challenges.

Another recurring challenge is the seemingly simple task of counting the number of patients and eyes in your data. This seems easy, but it can be daunting to count eyes because some patients have more than one eye involved and data entries are found like "both eyes", co-occurring with entries for right or left eyes only, and those should not be counted twice. This can cause a lot of recurring questions how to deal with this counting problem.

In the light of those recurring problems, I developed the *eye* package for R, which makes the conversion between different visual acuity notations very easy. It also allows for a very easy count of patients and eyes. In the following paragraphs,

the underlying functions will be explained.

A.2 Visual acuity notation conversion

This chapter details the underlying method for conversion of visual acuity notations. After automatic cleaning of data entries, the notation is detected automatically. After having detected the notation, the data is checked for plausibility and implausible entries will be removed. Only then happens the conversion to the desired notation. Each step will be detailed below.

A.2.1 Cleaning

1. A common problem with manual data entries are inconsistent codes for erroneous or missing data. This can be an empty cell which might or might not be correctly recognized as a missing value, or worse, a free text entry detailing why the measurement was not done or incorrect (instead of entering this into another column). The cleaning function replaces any value with missing values (*NA* in R) that cannot be visual acuity entries. 2. Another challenge is the inconsistent use of "(no) light perception" [(N)LP] or "(no) perception of light" [(N)PL], which the cleaning function simplifies for the subsequent conversion.

A.2.2 Notation detection

The notation is detected automatically, with a message to the user which notation was detected. The detection is based on the following rules:

- if the entry is one of "CF", "HM", "LP", "PL", "NLP", or "NPL", then this will be recognised as qualitative visual acuity entry, regardless of all other entries.

- The presence of those entries is very typical and very problematic, as it creates some challenges in data handling. In R, there is a broad distinction between data types that represent continuous variables on the one hand (numeric or integer mode) and those that represent categorical variables on the other hand (characters and factors). If all entries of a column in an excel sheet represent a number, R will correctly recognise this as continuous data. However, with

entries such as the above, not only the qualitative entries will be considered as categorical, but also the numbers. For example, 1 (one) will be then the category "1" rather than the number one with its expected value. In R, characters are typically printed with quotes, in order to make it clear to the user that one is dealing with categories rather than numbers. Thus, one cannot simply assume non-numeric entries simply based on the fact that the variable is of *character* type. In order to get around this problem, the *eye* package separates the qualitative entries from above from all other entries and will try a conversion to numeric data. R can correctly convert an entry such as "1" into a numeric entry, but any entry that does not easily convert (e.g., "one"), will result in a missing value on that transformation.

- The presence of new missing values ater that conversion will indicate the presence of character entries that are not convertible to numerics. Some of those are desired entries, in particular the qualitative entries, and if we deal with Snellen notation - R doesn't recognise entries such as 6/5 as fractions without specifically telling it so. Thus, it will see it as category "6/5".

- Having dealt with the qualitative entries, there will be rules for detection applied to all remaining entries:

- if all entries are integers bigger than 3 and smaller than 100, ETDRS is assumed.

- if all entries are integers, and between zero (0) and three (3), this can be in theory logMAR, decimal notation, or very low ETDRS values. The detection assumes logMAR by default, but the user can define the notation manually.

- if all entries are numeric (real numbers), then this is assumed to be either logMAR or snellen notation (as decimal visual acuity).

- if all entries are characters (or *R factors*) and contain a slash ("/"), then Snellen fractions are assumed.

A.2.3 Plausibility tests

Once the visual acuity notation was detected, there will be plausibility checks. If an entry is not plausible, it will be replaced with a missing value, with a warning to the user that this has happened.

- ETDRS measurements can only range from 0 to 100, any value beyond this range is not accepted.

- logMAR values beyond the range between -0.3 and 3.0 are not accepted. -0.3 is equivalent to a Snellen acuity of 6/3, and any higher value is extremely unlikely (because there are hardly any charts where this visual acuity is tested). It is also quite likely, that researchers who undertake studies where subjects would actually reach higher visual acuities than 6/3, have very specific research settings. It is more likely that they then use continous visual acuity notations such as logMAR or completely different ways of measurements such as sinusoid grids resulting in the unit cycle per degree (cpd). Those researchers will probably also not need the *eye* package for visual acuity notation conversion, but a feature request has already been put for conversion of cpd into logMAR.

- Snellen fractions *have to be entered* as a fraction with"/", whereby any fraction is allowed, e.g. 3/60 and 2/200 will be equally recognized. It doesn't play a role if the notation is in feet or meter or both (that data is entered in such ways is real life experience of the author), but if there is no "/", then the entry will not be recognised as Snellen fraction.

- Decimal visual acuity is nothing else than a numeric representation of Snellen fractions (thus, it is called *Snellen decimal* in the eye package). Therefore, values must be more than 0, and smaller or equal than 2.

- Qualitative must be either of "CF", "HM", "LP", "PL", "NLP", or "NPL" (any case is allowed).

A.2.4 Conversion

- Conversion from "pure" Snellen entries to logMAR is straight forward, as the numerical value of the fraction can be directly converted into a logMAR value with $logMAR = -\log_{10}(Snellenfraction)$
- More problematic are entries very often encountered in real life, containing "+" (plus) and "-" (minus) addition to the Snellen fractions, e.g. "6/5 - 2". This is naturally a violation of the visual acuity testing methods designed to assign one (!) unambiguous value to visual acuity, with non-arbitrary thresholds based on psychometric functions. It becomes even more ambiguous when considering that different charts have different numbers of optotypes per line, and some (many) charts even differ within themselves in number of optotypes for each visual acuity level (e.g., 6/60 will only be tested with one letter). Incorporating plus/minus add-ons to the results is thus quite problematic. There are currently three methods to deal with this in the eye package:

  1. for each additional (or removed) letter, a value of 0.02 logMAR will be added/ subtracted. (0.02 logmar for each optotype). This is based on the assumption on a typical chart with five optotypes in a row.
  2. the added letters are rounded to the next or previous Snellen level, such as that a new line commences with three more letters. I.e., and entry of 6/6+3 will be converted to 6/5.
  3. the entries are just ignored.

- *Snellenfraction* to *ETDRS* is converted with $ETDRS = 85 + 50\log_{10}(Snellenfraction)$. [138]
- *logMAR* to *ETDRS* is converted by rounding the logMAR value to the first digit and then converting with a chart.
- ETDRS to logMAR are converted with $logMAR = -0.02ETDRS + 1.7$. [139]
- Counting fingers and hand movements are converted 1.9 and 2.3 logMAR, respectively. [140]

- (No) light perception is an interesting case of debate, but to not convert it would mean to omit important data, e.g., complete loss of vision. They are converted following the suggestions by Michael Bach (see Appendix B).

- Conversion to snellen fraction: Although there seems to be no good statistical reason to convert back to Snellen, it is a very natural thing to eye specialists to think in Snellen. A conversion to snellen gives a good gauge of how the visual acuity for the patients are. However, back-conversion should not be considered an exact science and any attempt to use formulas will result in very weird Snellen values that have no correspondence to common charts. Therefore, Snellen matching the nearest ETDRS and logMAR value in the visual acuity conversion chart (Table A.1) are used.

A.3 Counting patients and eyes

The *eyes* function automatically counts number of patients and eyes in the given data. This data needs to be given as a so called *data frame*, a specific and very common way how relational data is stored and processed in R. It basically resembles an excel sheet but with clear constraints to the data (e.g., all columns have the same length, and all entries in one column must be of one type. This makes data analysis safer).

1. First, the columns are detected which code for patient ID and for eyes. This works by looking for specific "typical" names of those columns, e.g., "patient ID", or "eye". If those columns cannot be clearly identified, the user is prompted to specify it manually.

2. Then, the eye column is checked for plausible entries. A series of strings coding for eyes are allowed (i.e., right eyes can be coded as "r", "re", "od", "right"). It also allows numeric codes such as 1 and 2 for right and left eyes, respectively. If the user has different codes, this can be changed manually either for the entire session or just once. Changing it for the entire session

Snellen (feet)	Snellen (meter)	Decimal acuity	logMAR	ETDRS	Qualitative
20/20000	6/6000	0.001	3.00	0	NLP
20/10000	6/3000	0.002	2.70	0	LP
20/4000	6/1200	0.005	2.30	0	HM
20/2000	6/600	0.01	1.90	2	CF
20/800	6/240	0.025	1.60	5	NA
20/630	6/190	0.032	1.50	10	NA
20/500	6/150	0.04	1.40	15	NA
20/400	6/120	0.05	1.30	20	NA
20/320	6/96	0.062	1.20	25	NA
20/300	6/90	0.067	1.18	26	NA
20/250	6/75	0.08	1.10	30	NA
20/200	6/60	0.1	1.00	35	NA
20/160	6/48	0.125	0.90	40	NA
20/125	6/38	0.16	0.80	45	NA
20/120	6/36	0.167	0.78	46	NA
20/100	6/30	0.2	0.70	50	NA
20/80	6/24	0.25	0.60	55	NA
20/70	6/21	0.3	0.54	58	NA
20/63	6/19	0.32	0.50	60	NA
20/60	6/18	0.33	0.48	61	NA
20/50	6/15	0.4	0.40	65	NA
20/40	6/12	0.5	0.30	70	NA
20/32	6/9.6	0.625	0.20	75	NA
20/30	6/9	0.66	0.18	76	NA
20/25	6/7.5	0.8	0.10	80	NA
20/20	6/6	1.0	0.00	85	NA
20/16	6/5	1.25	-0.10	90	NA
20/15	6/4.5	1.33	-0.12	91	NA
20/13	6/4	1.5	-0.20	95	NA
20/10	6/3	2.0	-0.30	100	NA

Table A.1: This chart was underlying the conversion for visual acuity notations as detailed in subsection A.2.4

makes sense for example if the user has data in a different language than English.

3. Entries that are not matching any of the allowed codes for eyes are replaced with missing values - a warning will be given to the user that this has happened.

4. Then the number of right and left eyes are counted. It happens regularly in real life that the data sheet contains rows with entries for both eyes, and rows with entries for only one eye of the same patient. Care is taken not to count eyes twice if there are entries for both eyes as well.

5. The user can choose between a simple output just with the numbers of right and left eyes and number of patients, and a more detailed output containing the actual IDs for patients that have only right or only left eyes or who have both eyes documented.

Appendix B

Converting (no) perception of light into logMAR visual acuity

Electronic Letters to:

Visual Psychophysics and Physiological Optics:
Kilian Schulze-Bonsel, Nicolas Feltgen, Hermann Burau, Lutz Hansen, and Michael Bach
Visual Acuities "Hand Motion" and "Counting Fingers" Can Be Quantified with the Freiburg Visual Acuity Test
Invest. Ophthalmol. Vis. Sci. 2006; 47: 1236-1240 [Abstract] [Full text] [PDF]

eLetters: Submit a response to this article

Electronic letters published:

Numerical Imputation for Low Vision States
George F. Reed (26 July 2007)

Author Response: Numerical Imputation for Low Vision States
Michael Bach (26 July 2007)

Appendix C

Colophon

This document was set in the Times Roman typeface using LaTeX and BibTeX, composed with the text editor TextMate version 2.0.19. It was built on *ucl_thesis*, a LaTeX 2e class originally created in 1996 by Russel Winder, and later maintained and distributed with permission by Ian Kirker. All tables and figures were embedded in an *adjustbox* package environment. Figures were created with the *ggplot2* package in R and imported into LaTeX in jpeg format. In figure 2.6, the scatter plots have been produced with *ggplot2* and the macular pigment optical density images have been added with *Illustrator CC* (Adobe Inc., Delaware, United States). Figure 6.2 has been made with *Illustrator CC*. Figures 3.1, 3.2, 3.7, 4.1, 4.8, 6.1, 6.6 and 6.7 were created with *Photoshop CC* (Adobe Inc., Delaware, United States). In figures 4.6, 4.7 and 6.10, the fundus icon was created with *Photoshop CC* and imported to R with the *grImport* package.

General tables were generated in R using the *kableExtra* package, and saved to LaTeX . Tables summarising statistical models were created in R using the *sjPlot* package and saved to html, then converted to LaTeX with the *html2latex* package available on https://github.com/gorkang/html2latex.

Bibliography

[1] S. Vujosevic, T. F. C. Heeren, D. Florea, I. Leung, D. Pauleikhoff, F. Sallo, A. Bird, and T. Peto. Scotoma characteristics in macular telangiectasia type 2: Mactel project report no. 7-the mactel research group. *Retina*, 38 Suppl 1:S14–s19, 2018.

[2] T. F. C. Heeren, D. Kitka, D. Florea, T. E. Clemons, E. Y. Chew, A. C. Bird, D. Pauleikhoff, P. C. Issa, F. G. Holz, and T. Peto. Longitudinal correlation of ellipsoid zone loss and functional loss in macular telangiectasia type 2. *Retina*, 2017.

[3] T. F. C. Heeren, S. Tzaridis, R. Bonelli, M. Pfau, M. Fruttiger, M. Okada, C. Egan, P. Charbel Issa, and F. G. Holz. Dark-adapted two-color fundus-controlled perimetry in macular telangiectasia type 2. *Invest Ophthalmol Vis Sci*, 60(5):1760–1767, 2019.

[4] S. Muller, T. F. C. Heeren, R. Bonelli, M. Fruttiger, P. Charbel Issa, C. A. Egan, and F. G. Holz. Contrast sensitivity and visual acuity under low light conditions in macular telangiectasia type 2. *Br J Ophthalmol*, 103(3):398–403, 2019.

[5] Tjebo F.C. Heeren, Emily Y. Chew, Traci Clemons, Marcus Fruttiger, Konstantinos Balaskas, Roy Schwartz, Catherine A. Egan, and Peter Charbel Issa. Macular telangiectasia type 2: Visual acuity, disease end stage, and the MacTel area. *Ophthalmology*, 127(11):1539–1548, nov 2020.

[6] S. Tzaridis, P. Herrmann, P. Charbel Issa, S. Degli Esposti, S. K. Wagner, M. Fruttiger, C. Egan, G. Rubin, F. G. Holz, and T. F. C. Heeren. Binocular inhibition of reading in macular telangiectasia type 2. *Invest Ophthalmol Vis Sci*, 60(12):3835–3841, 2019.

[7] Marin L. Gantner, Kevin Eade, Martina Wallace, Michal K. Handzlik, Regis Fallon, Jennifer Trombley, Roberto Bonelli, Sarah Giles, Sarah Harkins-Perry, Tjebo F.C. Heeren, Lydia Sauer, Yoichiro Ideguchi, Michelle Baldini, Lea Scheppke, Michael I. Dorrell, Maki Kitano, Barbara J. Hart, Carolyn Cai, Takayuki Nagasaki, Mehmet G. Badur, Mali Okada, Sasha M. Woods, Catherine Egan, Mark Gillies, Robyn Guymer, Florian Eichler, Melanie Bahlo, Marcus Fruttiger, Rando Allikmets, Paul S. Bernstein, Christian M. Metallo, and Martin Friedlander. Serine and lipid metabolism in macular disease and peripheral neuropathy. *N Engl J Med*, 381(15):1422–1433, 2019.

[8] Y. Kihara, T. F. C. Heeren, C. S. Lee, Y. Wu, S. Xiao, S. Tzaridis, F. G. Holz, P. Charbel Issa, C. A. Egan, and A. Y. Lee. Estimating retinal sensitivity using optical coherence tomography with deep-learning algorithms in macular telangiectasia type 2. *JAMA Netw Open*, 2(2):e188029, 2019.

[9] S. Muller, P. Charbel Issa, T. F. C. Heeren, S. Thiele, F. G. Holz, and P. Herrmann. Macular pigment distribution as prognostic marker for disease progression in macular telangiectasia type 2. *Am J Ophthalmol*, 194:163–169, 2018.

[10] S. Müller, T. F. C. Heeren, J. Nadal, P. Charbel Issa, P. Herrmann, F. G. Holz, and B. K. Wabbels. Stereoscopic vision in macular telangiectasia type 2. *Ophthalmologica*, pages 1–9, 2018.

[11] M. Okada, C. A. Egan, T. F. C. Heeren, A. Tufail, M. Fruttiger, and P. M. Maloca. Macular telangiectasia type 2: Quantitative analysis of a novel phenotype and implications for the pathobiology of the disease. *Retina*, 38 Suppl 1:S97–s104, 2018.

[12] M. Okada, T. F. C. Heeren, C. A. Egan, V. Rocco, R. Bonelli, and M. Fruttiger. Effect of dark adaptation and bleaching on blue light reflectance imaging in macular telangiectasia type 2. *Retina*, 38 Suppl 1:S89–s96, 2018.

[13] M. Okada, A. G. Robson, C. A. Egan, F. B. Sallo, S. D. Esposti, T. F. C. Heeren, M. Fruttiger, and G. E. Holder. Electrophysiological characterization of macular telangiectasia type 2 and structure-function correlation. *Retina*, 38 Suppl 1:S33–s42, 2018.

[14] D. Pauleikhoff, R. Bonelli, A. M. Dubis, F. Gunnemann, K. Rothaus, P. Charbel Issa, T. F. Heeren, T. Peto, T. E. Clemons, E. Y. Chew, A. C. Bird, and F. B. Sallo. Progression characteristics of ellipsoid zone loss in macular telangiectasia type 2. *Acta Ophthalmol*, 97(7):e998–e1005, 2019.

[15] T. Peto, T. F. C. Heeren, T. E. Clemons, F. B. Sallo, I. Leung, E. Y. Chew, and A. C. Bird. Correlation of clinical and structural progression with visual acuity loss in macular telangiectasia type 2: Mactel project report no. 6-the mactel research group. *Retina*, 38 Suppl 1:S8–s13, 2018.

[16] S. Tzaridis, T. Heeren, C. Mai, S. Thiele, F. G. Holz, P. Charbel Issa, and P. Herrmann. Right-angled vessels in macular telangiectasia type 2. *Br J Ophthalmol*, 2019.

[17] S. Tzaridis, M. W. M. Wintergerst, C. Mai, T. F. C. Heeren, F. G. Holz, P. Charbel Issa, and P. Herrmann. Quantification of retinal and choriocapillaris perfusion in different stages of macular telangiectasia type 2. *Invest Ophthalmol Vis Sci*, 60(10):3556–3562, 2019.

[18] C. A. Curcio, K. R. Sloan, R. E. Kalina, and A. E. Hendrickson. Human photoreceptor topography. *J Comp Neurol*, 292(4):497–523, 1990.

[19] Jan M. Provis. Development of the primate retinal vasculature. *Progress in Retinal and Eye Research*, 20(6):799 – 821, 2001.

[20] Richard F. Spaide and Christine A. Curcio. Evaluation of segmentation of the superficial and deep vascular layers of the retina by optical coherence tomography angiography instruments in normal eyes. *JAMA Ophthalmology*, 135(3):259, mar 2017.

[21] Jan M. Provis, Adam M. Dubis, Ted Maddess, and Joseph Carroll. Adaptation of the central retina for high acuity vision: Cones, the fovea and the avascular zone. *Progress in Retinal and Eye Research*, 35:63–81, jul 2013.

[22] Philip L Penfold, Michele C Madigan, Mark C Gillies, and Jan M Provis. Immunological and aetiological aspects of macular degeneration. *Progress in Retinal and Eye Research*, 20(3):385 – 414, 2001.

[23] J. D. Gass. *Stereoscopic Atlas of Macular Diseases*. Mosby, 1977.

[24] J. D. Gass and B. A. Blodi. Idiopathic juxtafoveolar retinal telangiectasis. update of classification and follow-up study. *Ophthalmology*, 100(10):1536–46, 1993.

[25] J. D. Gass and R. T. Oyakawa. Idiopathic juxtafoveolar retinal telangiectasis. *Arch Ophthalmol*, 100(5):769–80, 1982.

[26] Algernon B. Reese. Telangiectasis of the retina and coats' disease. *American Journal of Ophthalmology*, 42(1):1–8, jul 1956.

[27] Photocoagulation for diabetic macular edema. early treatment diabetic retinopathy study report number 1. early treatment diabetic retinopathy study research group. *Arch Ophthalmol*, 103(12):1796–806, 1985.

[28] A. Hendrickson and C. Kupfer. The histogenesis of the fovea in the macaque monkey. *Invest Ophthalmol Vis Sci*, 15(9):746–56, 1976.

[29] A. Hendrickson, D. Possin, L. Vajzovic, and C. A. Toth. Histologic development of the human fovea from midgestation to maturity. *Am J Ophthalmol*, 154(5):767–778.e2, 2012.

[30] A. E. Hendrickson and C. Yuodelis. The morphological development of the human fovea. *Ophthalmology*, 91(6):603–12, 1984.

[31] C. Yuodelis and A. Hendrickson. A qualitative and quantitative analysis of the human fovea during development. *Vision Res*, 26(6):847–55, 1986.

[32] Peter Charbel Issa, Mark C. Gillies, Emily Y. Chew, Alan C. Bird, Tjebo F.C. Heeren, Tunde Peto, Frank G. Holz, and Hendrik P.N. Scholl. Macular telangiectasia type 2. *Progress in Retinal and Eye Research*, 34:49–77, may 2013.

[33] Harold R. Novotny and David L. Alvis. A method of photographing fluorescence in circulating blood in the human retina. *Circulation*, 24(1):82–86, 1961.

[34] D Huang, EA Swanson, CP Lin, JS Schuman, WG Stinson, W Chang, MR Hee, T Flotte, K Gregory, CA Puliafito, and al. et. Optical coherence tomography. *Science*, 254(5035):1178–1181, 1991.

[35] Michael R. Hee. Optical coherence tomography of the human retina. *Archives of Ophthalmology*, 113(3):325, mar 1995.

[36] P. M. Maloca, J. E. R. de Carvalho, T. Heeren, P. W. Hasler, F. Mushtaq, M. Mon-Williams, H. P. N. Scholl, K. Balaskas, C. Egan, A. Tufail, L. Wittthauer, and P. C. Cattin. High-performance virtual reality volume rendering of original optical coherence tomography point-cloud data enhanced with real-time ray casting. *Transl Vis Sci Technol*, 7(4):2, 2018.

[37] Peter Charbel Issa, Tjebo F. C. Heeren, Elke H. Kupitz, Frank G. Holz, and Tos T. J. M. Berendschot. Very early disease manifestations of macular telangiectasia type 2. *Retina*, 36(3):524–534, mar 2016.

[38] Evangelos S. Gragoudas, Anthony P. Adamis, Emmett T. Cunningham, Matthew Feinsod, and David R. Guyer. Pegaptanib for neovascular

age-related macular degeneration. *New England Journal of Medicine*, 351(27):2805–2816, 2004. PMID: 15625332.

[39] F. B. Sallo, I. Leung, T. E. Clemons, T. Peto, E. Y. Chew, D. Pauleikhoff, and A. C. Bird. Correlation of structural and functional outcome measures in a phase one trial of ciliary neurotrophic factor in type 2 idiopathic macular telangiectasia. *Retina*, 2017.

[40] F. B. Sallo, T. Peto, C. Egan, U. E. Wolf-Schnurrbusch, T. E. Clemons, M. C. Gillies, D. Pauleikhoff, G. S. Rubin, E. Y. Chew, A. C. Bird, and Group MacTel Study. The is/os junction layer in the natural history of type 2 idiopathic macular telangiectasia. *Invest Ophthalmol Vis Sci*, 53(12):7889–95, 2012.

[41] F. B. Sallo, T. Peto, C. Egan, U. E. Wolf-Schnurrbusch, T. E. Clemons, M. C. Gillies, D. Pauleikhoff, G. S. Rubin, E. Y. Chew, and A. C. Bird. "en face" oct imaging of the is/os junction line in type 2 idiopathic macular telangiectasia. *Invest Ophthalmol Vis Sci*, 53(10):6145–52, 2012.

[42] T. F. Heeren, T. Clemons, H. P. Scholl, A. C. Bird, F. G. Holz, and P. Charbel Issa. Progression of vision loss in macular telangiectasia type 2. *Invest Ophthalmol Vis Sci*, 56(6):3905–12, 2015.

[43] Stefanie Mueller, Frederic Gunnemann, Kai Rothaus, Marius Book, Henrik Faatz, Alan Bird, and Daniel Pauleikhoff. Incidence and phenotypical variation of outer retina-associated hyperreflectivity in macular telangiectasia type 2. *British Journal of Ophthalmology*, pages bjophthalmol–2020–317997, jan 2021.

[44] Valérie Krivosic, Carlo Lavia, Anais Aubineau, Ramin Tadayoni, and Alain Gaudric. Oct of outer retinal hyperreflectivity, neovascularization, and pigment in macular telangiectasia type 2. *Ophthalmology Retina*, 2020.

[45] FC Delori, CK Dorey, G Staurenghi, O Arend, DG Goger, and JJ Weiter. In vivo fluorescence of the ocular fundus exhibits retinal pigment epithelium

lipofuscin characteristics. *Invest Ophthalmol Vis Sci*, 36(3):718—729, March 1995.

[46] FC Delori, DG Goger, and CK Dorey. Age-related accumulation and spatial distribution of lipofuscin in rpe of normal subjects. *Invest Ophthalmol Vis Sci*, 42(8):1855—1866, July 2001.

[47] Ruth Hubbard. Absorption spectrum of rhodopsin: 500 nm absorption band. *Nature*, 221(5179):432–435, feb 1969.

[48] Laurenz Pauleikhoff, Tjebo F.C. Heeren, Martin Gliem, Ernest Lim, Daniel Pauleikhoff, Frank G. Holz, Traci Clemons, Konstantinos Balaskas, Catherine A. Egan, and Peter Charbel Issa. Fundus autofluorescence imaging in macular telangiectasia type 2: MacTel study report number 9. *American Journal of Ophthalmology*, 228:27–34, aug 2021.

[49] W. T. Wong, F. Forooghian, Z. Majumdar, R. F. Bonner, D. Cunningham, and E. Y. Chew. Fundus autofluorescence in type 2 idiopathic macular telangiectasia: correlation with optical coherence tomography and microperimetry. *Am J Ophthalmol*, 148(4):573–83, 2009.

[50] JJ Nussbaum, RC Pruett, and FC Delori. Historic perspectives. macular yellow pigment. the first 200 years. *Retina (Philadelphia, Pa.)*, 1(4):296—310, 1981.

[51] D. M. Snodderly, J. D. Auran, and F. C. Delori. The macular pigment. ii. spatial distribution in primate retinas. *Invest Ophthalmol Vis Sci*, 25(6):674–85, 1984.

[52] D. M. Snodderly, P. K. Brown, F. C. Delori, and J. D. Auran. The macular pigment. i. absorbance spectra, localization, and discrimination from other yellow pigments in primate retinas. *Invest Ophthalmol Vis Sci*, 25(6):660–73, 1984.

[53] François C. Delori. Autofluorescence method to measure macular pigment optical densities fluorometry and autofluorescence imaging. *Archives of Biochemistry and Biophysics*, 430(2):156–162, oct 2004.

[54] M. B. Zeimer, I. Kromer, G. Spital, A. Lommatzsch, and D. Pauleikhoff. Macular telangiectasia: patterns of distribution of macular pigment and response to supplementation. *Retina*, 30(8):1282–93, 2010.

[55] H. M. Helb, P. Charbel Issa, Van Der Veen RL, T. T. Berendschot, H. P. Scholl, and F. G. Holz. Abnormal macular pigment distribution in type 2 idiopathic macular telangiectasia. *Retina*, 28(6):808–16, 2008.

[56] P. Charbel Issa, T. T. Berendschot, G. Staurenghi, F. G. Holz, and H. P. Scholl. Confocal blue reflectance imaging in type 2 idiopathic macular telangiectasia. *Invest Ophthalmol Vis Sci*, 49(3):1172–7, 2008.

[57] S. Degli Esposti, C. Egan, C. Bunce, J. D. Moreland, A. C. Bird, and A. G. Robson. Macular pigment parameters in patients with macular telangiectasia (mactel) and normal subjects: implications of a novel analysis. *Invest Ophthalmol Vis Sci*, 53(10):6568–75, 2012.

[58] Simone Müller, Peter Charbel Issa, Tjebo F.C. Heeren, Sarah Thiele, Frank G. Holz, and Philipp Herrmann. Macular pigment distribution as prognostic marker for disease progression in macular telangiectasia type 2. *American Journal of Ophthalmology*, 194:163–169, oct 2018.

[59] P. Charbel Issa, R. P. Finger, H. M. Helb, F. G. Holz, and H. P. Scholl. A new diagnostic approach in patients with type 2 macular telangiectasia: confocal reflectance imaging. *Acta Ophthalmol*, 86(4):464–5, 2008.

[60] F. B. Sallo, I. Leung, M. Zeimer, T. E. Clemons, A. M. Dubis, M. Fruttiger, D. Pauleikhoff, E. Y. Chew, C. Egan, T. Peto, and A. C. Bird. Abnormal retinal reflectivity to short-wavelength light in type 2 idiopathic macular telangiectasia. *Retina*, 38 Suppl 1(Suppl 1):S79–s88, 2018.

[61] Talha Soorma, Tjebo Heeren, Daniela Florea, Irene Leung, and Tunde Peto. Identification of increased blue light reflectivity in macular telangiectasia type 2 using scanning laser ophthalmoscopy versus red-free fundus photography. *Retinal Cases & Brief Reports*, 13(2):115–117, 2019.

[62] Holger Dietze. Die bestimmung der sehschärfe. *Klinische Monatsblätter für Augenheilkunde*, 235(09):1057–1075, aug 2018.

[63] F. Ricci, C. Cedrone, and L. Cerulli. Standardized measurement of visual acuity. *Ophthalmic Epidemiology*, 5(1):41–53, jan 1998.

[64] Frederick L. Ferris, Aaron Kassoff, George H. Bresnick, and Ian Bailey. New visual acuity charts for clinical research. *American Journal of Ophthalmology*, 94(1):91–96, jul 1982.

[65] G. Westheimer. Scaling of visual acuity measurements. *Archives of Ophthalmology*, 97(2):327–330, feb 1979.

[66] T. E. Clemons, M. C. Gillies, E. Y. Chew, A. C. Bird, T. Peto, M. J. Figueroa, M. W. Harrington, and Group MacTel Research. Baseline characteristics of participants in the natural history study of macular telangiectasia (mactel) mactel project report no. 2. *Ophthalmic Epidemiol*, 17(1):66–73, 2010.

[67] Ethan A Rossi and Austin Roorda. The relationship between visual resolution and cone spacing in the human fovea. *Nature Neuroscience*, 13(2):156–157, dec 2009.

[68] Gary S. Rubin. Measuring reading performance. *Vision Research*, 90:43–51, sep 2013.

[69] W. Radner. Reading charts in ophthalmology. *Graefe's Archive for Clinical and Experimental Ophthalmology*, 255(8):1465–1482, apr 2017.

[70] R. P. Finger, P. Charbel Issa, R. Fimmers, F. G. Holz, G. S. Rubin, and H. P. Scholl. Reading performance is reduced by parafoveal scotomas in patients

with macular telangiectasia type 2. *Invest Ophthalmol Vis Sci*, 50(3):1366–70, 2009.

[71] Susanne Trauzettel-Klosinski. Reading disorders due to visual field defects: a neuro-ophthalmological view. *Neuro-Ophthalmology*, 27(1-3):79–90, 2002.

[72] Maximilian Pfau, Jasleen Kaur Jolly, Zhichao Wu, Jonathan Denniss, Eleonora M. Lad, Robyn H. Guymer, Monika Fleckenstein, Frank G. Holz, and Steffen Schmitz-Valckenberg. Fundus-controlled perimetry (microperimetry): Application as outcome measure in clinical trials. *Progress in Retinal and Eye Research*, 82:100907, may 2021.

[73] P. Charbel Issa, H. M. Helb, K. Rohrschneider, F. G. Holz, and H. P. Scholl. Microperimetric assessment of patients with type 2 idiopathic macular telangiectasia. *Invest Ophthalmol Vis Sci*, 48(8):3788–95, 2007.

[74] Emily Y. Chew, Traci E. Clemons, Tunde Peto, Ferenc B. Sallo, Avner Ingerman, Weng Tao, Lawrence Singerman, Steven D. Schwartz, Neal S. Peachey, and Alan C. Bird. Ciliary neurotrophic factor for macular telangiectasia type 2: Results from a phase 1 safety trial. *American Journal of Ophthalmology*, 159(4):659–666.e1, apr 2015.

[75] D. G. Pelli and P. Bex. Measuring contrast sensitivity. *Vision Res*, 90:10–4, 2013.

[76] D. G. Pelli, J. G. Robson, and A. J. Wilkins J. The design of a new letter chart for measuring contrast sensitivity. *Clinical Vision Sciences*, pages 187–199, 1988.

[77] David B. Elliott, Kay Sanderson, and Alison Conkey. The reliability of the pelli-robson contrast sensitivity chart. *Ophthalmic and Physiological Optics*, 10(1):21–24, 1990.

[78] J. M. Nolan, J. Loughman, M. C. Akkali, J. Stack, G. Scanlon, P. Davison, and S. Beatty. The impact of macular pigment augmentation on visual performance in normal subjects: Compass. *Vision Res*, 51(5):459–69, 2011.

[79] John M. Nolan, Rebecca Power, Jim Stringham, Jessica Dennison, Jim Stack, David Kelly, Rachel Moran, Kwadwo O. Akuffo, Laura Corcoran, and Stephen Beatty. Enrichment of macular pigment enhances contrast sensitivity in subjects free of retinal disease: Central retinal enrichment supplementation trials – report 1central retinal enrichment supplementation trials. *Investigative Ophthalmology & Visual Science*, 57(7):3429–3439, 2016.

[80] J. S. Sunness, G. S. Rubin, A. Broman, C. A. Applegate, N. M. Bressler, and B. S. Hawkins. Low luminance visual dysfunction as a predictor of subsequent visual acuity loss from geographic atrophy in age-related macular degeneration. *Ophthalmology*, 115(9):1480–8, 1488.e1–2, 2008.

[81] Tjebo F.C. Heeren. *The eye package for R: A tool to facilitate analysis of ophthalmic data*. London, UK, 2020. version 1.0.1.

[82] Jose Pinheiro, Douglas Bates, Saikat DebRoy, Deepayan Sarkar, and R Core Team. *nlme: Linear and Nonlinear Mixed Effects Models*, 2020. R package version 3.1-149.

[83] R Core Team. *R: A Language and Environment for Statistical Computing*. R Foundation for Statistical Computing, Vienna, Austria, 2020.

[84] W. N. Venables and B. D. Ripley. *Modern Applied Statistics with S*. Springer, New York, fourth edition, 2002. ISBN 0-387-95457-0.

[85] S Della Sala, G Bertoni, L Somazzi, F Stubbe, and A J Wilkins. Impaired contrast sensitivity in diabetic patients with and without retinopathy: a new technique for rapid assessment. *British Journal of Ophthalmology*, 69(2):136–142, feb 1985.

[86] T. E. Clemons, M. C. Gillies, E. Y. Chew, A. C. Bird, T. Peto, J. J. Wang, P. Mitchell, W. D. Ramdas, and J. R. Vingerling. Medical characteristics of patients with macular telangiectasia type 2 (mactel type 2) mactel project report no. 3. *Ophthalmic Epidemiol*, 20(2):109–13, 2013.

[87] T. S. Scerri, A. Quaglieri, C. Cai, J. Zernant, N. Matsunami, L. Baird, L. Scheppke, R. Bonelli, L. A. Yannuzzi, M. Friedlander, C. A. Egan, M. Fruttiger, M. Leppert, R. Allikmets, and M. Bahlo. Genome-wide analyses identify common variants associated with macular telangiectasia type 2. *Nat Genet*, 2017.

[88] Roberto Bonelli, Sasha M. Woods, Brendan R. E. Ansell, Tjebo F. C. Heeren, Catherine A. Egan, Kamron N. Khan, Robyn Guymer, Jennifer Trombley, Martin Friedlander, Melanie Bahlo, and Marcus Fruttiger. Systemic lipid dysregulation is a risk factor for macular neurodegenerative disease. *Scientific Reports*, 10(1), jul 2020.

[89] M. S. Eckmiller. Defective cone photoreceptor cytoskeleton, alignment, feedback, and energetics can lead to energy depletion in macular degeneration. *Prog Retin Eye Res*, 23(5):495–522, 2004.

[90] R. B. Barlow, M. Khan, and B. Farell. Metabolic modulation of human visual sensitivity. *Investigative Ophthalmology & Visual Science*, 44(13):2708–2708, 2003.

[91] R. F. Hess, K. Nordby, and J. S. Pointer. Regional variation of contrast sensitivity across the retina of the achromat: sensitivity of human rod vision. *J Physiol*, 388:101–19, 1987.

[92] S. Schmitz-Valckenberg, K. Fan, A. Nugent, G. S. Rubin, T. Peto, A. Tufail, C. Egan, A. C. Bird, and F. W. Fitzke. Correlation of functional impairment and morphological alterations in patients with group 2a idiopathic juxtafoveal retinal telangiectasia. *Arch Ophthalmol*, 126(3):330–5, 2008.

[93] Rene Y. Choi, Aruna Gorusupudi, Kimberley Wegner, Mohsen Sharifzadeh, Werner Gellermann, and Paul S. Bernstein. Macular pigment distribution responses to high-dose zeaxanthin supplementation in patients with macular telangiectasia type 2. *Retina*, 37(12):2238–2247, dec 2017.

[94] Simone Müller, Jean-Pierre Allam, Christopher G. Bunzek, Traci E. Clemons, Frank G. Holz, and Peter CHARBEL Issa. Sex steroids and macular telangiectasia type 2. *Retina*, 38(1):S61–S66, jan 2018.

[95] T. F. Heeren, F. G. Holz, and P. Charbel Issa. First symptoms and their age of onset in macular telangiectasia type 2. *Retina*, 34(5):916–9, 2014.

[96] K. Rohrschneider, S. Bultmann, and C. Springer. Use of fundus perimetry (microperimetry) to quantify macular sensitivity. *Prog Retin Eye Res*, 27(5):536–48, 2008.

[97] Peter Charbel Issa, Eric Troeger, Robert Finger, Frank G. Holz, Robert Wilke, and Hendrik P. N. Scholl. Structure-function correlation of the human central retina. *PLoS ONE*, 5(9):e12864, sep 2010.

[98] Fred K. Chen, Praveen J. Patel, Wen Xing, Catey Bunce, Catherine Egan, Adnan T. Tufail, Peter J. Coffey, Gary S. Rubin, and Lyndon Da Cruz. Test–retest variability of microperimetry using the nidek MP1 in patients with macular disease. *Investigative Opthalmology & Visual Science*, 50(7):3464, jul 2009.

[99] Q. Wang, W. S. Tuten, B. J. Lujan, J. Holland, P. S. Bernstein, S. D. Schwartz, J. L. Duncan, and A. Roorda. Adaptive optics microperimetry and OCT images show preserved function and recovery of cone visibility in macular telangiectasia type 2 retinal lesions. *Investigative Ophthalmology & Visual Science*, 56(2):778–786, jan 2015.

[100] D. Scoles, J. A. Flatter, R. F. Cooper, C. S. Langlo, S. Robison, M. Neitz, D. V. Weinberg, M. E. Pennesi, D. P. Han, A. Dubra, and J. Carroll. Assessing

photoreceptor structure associated with ellipsoid zone disruptions visualized with optical coherence tomography. *Retina*, 36(1):91–103, 2016.

[101] Katie M. Litts, Mali Okada, Tjebo F. C. Heeren, Angelos Kalitzeos, Vincent Rocco, Rebecca R. Mastey, Navjit Singh, Thomas Kane, Melissa Kasilian, Marcus Fruttiger, Michel Michaelides, Joseph Carroll, and Catherine Egan. Longitudinal assessment of remnant foveal cone structure in a case series of early macular telangiectasia type 2. *Translational Vision Science & Technology*, 9(4):27, mar 2020.

[102] M. B. Powner, M. C. Gillies, M. Tretiach, A. Scott, R. H. Guymer, G. S. Hageman, and M. Fruttiger. Perifoveal muller cell depletion in a case of macular telangiectasia type 2. *Ophthalmology*, 117(12):2407–16, 2010.

[103] M. B. Powner, M. C. Gillies, M. Zhu, K. Vevis, A. P. Hunyor, and M. Fruttiger. Loss of muller's cells and photoreceptors in macular telangiectasia type 2. *Ophthalmology*, 120(11):2344–52, 2013.

[104] S. Schmitz-Valckenberg, E. E. Ong, G. S. Rubin, T. Peto, A. Tufail, C. A. Egan, A. C. Bird, and F. W. Fitzke. Structural and functional changes over time in mactel patients. *Retina*, 29(9):1314–20, 2009.

[105] Janet S. Sunness, Carol A. Applegate, David Haselwood, and Gary S. Rubin. Fixation patterns and reading rates in eyes with central scotomas from advanced atrophic age-related macular degeneration and stargardt disease. *Ophthalmology*, 103(9):1458–1466, 1996.

[106] G. S. Rubin, B. Munoz, K. Bandeen-Roche, and S. K. West. Monocular versus binocular visual acuity as measures of vision impairment and predictors of visual disability. *Invest Ophthalmol Vis Sci*, 41(11):3327–34, 2000.

[107] L. Frisen and B. Lindblom. Binocular summation in humans: evidence for a hierarchic model. *J Physiol*, 402:773–82, 1988.

[108] H. M. Robinson. Factors related to monocular and binocular reading efficiency. *Am J Optom Arch Am Acad Optom*, 28(7):337–46, 1951.

[109] George Spache. One-eyed and two-eyed reading. *The Journal of Educational Research*, 37(8):616–618, 1944.

[110] J. Johansson, T. Pansell, J. Ygge, and G. O. Seimyr. Monocular and binocular reading performance in subjects with normal binocular vision. *Clin Exp Optom*, 97(4):341–8, 2014.

[111] E. Stifter, F. Konig, T. Lang, P. Bauer, S. Richter-Muksch, M. Velikay-Parel, and W. Radner. Reliability of a standardized reading chart system: variance component analysis, test-retest and inter-chart reliability. *Graefes Arch Clin Exp Ophthalmol*, 242(1):31–9, 2004.

[112] Maurizio Battaglia Parodi, Giacinto Triolo, Marco Morales, Enrico Borrelli, Maria V. Cicinelli, Maria L. Cascavilla, and Francesco Bandello. Mp1 and maia fundus perimetry in healthy subjects and patients affected by retinal dystrophies. *Retina*, 35(8):1662–1669, aug 2015.

[113] Keith Rayner, Arnold D. Well, and Alexander Pollatsek. Asymmetry of the effective visual field in reading. *Perception & Psychophysics*, 27(6):537–544, 1980.

[114] S. A. Kabanarou and G. S. Rubin. Reading with central scotomas: is there a binocular gain? *Optom Vis Sci*, 83(11):789–96, 2006.

[115] M. Pfau, M. Lindner, M. Fleckenstein, R. P. Finger, G. S. Rubin, W. M. Harmening, M. U. Morales, F. G. Holz, and S. Schmitz-Valckenberg. Test-retest reliability of scotopic and mesopic fundus-controlled perimetry using a modified maia (macular integrity assessment) in normal eyes. *Ophthalmologica*, 237(1):42–54, 2017.

[116] M. Pfau, M. Lindner, P. L. Müller, J. Birtel, R. P. Finger, W. M. Harmening, M. Fleckenstein, F. G. Holz, and S. Schmitz-Valckenberg. Effec-

tive dynamic range and retest reliability of dark-adapted two-color fundus-controlled perimetry in patients with macular diseases. *Invest Ophthalmol Vis Sci*, 58(6):Bio158–bio167, 2017.

[117] M. Pfau, M. Lindner, J. S. Steinberg, S. Thiele, C. K. Brinkmann, M. Fleckenstein, F. G. Holz, and S. Schmitz-Valckenberg. Visual field indices and patterns of visual field deficits in mesopic and dark-adapted two-colour fundus-controlled perimetry in macular diseases. *Br J Ophthalmol*, 102(8):1054–1059, 2018.

[118] A. J. Zele and D. Cao. Vision under mesopic and scotopic illumination. *Front Psychol*, 5:1594, 2014.

[119] Vincent Michael Patella. Douglas R. Anderson. *Automated Static Perimetry, 2nd ed.* St. Louis: Mosby, 1999.

[120] Douglas Bates, Martin Mächler, Ben Bolker, and Steve Walker. Fitting linear mixed-effects models using lme4. *Journal of Statistical Software*, 67(1):1–48, 2015.

[121] C. A. Curcio, C. L. Millican, K. A. Allen, and R. E. Kalina. Aging of the human photoreceptor mosaic: evidence for selective vulnerability of rods in central retina. *Invest Ophthalmol Vis Sci*, 34(12):3278–96, 1993.

[122] M. P. Simunovic, A. T. Moore, and R. E. MacLaren. Selective automated perimetry under photopic, mesopic, and scotopic conditions: Detection mechanisms and testing strategies. *Transl Vis Sci Technol*, 5(3):10, 2016.

[123] Maximilian Pfau, Philipp L. Müller, Leon von der Emde, Moritz Lindner, Philipp T. Möller, Monika Fleckenstein, Frank G. Holz, and Steffen Schmitz-Valckenberg. Mesopic and dark-adapted two-color fundus-controlled perimetry in geographic atrophy secondary to age-related macular degeneration. *Retina*, 40(1):169–180, jan 2020.

[124] C. Owsley, G. R. Jackson, A. V. Cideciyan, Y. Huang, S. L. Fine, A. C. Ho, M. G. Maguire, V. Lolley, and S. G. Jacobson. Psychophysical evidence for rod vulnerability in age-related macular degeneration. *Invest Ophthalmol Vis Sci*, 41(1):267–73, 2000.

[125] Peter Charbel Issa, Rob L.P. van der Veen, Astrid Stijfs, Frank G. Holz, Hendrik P.N. Scholl, and Tos T.J.M. Berendschot. Quantification of reduced macular pigment optical density in the central retina in macular telangiectasia type 2. *Experimental Eye Research*, 89(1):25–31, jun 2009.

[126] J. Schindelin, I. Arganda-Carreras, E. Frise, V. Kaynig, M. Longair, T. Pietzsch, S. Preibisch, C. Rueden, S. Saalfeld, B. Schmid, J. Y. Tinevez, D. J. White, V. Hartenstein, K. Eliceiri, P. Tomancak, and A. Cardona. Fiji: an open-source platform for biological-image analysis. *Nat Methods*, 9(7):676–82, 2012.

[127] María Nieves-Moreno, Jose M. Martínez-de-la Casa, Pilar Cifuentes-Canorea, Marina Sastre-Ibáñez, Enrique Santos-Bueso, Federico Sáenz-Francés, Laura Morales-Fernández, and Julián García-Feijoó. Normative database for separate inner retinal layers thickness using spectral domain optical coherence tomography in caucasian population. *PloS one*, 12(7):e0180450–e0180450, 2017.

[128] Hadley Wickham. *ggplot2: Elegant Graphics for Data Analysis.* Springer-Verlag New York, 2016.

[129] Daniel Lüdecke. *sjPlot: Data Visualization for Statistics in Social Science*, 2021. R package version 2.8.7.

[130] Thomas Lin Pedersen. *patchwork: The Composer of Plots*, 2020. R package version 1.1.1.

[131] M Hillemanns. Die funktionelle asymmetrie der augen, die vorherrschaft eines derselben und die binokulare richtungslokalisation. *Klin Monbl Augenheilkd*, 78:737–761, 1927.

[132] E. Y. Chew, R. P. Murphy, D. A. Newsome, and S. L. Fine. Parafoveal telangiectasis and diabetic retinopathy. *Arch Ophthalmol*, 104(1):71–5, 1986.

[133] G. B. Jaissle, C. A. May, S. A. van de Pavert, A. Wenzel, E. Claes-May, A. Giessl, P. Szurman, U. Wolfrum, J. Wijnholds, M. D. Fischer, P. Humphries, and M. W. Seeliger. Bone spicule pigment formation in retinitis pigmentosa: insights from a mouse model. *Graefes Arch Clin Exp Ophthalmol*, 248(8):1063–70, 2010.

[134] Ecosse L. Lamoureux, Rebecca M. Maxwell, Manjula Marella, Mohamed Dirani, Eva Fenwick, and Robyn H. Guymer. The longitudinal impact of macular telangiectasia (mactel) type 2 on vision-related quality of life. *Investigative Ophthalmology & Visual Science*, 52(5):2520–2524, 2011.

[135] Alexandre Matet, Suzanne Yzer, Emily Y. Chew, Alejandra Daruich, Francine Behar-Cohen, and Richard F. Spaide. Concurrent idiopathic macular telangiectasia type 2 and central serous chorioretinopathy. *Retina*, 38(1):S67–S78, jan 2018.

[136] Emily Y. Chew, Traci E. Clemons, Glenn J. Jaffe, Charles A. Johnson, Sina Farsiu, Eleonora M. Lad, Robyn Guymer, Philip Rosenfeld, Jean-Pierre Hubschman, Ian Constable, Henry Wiley, Lawrence J. Singerman, Mark Gillies, Grant Comer, Barbara Blodi, Dean Eliott, Jiong Yan, Alan Bird, and Martin Friedlander. Effect of ciliary neurotrophic factor on retinal neurodegeneration in patients with macular telangiectasia type 2. *Ophthalmology*, 126(4):540–549, apr 2019.

[137] Ryan Poplin, Avinash V. Varadarajan, Katy Blumer, Yun Liu, Michael V. McConnell, Greg S. Corrado, Lily Peng, and Dale R. Webster. Prediction of cardiovascular risk factors from retinal fundus photographs via deep learning. *Nature Biomedical Engineering*, 2(3):158–164, feb 2018.

[138] N. Z. Gregori, W. Feuer, and P. J. Rosenfeld. Novel method for analyzing snellen visual acuity measurements. *Retina*, 30(7):1046–50, 2010.

[139] Roy W Beck, Pamela S Moke, Andrew H Turpin, Frederick L Ferris, John Paul SanGiovanni, Chris A Johnson, Eileen E Birch, Danielle L Chandler, Terry A Cox, R.Clifford Blair, and Raymond T Kraker. A computerized method of visual acuity testing. *American Journal of Ophthalmology*, 135(2):194–205, feb 2003.

[140] Kilian Schulze-Bonsel, Nicolas Feltgen, Hermann Burau, Lutz Hansen, and Michael Bach. Visual acuities "hand motion" and "counting fingers" can be quantified with the freiburg visual acuity test. *Investigative Opthalmology & Visual Science*, 47(3):1236, mar 2006.